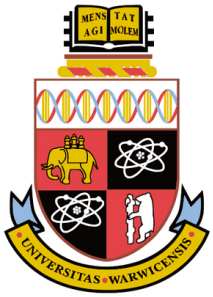

CHARACTERISING THE ROLE OF ATSCL26 IN ROOT DEVELOPMENT

MATT TEFT

Thesis submitted to the

University of Warwick

for the degree of

DOCTOR OF PHILOSOPHY

School of Life Sciences

WARWICK
THE UNIVERSITY OF WARWICK

Table of Contents

List of figures

List of tables

Acknowledgements

I would firstly like to dedicate this thesis to my late Grandfather who always supported my decisions and who made it possible for me to be where I am today. Whilst he is not here to see me complete this thesis, I know that he would be proud of what I have accomplished.

I would like to acknowledge and sincerely thank my supervisor, Dr Miriam Gifford, for her never-ending patience and for the support she has shown me throughout my PhD. I joined the lab with very little plant biology experience, and not a great deal of confidence. I owe Miriam a huge thank you for giving me the time I needed to develop these skills and also the support in doing so. I also owe a huge debt of gratitude to Dr Beatriz Lagunas-Castan who has kept me on my toes and helped me find motivation when I was running low.

I would also like to thank the members of my advisory panel, Prof Eric Holub and Dr Patrick Schäfer. Their advice and opinions really helped me develop as a PhD candidate and gave me a broader perspective as to what was expected of me as not only a PhD candidate within the lab, but where I should be aiming for externally. They gave me fresh eyes when looking at my project.

Finally, I would like to thank my colleagues who have in helped and guided me through times when I was unsure and uncertain.

Declaration

This thesis is submitted to the University of Warwick in support of my application for the degree of Doctor of Philosophy. It has been composed by myself and has not been submitted in any previous application for a degree.

All research and analyses was carried out by the author except for the qPCR of *AtSCL26,* which was carried out by Anthony Carter, a previous student (chapter 3). Phenotyping *AtSCL26* root systems on KNO_3 (chapter 3) and micro RNA of the cortex and epidermis layers (chapter 5) was carried out by Dr Beatriz Lagunas-Castan.

Abstract

Variations in root phenotype in response to the limiting nutrient nitrogen is of great importance in light of current agricultural challenges. Understanding the molecular processes that determine phenotype can also help further understanding of how root architecture systems are regulated and the overall effect that N has on molecular processes. Links between divergent root systems can also offer answers as to how plants have adapted to meet changes in their environmental conditions over evolutionary time. *NSP2* is a *Medicago truncatula* gene known to regulate processes involved in the formation of nodules in legumes, and has a putative homolog in the non-nodulating plant *Arabidopsis thaliana*, *AtSCL26*. This thesis has shown that there is a root system architecture phenotype, as well as a molecular transcriptomic phenotype in *atscl26* mutants, and that these phenotypes are nitrogen dependant. *AtSCL26* acts to regulate transport of auxin signalling genes in deplete nitrogen conditions, as well as repress other molecular regulatory processes that are involved in regulating growth and root development. Overall *AtSCL26* has a repressive effect on root development in nitrogen-deplete conditions, and this is also nitrogen source dependant, as there is a stronger phenotype on potassium nitrate when compared to ammonium nitrate. Overall this investigation suggests that, like *NSP2*, *AtSCL26* could be a nitrogen-regulated transcription factor that coordinates root development according to environmental cues.

Abbreviations

ANOVA	Analysis of variance
AtSCL	*Arabidopsis thaliana* SCARECROW-LIKE
Bp	Base pair
cDNA	Complementary DNA
CK	Cytokinin
DNA	Deoxyribonucleic acid
dNTP	Deoxyribonucleic triphosphate
FACS	Fluorescence activated cell sorting
GO	Gene ontology
GOGAT	Glutamine oxoglutarate aminotransferase
GS	Glutamine synthase
KNO_3	Potassium nitrate
LB	Luria broth
LBA	Luria broth agar
LR	Lateral root
LRFC	Lateral root founder cell
mRNA	Messenger RNA
N_2	Diatomic nitrogen
NH_3	Ammonia

NH_4+	Ammonium
NH_4NO_3	Ammonia nitrate
NO_2-	Nitrite
NO_3-	Nitrate
NSP	Nodulation signalling pathway
PCR	Polymerase chain reaction
PR	Primary root
qPCR	Quantitative PCR
RNA	Ribonucleic acid
RSA	Root system architecture
tDNA	transfer DNA
XPP	Xylem pole pericycle

Chapter 1 Introduction

1.1 Context for the need to improve agricultural yield whilst also reducing dependence on fertiliser

As of 2016, the Earth's population stood at around 7.6 billion, growing at a net increase of approximately 1.1% each year (Population and History, 2008). Whilst this rate of increase is at an all-time low when you look back over the last 50 years (peak of growth of 2.19% in 1963) and is predicted to decrease to less than 1% in 2020 and less than 0.5% in 2050, the fact still remains that the population has more than doubled since 1960 when the population stood at 3 billion. At even the low rate of increase the United Nations is currently predicting the population to reach 9.8 billion by 2050 (United Nations News Service, 2013). The growth in the population has led to an increase in demand for sustainable crop supplies, leading to pressure on farmers, agriculture, and the food sector. One of the biggest breakthroughs which answered the increasing demand for food in modern times was led by Norman Borlaug. He led a global initiative to increase yield in wheat and rice by reducing the length of stems, which stopped them falling over and reducing harvestable parts. This 'Green Revolution' lasted between the 1930s and 1960s and saved an estimated 1 billion people from starvation. In recognition for the initiatives research, Borlaug was awarded the Nobel Peace Prize in 1970.

To combat the ever-increasing demand for food, farmers have had to make use of land with a poorer nutrient profile to grow crops and thus enlist the aid of artificial fertilisers to provide phosphorous, nitrogen, and potassium. With a decreasing area of nutrient-rich land in modern times (Bren d'Amour et al., 2016), plant and crop researchers are challenged with developing and improving on current methods of production to meet new yield demands. Areas of focus for research include optimising

and improving the photosynthetic pathway, increasing pest resistance and reducing losses due to disease, and developing ways to increase nutrient and water uptake or increase nutrient use efficiency (Moshelion and Altman, 2015). Exploiting the high degree of root architecture plasticity to the environment is another promising approach (Tian and Doerner, 2013). These improvements are also needed to address the economic and environmental cost of fertiliser use in agriculture as the demand increases. Demands for fertilizer nutrients have increased since 2015 and are estimated to rise even further by 2020; demands on nitrogen have risen from 110,027 kt to an estimated 118,763 kt (2020 estimation), phosphate has risen from 41,151 kt to 45,858 kt, potash (K_2O) rose from 32,838 kt to 37,042 kt (FAO, 2015).

One of the main direct environmental costs of N fertiliser production is in the energy that it takes to produce, it is estimated that 1.2% of the worlds global energy production goes towards producing fertilisers (Worrell et al., 2009), taking approx. 3 units of carbon to produce 1 unit of nitrogen (Fossum, 2014).

1.2 Environmental impacts of eutrophication

Whilst not a direct consequence of producing artificial fertilisers, another devastating consequence of nutrient supplementation is a process called eutrophication, whereby the nutrients leak into surrounding ground water and habitats (Fenn et al., 2003). This increase in nutrients causes excessive growth in plant and algae which has a number of effects; initially it causes a depletion of available light to plants in the littoral zones and also leads to reduced success of predation by organisms that rely on light (Salonen et al., 2009). In addition to these changes, the increased demand on inorganic carbon for photosynthesis can cause increases in pH during the day that would leave organisms that rely on chemical cues to sense their environment

severely limited (Turner and Chislock, 2010). One of the last effects, but also one of the most devastating in terms of ecological damage comes when then algae begin to die and microbial decomposition begins. This process creates hypoxic and anoxic 'dead zones' which are depleted of oxygen during the decomposition process and are left unable to support oxygen dependant life (Rabalais et al., 2002).

1.3 The role of nitrogen in controlling plant development

Apart from phosphorus, nitrogen is considered to be the most limiting nutrient for plant growth and development. All living organisms require nitrogen to synthesise the amino acids needed from DNA and proteins, but plants also require nitrogen to synthesise chlorophyll. This pigment, when exposed to sunlight, oxidises and releases electrons into the electron transport chain pathway that chloroplasts use to produce ATP (Muldoon, M., *et al*., 1985). Nitrogen, as building block and nutrient is thus crucial for all aspects of development, from germination to seed set.

With the increase in the demand for yield, ensuring that the correct quantity and source of nitrogen is produced and utilised has never been more important. Whilst the atmosphere is comprised of 78% nitrogen, in this gaseous form it is not possible for plants to directly fix diatomic nitrogen (N_2) from the vast supply in the air. Gaseous N_2 can be fixed, which can happen either of two-ways, either N_2 is converted directly to NO_3^-, which requires a large amount of energy, heat and pressure, such as a volcanic event or lightning, or energy used in the manufacturing Harber-Bosch process. Alternatively, the change can occur via biological nitrogen fixation that can be carried out by a small group of bacteria that are able to produce and utilise nitrogenase enzymes. In the absence of oxygen (O_2) these enzymes are capable of breaking the

strong N-N triple bonds that bind the diatomic nitrogen atoms and replace them with hydrogen atoms to produce un-ionised ammonia gas (NH_3) and ammonium (NH_4^+).

Biological nitrogen fixation occurs either in free-living organisms including cyanobacteria, heterotrophic or autotrophic bacteria, or bacteria that are associated with plants. N fixation by bacteria is a very energy intensive process and for every mole of N reduced, it takes 16 moles of adenosine triphosphate (ATP) (Kim and Rees, 1994; Rees and Howard, 2000; Hoffman et al., 2013). Biological nitrogen fixation can be expressed in the follow equation:

$$N_2 + 8e^- + 16\,ATP + 8H_2^+ \rightarrow 2NH_3 + H_2 + 16ADP + 16P$$

The energy to reduce N is obtained by the oxidation of organic molecules either provided by the host plant directly, as in the case of nodulation, or from the surrounding soil.

In nitrifying bacteria including *Nitrosomonas* and *Nitrococcus* species there is a two-step nitrification process where NH_4^+ is oxidised to NO_2-, then NO_2^- is oxidised to NO_3^- by *Nitrobacter* (Masson-Boivin and Sachs, 2018).

1.4 Nitrogen uptake by plants and communication of nitrogen status

Free nitrate in the soil is taken up by plant cells via a combination of high and low affinity nitrogen transport systems (reviewed in O'Brien et al 2016). Of these, the *Nitrate Transporter 1.1* (*NRT1.1*) plays a particularly key regulatory role in not only transporting nitrate but sensing it (Gojon et al., 2011). Once absorbed through the root, nitrate can either be reduced by the plant using nitrate reductase (NR) in the cytosol, transported, or stored in a vacuole. Nitrate is reduced to ammonium by nitrite reductase (NIR) in the plastid which is then fixed into glutamine/glutamate amino acids by the

glutamine synthase/glutamine oxoglutarate aminotransferase (GS/GOGAT) pathway (Figure 1) (Tischner, 2000).

During early nitrate responses *NRT1.1* also plays a regulatory role, activating a wide number of genes that are involved in the assimilation of nitrate. Regulation of nitrate transport also occurs downstream of *NRT1.1* action; bZIP family transcription factors *TGA1* and *TGA4* regulate expression of the nitrate transporters *NRT2.1* and *NRT2.2* (Alvarez et al., 2014).

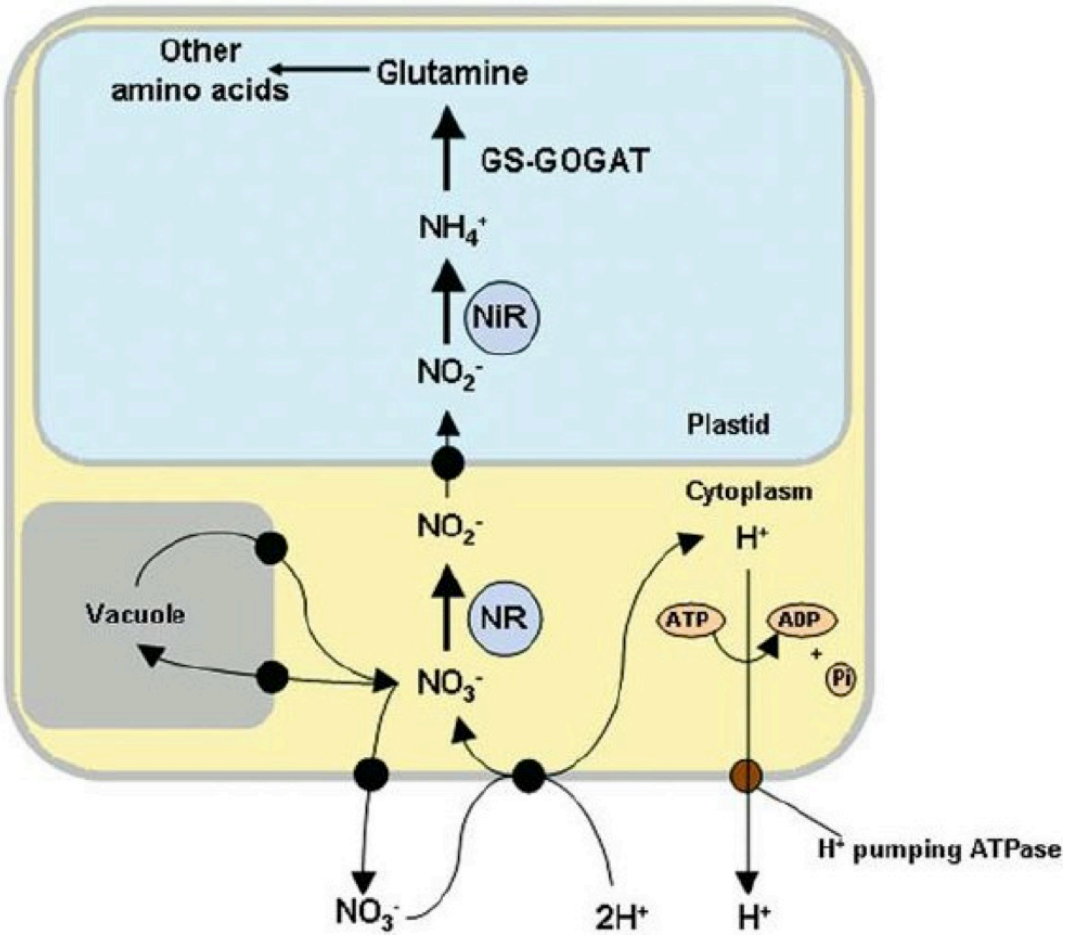

Figure 1: NO3- uptake and assimilation in plant cells. NO_3^- enters the plant cell and is reduced through redox action of NR to NO_2^-. NO^{2-} enters the plastid and is further reduced to NH_4^+ by NIR, then enters the GS-GOGAT pathway, ultimately leading to production of glutamine and other amino acids (Tischner, 2000).

Arabidopsis thaliana (*A. thaliana*) has four main families of genes which are involved in the uptake and systemic transport of nitrogen identified; NITROGEN TRANSPORTER 1/PEPTIDE TRANSPORT (NRT1/PTR), NITROGEN TRANSPORTER 2 (NRT2), CHLORIDE CHANNELS (CLC), and SLOQ ANION CHANNEL-ASSOCIATED 1 HOMOLOGS (SLAC1/SLAH) (Lin et al., 2008).

1.5 Developmental differences between seedlings grown on different nitrogen sources

Although both NH_4^+ and NO_3^- are able to be assimilated directly by plants, there have been recorded differences in their effect on root development and root architecture. One key difference is that, whilst both are actively taken up through membrane transport, ammonia transport is facilitated by 6 high affinity ammonia transporters of the AMT/MEP/Rh (AMT superfamily) (Yuan et al., 2007) whereas transport of nitrate across the membrane is mediated by the NITRATE TRANSPORTER1/PEPTIDE TRANSPORTER super family (NPF). This family contains 53 genes which encode for low affinity nitrate transporters. In addition the NRT2 family is comprised of 7 members that code for high affinity nitrate transporters (Nacry et al., 2013). It has been shown in previous investigations that high affinity transporters are pivotal to the uptake of N in deplete conditions (Krapp et al., 2011).

Shtratnikova (2015) conducted a series of experiments on *A. thaliana* to evaluate root system architecture on different nitrogen sources; MS medium containing either 2mM KNO_3, 10mM $(NH_4)SO_4$ or 1mM $(NH_4)SO_4$ (Figure 2). Seedlings that were grown on 2mM KNO_3 as their nitrogen source had much greater total root length (primary plus lateral) and total lateral root length (~230mm and

~200mm respectively) compared to seedlings grown on 10mM $(NH_4)SO_4$ which had a total root length of ~50mm and total lateral root length of ~20mm.

Molecularly there are strong links between nitrogen uptake/accumulation and the induction of cytokinin (CK) synthesis. The CK pathway enzymes are involved in signalling in response to nitrate nutrition as well as in many aspects of plant growth and development including leaf growth, and long distance signalling in response to nitrogen nutrition (Mok and Mok, 2001). The seedling lines used by Shtratnikaetal (2015) carried a cytokinin dependant promoter of the *Arabidopsis* response regulators (ARR5) driving a GUS reporter line to visualise cytokinin pathway induction and how it varied depending on N input. The observed an increase in cytokinin accumulation during leaf growth, and also noticed that it was increased due to nitrate in the soil and that ammonium actually supressed growth of leaves and roots.

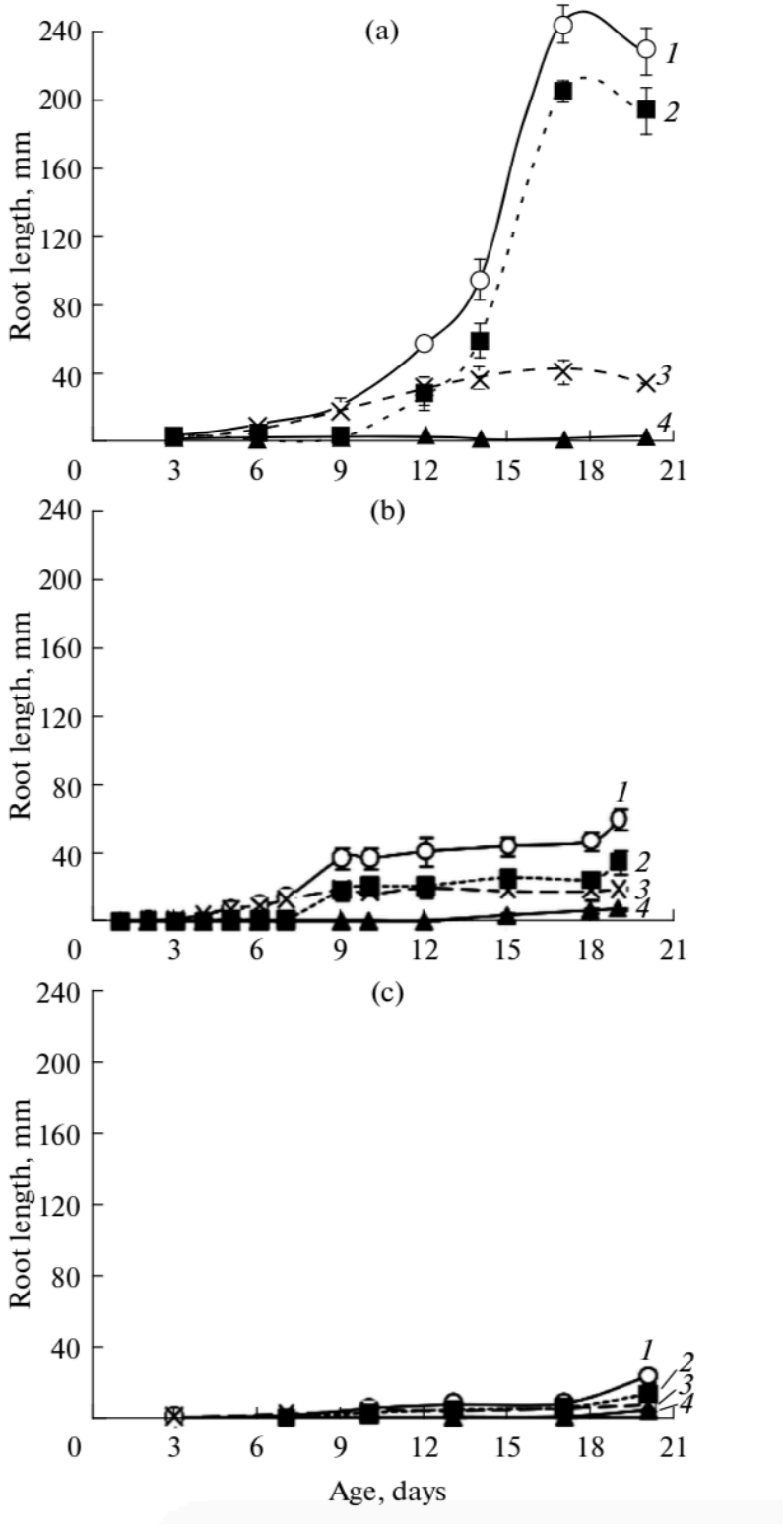

Figure 2: Root system architecture under different nitrogen regimes. Seedlings grown on 2mM KNO_3 (a), 10mM $(NH_4)SO_4$ (b), or 1mM $(NH_4)SO_4$ (c). Lengths of total root system (1), 1st order lateral roots (2), primary root (3), and 2nd order lateral roots (4) (Shtratnikova et al., 2015).

1.6 The process of lateral root development in *A. thaliana*

The primary root of a dicot plant is comprised of 15 cell types with a range of distinct functions and structural features that have been elucidated using detailed analysis of each cell type (reviewed in Brady *et al.*, 2007). Lateral roots that arise from the primary root are similarly organised (Figure 3). Lateral root development is regulated by many interacting pathways that respond to nutrient and water availability as well as biotic factors and is influenced by a number of key hormone pathways including cytokinin (CK), gibberellin (GA) and auxin (e.g. reviewed in Péret *et al.*, 2009). The combined regulation of primary and lateral root architecture results in variation in lateral root characteristics including number, length, direction of outgrowth and spacing over the primary root (lateral root density). Studies using ecotypes have shown that these characteristics can be independently regulated by nitrogen in the environment (Gifford et al., 2013).

Whilst it is true that lateral roots originate from division in the pericycle, this only takes place in xylem pole pericycle (XPP) cells. Through a mechanism involving readout of auxin levels and the activation of regulatory genes, these cells are primed to become lateral root founder cells (LRFC). Activation of cell division occurs where the nucleus of each XPP cell migrates towards each other and the cells undergo periclinal asymmetric division to form stage 1 LR primordia. The established LR primordia then divides anticlinally through the other cell layers until it emerges as an established LR (Figure 3).

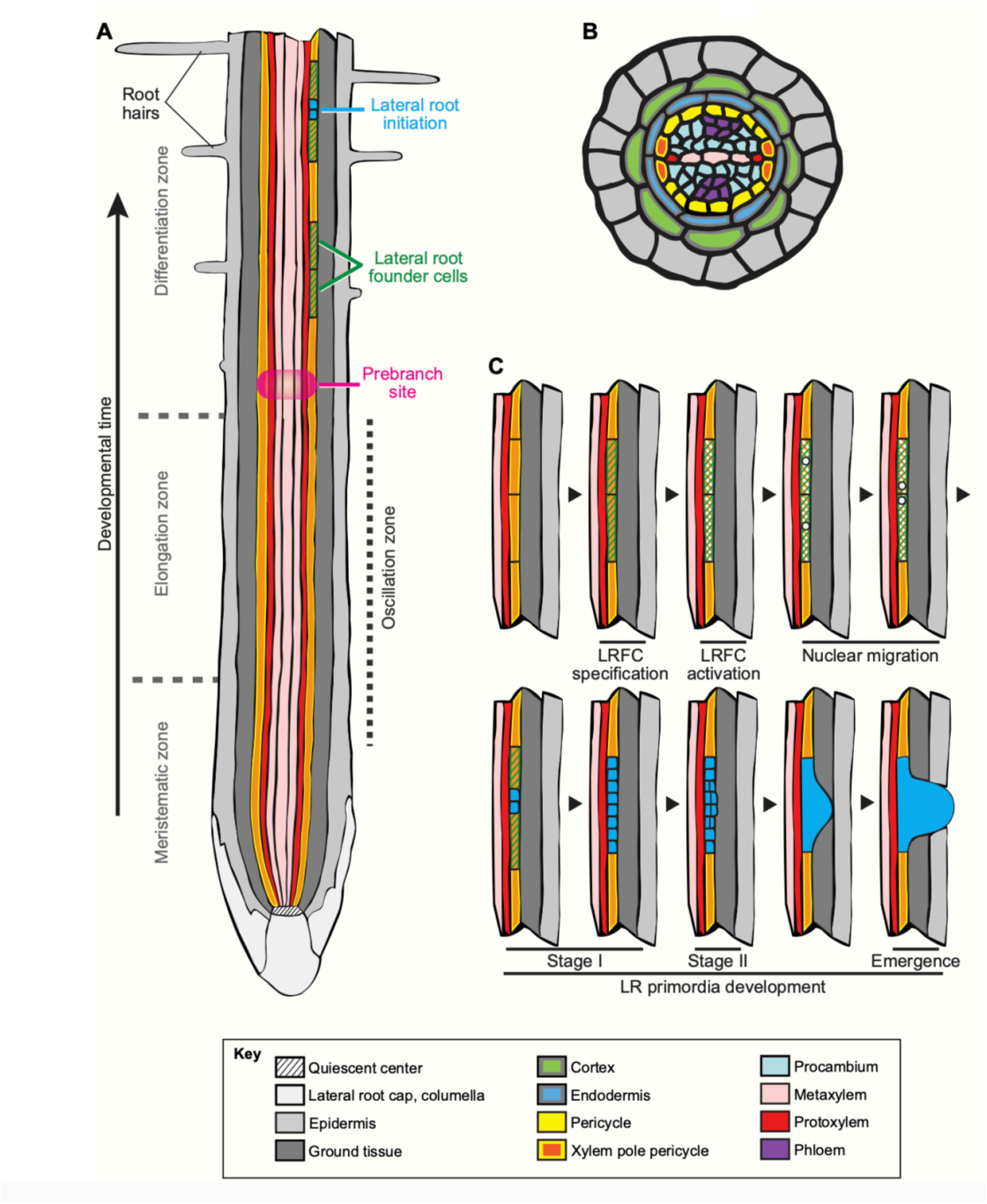

Figure 3: *A. thaliana* root organisation. (A) Longitudinal section, with the meristematic region, the zone of elongation, the zone of cell differentiation and the location of lateral root initiation indicated. (B) A transverse section of the same root taken at a point within the differentiation zone. Concentric layers of cells with distinct cell types are visible. (C) The establishment of LRFCs and initiation of a LR, starting with asymmetrical anticlinal cell division of the pericycle. (Van Norman et al., 2013)

1.7 The regulation of lateral root development by nitrogen

Signalling pathways (both local and long distance) are able to assert control over the distribution and transport of nitrogen, which allows the plant to regulate its response in relation to nitrogen demands and nitrogen content. Communication of nitrogen demand between cells in the form of microRNA and phytohormone synthesis/transport, and transcription factor regulation have all been documented in previous research. For example, in one such mechanism the auxin receptor gene AUXIN SIGNALLING F BOX 3(AFB3), which regulates nitrogen-responsive lateral root initation, is modulated by miR393 (Liu et al., 2015).

The limiting effect of nitrogen on LR growth has been seen by genes expressed in the pericycle cell when nitrogen in low. CLAVATA3/ENDOSPERM SURROUNDING REGION-*related* (CLE) genes encode for peptides which target CLAVATA1 (CLV1) leucine-rich repeat receptor-like kinases to inhibit lateral root growth, however during this time of nitrogen shortages, C-TERMINALLY ENCODED PEPTIDES (CEP) are translocated long distance to the shoots, where they are crucial for inducing a foraging like behaviour in the roots (Tabata et al., 2014). Both of these examples indicate the importance of communication on a cellular and longer distanced level within the plant to enable survival in times when nitrogen levels are poor.

A large number of genetic regulators have been found to be involved in sensing and responding to N in plants that control lateral root development. Of particular note is the hormone pathway involving the plant growth regulator auxin, indole-3-acetic acid (IAA) (Overvoorde et al., 2010). Research has identified that auxin biosynthesis, polar transport and signal transduction are all important regulators in the development of LRs in higher plants (Casimiro et al., 2001; Overvoorde et al., 2010). Auxin

biosynthesis is upregulated in low nitrogen levels and this has been attributed to the N-dependent up-regulation of tryptophan aminotransferase related 2 (TAR2) which converts tryptophan into indole-3-pyruvic acid (IPyA); one of the four pathways of IAA biosynthesis (Ma et al., 2014; Kiba and Krapp, 2016). In over-expressers of TAR2, there is an increase of LRs and specifically an increase in shoot to root IAA accumulation. Conversely, in *tar2-c* mutants there is a reduction in LR number and length (Ma et al., 2014). *NRT1.1* also represses lateral root branching when nitrogen levels are deplet, by diverting accumulating auxin from lateral root primordia (Bouguyon et al., 2015). Low nitrogen also up-regulates *AGL21*, another gene known to affect the expression of auxin. In *AGL21*-overexpressing plants grown on low N, there was a significant increase in the expression of genes involved in the biosynthesis of auxin (*YUC5*, *YUC8*, and *TAR3*), which were all down regulated in *agl21* mutants (Yu et al., 2014).

A number of transcription factors have been found to control lateral root numbers in a nitrogen-dependent way. These include two WRKY transcription factors, *WRKY75*, *WKY15* and the GRAS transcription factor *HRS1* (Medici et al., 2015), that integrates both N and P signalling in the root (Devaiah et al., 2007; Walker et al., 2017).

Whilst LR initiation is visible in the differentiation zone of the plant root (Figure 3), the process actually begins a long closer to the basal meristem portion of the root. Along the length of the root, there are a number of key areas that have been characterised by their function, or by the developmental process that are attributed to it. DeSmet *et al* (2007) showed that fluctuations in transcriptional responses in auxin biosynthesis and transport, using the DR5:GUS reporter, occur in the area of the root between the meristem and the differentiation zone (De Smet, I., *et al,* 2007), in a

mechanism termed ‘priming’ of lateral root founder cells. This was further investigated using DR5:LUC as a reporter, which showed similar fluctuating patterning. However, some of the cells maintained the concentrations of DR5:LUC and later developed into LRs, indicating that if cells that are developing within the oscillation zone experience high concentrations of auxin, they are primed and go on to develop into LRs (Moreno-Risueno, *et al*, 2010).

1.8 Nodulation formation in legume plants

As sessile organisms, plants are forced to either exploit their immediate surrounds, or adapt (or both) one way in which some plants have evolved to do this is by recruiting nitrogen fixing bacteria as symbiotes in a nitrogen-carbohydrate exchange. In the case of plant-associated bacteria, the most common interactions are of rhizobial bacteria with legumes, in a process termed nodulation (Downie, 2014; Suzaki et al., 2015; Kassaw et al., 2017). The majority of plant species that belong to the Fabacean (legume) family have the ability to initiate interactions with rhizobial bacteria following exchange of molecular signals. The process of nodulation is firstly initiated through chemical signalling between host legume and nearby rhizobacteria at plant root hairs. The legume exudes flavonoids into the surrounding soil and these can be detected by the rhizobia, that begin to produce a litochitoligosaccharide called Nod factor. The structures of both flavonoid and Nod factor are sensed specifically, enabling particular rhizobia-legume synmbiotic interactions to form. Plant epidermal cells can detect Nod factor through receptor-like kinases (NFR1/NFR5). The LysM domains of thesee kinases is where Nod factor can bind, leading to oscillations in Ca^{2+} in the epidermal cytoplasm and activation of the CALCIUM-CALMODULIN

DEPENDENT KINASE. CCamK is an important step in the nodulation process as once CCamK has been produced, the components upstream of this pathway are no longer required for successful nodulation to occur. This CCamK phosphorylates CYCLOPS, which is hypothesised to regulate transcription of transcription factors important in controlling the formation of nodules, including NODULATION SIGNALLING PATHWAY 1 and 2 (NSP1 and 2), ERF REQUIRED FOR NODULATION (ERN), and NODULE INCEPTION (NIN) (Oldroyd, G., Murray, J. Poole, P., 2011)

At the same time as CCamK and CYCLOPS control responses in the epidermis, cytokinin signalling is initiated by the production of CCamK and CYCLOPS. This results in initiation of cortical cell division and the formation of pre-infection threads (pIT) that lead from to the root hair to the cortex cells. Within root hairs rhizobia are encapsulated, then travel down pITs as they are established as infection threads (IT) (Figure 4) (reviewed in (Gibson et al., 2008)).

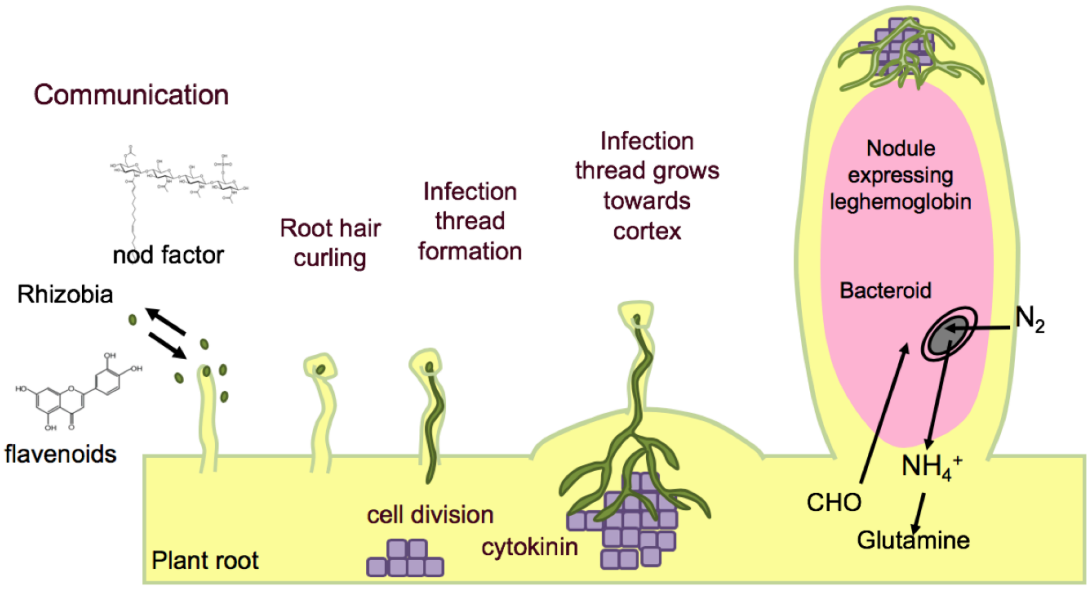

Figure 4: The formation of nodules in legume plants. Nodulation is initiated after a molecular signalling interaction between host plant and rhizobia involving Nod-factor production from rhizobia and flavonoid release by the plant. The plant root hair curls

around the detected bacteria and the growth of an infection thread is initiated. At the same time the nodule organ begins to develop through cortical cellular division. Image adapted from Gibson *et al* (2008) and The Plant Cell Teaching Resources.

The ability of legumes to symbiotically interact with nitrogen-fixing bacteria in the surrounding rhizosphere has been of great evolutionary advantage for plants that experience nitrogen-deficient growth conditions. Part of the mechanism that enables this is the ability to sense the rhizobia as a symbioint, rather than pathogen. As part of plant immunity and defense mechanisms, plants can recognise fungal and bacterial pathogens via plasma-membrane receptor-like kinases. These receptors recognise highly conserved pathogen/microbe-associated molecular patterns (PAMPs/MAMPs) in a process termed PAMP-triggered immunity (PTI). This is a very early stage in pathogen identification and the point at which differentiation between potential symbiont and potential pathogen can be made. It has been proposed that rhizobia are able to either supress the immune response, or pass undetected through the IT to the nodule. This has been shown using time course experiments conducted in several legumes, *Glycine max* (Libault, *et al.* 2010), *Medicago truncatula* (Lohart, *at al*., 2006)), and *Lotus japonicus* (Kouchi, *et al*., 2004). An upregulation of immune response genes is seen at the time of rhizobial infiltration, however the expression levels return to basal rates, and were even supressed at times coinciding with the initiation of ITs.

1.9 Links between nodulation and lateral root development

Based on a range of genetic and physiological evidence, it is hypothesised that the developmental pathway of nodulation is an evolutionary adaptation of the genetic

blueprint involved in formation of lateral roots (Bensmihen, 2015; Lagunas *et al*, 2015). Both organs are controlled over time and in a cell type specific manner and formed by reactivation of cell division in differentiated cells in specific developmental zones (Malamy and Benfey, 1997; Stougaard, 2000; Brady et al., 2007). When a number of genes controlling nodulation in *Medicago truncatula* have been altered, including the cytokinin receptor *MtCRE1*(Gonzalez-Rizzo et al., 2006) and *MsRH2-1*, a RING-H2 domain protein(Karlowski and Hirsch, 2003), it has been found that this also leads to defects in lateral root development.

Induction of both LR and nodule development are strongly affected by levels of nitrogen in the surrounding soil and within the root. Research has shown that the roots of a plant grown in low N conditions produces longer lateral roots and the root system takes on a more exploratory or foraging nature (Tian and Doerner, 2013; Araya et al., 2014). In low N conditions or 'mild' deficiency there is a significant increase in average LR length, however this effect diminishes when plants are grown in N deficient conditions where LR outgrowth is much reduced (Krouk et al., 2011; Gruber et al., 2013). Much higher concentrations of N supplementation (>10mM) can have an inhibitory effect on LR length and number, attributed to N-induced changes in the hormone pathways associated with LR development (Simonson, 1956).Similar effects of high N can be seen to inhibit nodulation in legumes. For example, in the model legume *Medicago truncatula* flavonoids are secreted by the plant roots in low N conditions, as part of the plant-rhizobia communication, but at high N levels flavonoid secretion is much reduced (Liu and Murray, 2016; Xia et al., 2017).

GRAS transcription factors (named after the first three members of the family: GIBBERELLIC-ACID INSENSITIVE (GAI), REPRESSOR of GAI (RGA) and

SCARECROW (SCR)) are well known to be involved in the regulation of root architecture (Hirsch and Oldroyd, 2009; Heo et al., 2011; Bolle, 2015).

In legumes the GRAS transcription factors *NSP1* and *NSP2* play an important role in the nodulation process (Kaló et al., 2005; Smit et al., 2005; Eckardt, 2009). Part of their role is in regulating genes that regulate the de-oxygenated environment that is required for nitrogen fixation to occur. *NSP2* has been found to be a pivotal gene for successful nodulation, with *nsp2* mutants unable to signal for infection thread initiation and also exhibit a reduction in deformation of the root hair (Figure 5) (Oldroyd, 2003; Kaló et al., 2005, 2005; Heckmann et al., 2006) (Kaló et al., 2005; Heckmann et al., 2006). also show a complete block of expression of EARLY NODULIN-11 (*ENOD11*) one of the key initial genes in Nod-factor detection, pre-infection, and infection in legumes (Journet et al., 2001). NSP2 has been shown to have a putative homolog in *A. thaliana* called ARABIDOPSIS THALIANA SCARECROW-LIKE 26 (AtSCL26), which is a GRAS protein within the *A. thaliana* genome that shows the greatest similarity to NSP2 (Kaló et al., 2005).

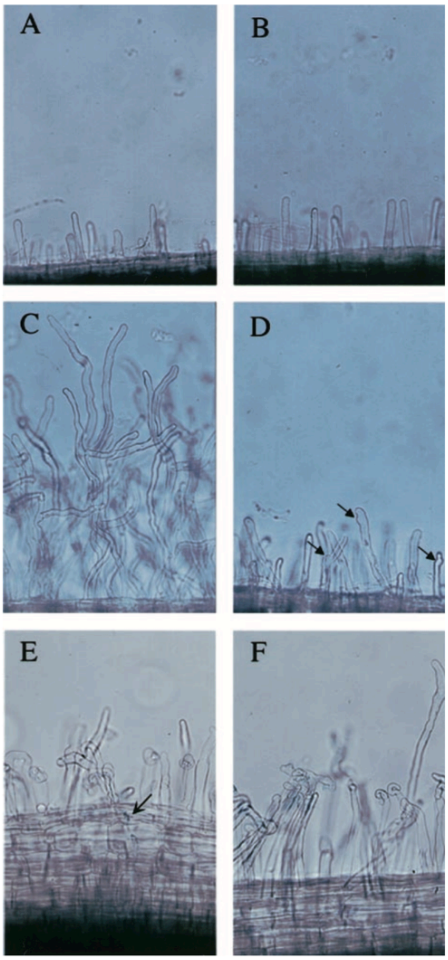

Figure 5: Nod factor induced root hair deformation is reduced in *nsp2* mutants. Root hairs of wild-type and *nsp2-2* mutants exhibit no difference in phenotype when grown in the absence of Nod factor (A,B). Roots supplemented with Nod factor to simulate the presence of suitable bacteria (C,D) show root hair deformations in WT (C) which are significantly reduced in *nsp2-2* mutants (indicated by arrows) (D). When roots were infected with *Sinorhizobium melliloti* both wild-type and *nsp2-1* exhibited root hair deformations (E,F) however only the wild-type showed evidence of an infection event (E, indicated by arrow) (Oldroyd, 2003).

1.10 Links between NSP2 and dimerisation partner NSP1, with putative orthologs in Arabidopsis, AtSCL26 and AtSCL29

As discussed earlier in this chapter, in *M. truncatula NSP2* and *NSP1* are expressed during the initial steps involved in the nodulation pathway, downstream of CCamK. NSP1 encodes for a GRAS protein which binds to the promoter region of EARLY

NODULIN 11 (ENOD11), a protein pivotal in the formation of nodules, however NSP1 must heterodimerise with NSP2 to successfully bind to ENOD11. Although both NSP1 and NSP2 (putatively) encode for GRAS protein, they are not similar in sequence, only showing a 17% similarity (Smit, *et* al, 2005). Both genes however do have homology in other species; in Arabidopsis the NSP1 putative homolog is AtSCL29 (Smit, *et al*, 2005) and the putative NSP2 homolog is AtSCL26 (Kaló *et al*, 2005. Until now very little is known about the functions of either AtSCL26 or AtSCL29, other than that they are both assigned to the GRAS family of putative transcription factors.

1.11 The diverse role of flavonoids in plants

Flavonoids are an important group of secondary metabolites that provide a diverse range of functions to plants depending on their chemical structure. They can be divided into 9 distinct subclasses of flavonoid: chalcones, flavones, flavonols, dihydroflavonols, flavandiols, anthocyanins, proanthocyanidins, isoflavonoids, and aurones. The biosynthesis of flavonoids begins with the phenylpropanoid pathway where PHENYLALANINE AMMONIA-LYASE (PAL) catalyses phenylalanine to *trans*-cinnamic acid which is then catalysed to 4-Courmaroyl-CoA by CINNAMIC ACID 4-HYDROXYLASE. 3-Malonyl-CoA is a product deriving from the carboxylation of acetyl-CoA by the ACETYL-COA CARBOXYLASE (ACC), These two compounds create naringenin chalcone through a Claisen condensation reaction which is catalysed by the enzyme CHALCONE SYNTHASE (CHS). There is then a branching to form either isoflavonoids (not present in *A. thaliana*) or flavonoids (Figure 6).

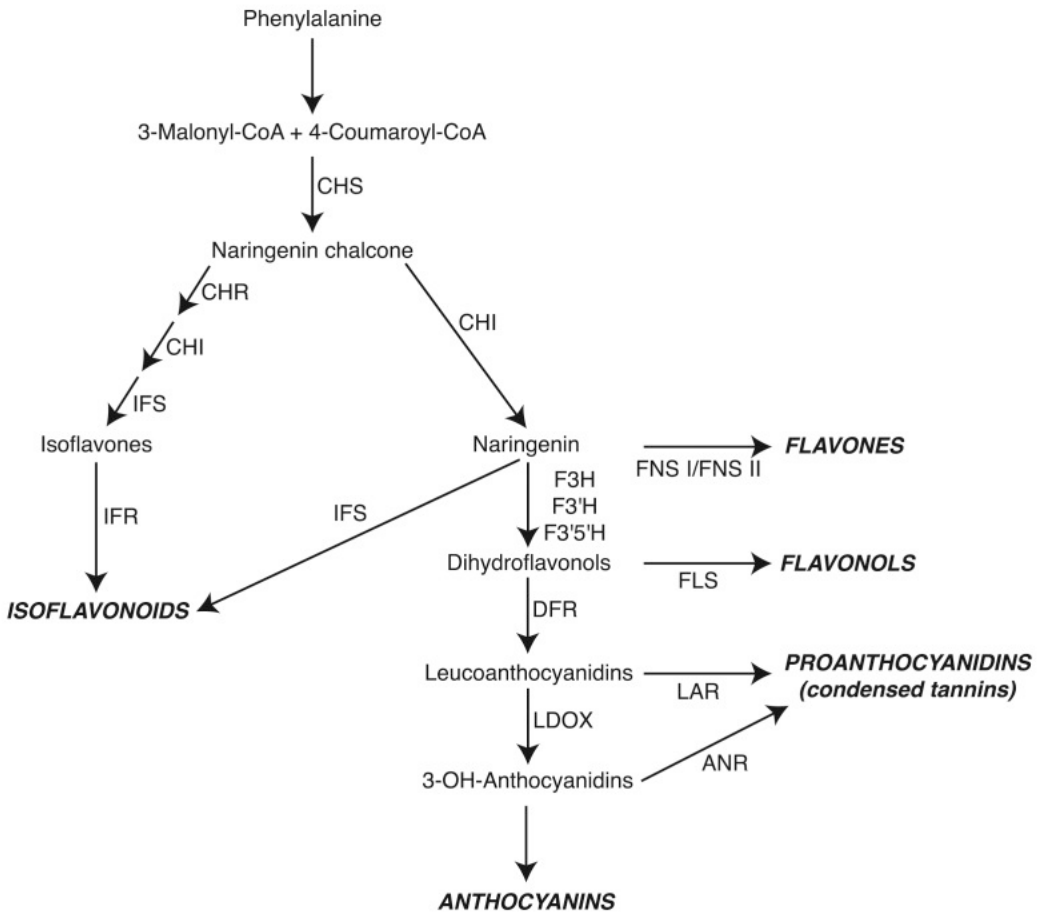

Figure 6: The flavonoid biosynthetic pathway. Naringenin chalcone can be directed towards either isoflavonoid biosynthesis through a cascade of enzymatic reactions with catalytic enzymes, or into the synthesis of other major groups of flavonoids such as flavones, flavonols, anthocyanins, and proanthocyanidins**.** The diagram shows the critical enzymes which are involved in the production of these metabolites and at which point they are introduced to the pathway: chalcone reductase (CHR); chalcone isomerase (CHI); isoflavone synthase (IFS); isoflavone reductase (IFR); flavanone-3-hydroxylase (F3H); flavonoid-3'-hydroxylase (F3'H); flavonoid-3',5'-hydroxylase (F3',5'H); dihydro-flavonol reductase (DFR); flavone synthase (FNS); flavonol synthase (FLS); leucoan-thocyanidin dioxygenase; (LDOX); leucanthocyanidin reductase (LAR); anthocyanidin reductase (ANR), (Abdel Lateif, *et al*. 2012).

The diversity of the flavonoids underlies the diversity of processes and roles that they have been found to play in plant development. Flavonoids are a key player in successful nodulation in plants as they are chemo-detected by rhizobia that release Nod factor as part of molecular communication with legumes during establishment of

nodulation. Legumes have a unique branch of flavonoids, called isoflavonoids which are involved in pathogen detection and the initiation of symbiotic pathways. This has been documented to have occurred due to the legume producing a novel isoform early on in the flavonoid pathway, isoliquiritigenin, by CHALCONE REDUCTASE (CHR) acting in combination with CHALCONE SYNTHASE (CHS). The enzyme CHALCONE ISOMERASE (CHI) in legumes has a preference for isoliquiritigenin over the non-legume version liquiritigenin as a substrate, which is converted into isoflavonoid by ISOFLAVONOID SYNTHASE (IFS) (Liu, C-W., Murray, J.D. 2016). Flavonoid biosynthesis is known to be important in nitrogen starvation responses during root development (Peng et al., 2008) and thus it can be hypothesised that transcription factors that control nodulation and lateral root development could also regulate flavonoid biosynthesis.

1.12 Cell sorting in plants can be used to isolate cell types of the root for study

Due to the highly cell type specific nature of lateral root developmental and nodulation, methods that enable investigation of processes within particular cells is crucial. Fluorescence Activated Cell Sorting (FACS) flow cytometry in plants has becomes a valuable tool in investigating cell-type specific expression differences and is very useful for doing this in response to differing experimental conditions (Birnbaum et al., 2005; Carter et al., 2013). In plants, FACS is carried out using protoplasts (from which the cell wall has been digested), with live cells identified based on forward scatter (size) or side scatter (cell surface profile) parameters. In order to detect, differentiate between and isolate cell types, florescent markers expressed under the control of cell-type specific promoters are commonly employed.

FACS involves the introduction of a sample into a fluidics system controlled under negative pressure to produce a steady stream. The sample is hydrodynamically focussed and vibrating plates resonate to break the sample line up into droplets, ideally each containing an individual protoplast. Each droplet is interrogated by a specific laser which will excite any fluorophores contained within the droplet/protoplast, and sensors are used to detect the emission wavelengths. The FACS user can then set the machine to apply a positive or negative charge droplets based on their emission spectra. Charged droplets are then deflected into collection receptacles (Figure 7) (Carter et al., 2013).

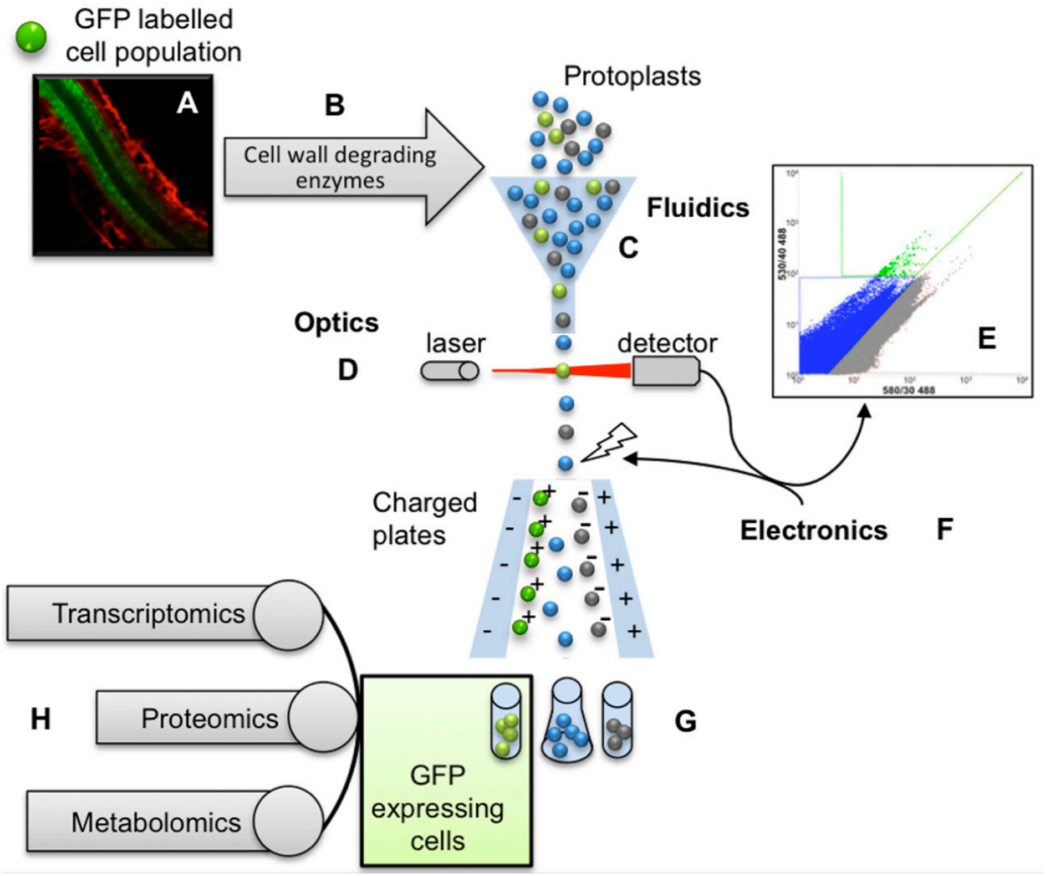

Figure 7: The workflow of a FACS cell sorter. Protoplasts from plant tissue (in this case carrying a transgenic fluorescent reporter) are generated (A,B) and introduced into the fluidics system of the FACS machine (C). Laser light is used to excite fluorophores within protoplasts, or cell material, then the emission wavelength from reflected or transmitted light can be detected (D). Gates can be chosen to capture or

omit protoplasts (or events) with particular profiles (E). The selected droplets containing protoplasts within each gate range are then charged, leading to them to being deflected into chosen collection receptacle (F,G) for analysis (H); Carter *et al* (2013).

The study of roots FACS has been used in a range of experiments, for example Gifford *et al* (2008) utilised FACS to isolate specific cells from *A. thaliana* whole root samples to assess the influence of N on a transcriptomic level in specific cell lines and were able to demonstrate that there were previously undetected vast cell type specific responses. Walker *et al* (2017) focussed on analysing *A. thaliana* cortical and pericycle cells after a nitrogen treatment over a 48 hour timeseries, to ask how nitrogen controlled early stages of lateral root development regulation, and how different nitrogen responses were shared between different cells. Brady *et al* (2008) used FACS to develop a map of all cell types of the root.

1.13 Aims and Objectives

The aims of this project are to establish the role of the GRAS family transcription factor *AtSCL26* in *A. thaliana* and to determine if the functions of *AtSCL26* are N-dependent. *AtSCL26* is the putative ortholog of *NSP2*, a pivotal gene in nodulation. Comparing the functions of these genes will enable us to investigate the molecular mechanism and possible evolutionary links between nodulation and lateral root development. Given that there are already elements of signalling in common between nodulation and lateral root development, as well as common regulation by hormones such as cytokinin, it is possible that nodulation-like responses could be activated in non-legumes if genes involved in lateral root development are altered. This would offer new insights into the ancestral links between these pathways.

1.13.1 Evaluate the *atscl26* phenotype

Phenotypic comparison between Col-0 and two *atscl26* mutants grown on deplete and replete N-supplemented agar plates will be carried out (Chapter 3). The metrics that will be measured during this analysis will be PR length, LR length, LR number, and total LR length. This data will determine if there are any developmental differences in phenotype but also determine if these phenotypes vary depending on the mutant allele or are N-dependant.

1.13.2 Establish the protein localisation pattern of AtSCL26

To understand the role that *AtSCL26* plays, and also to investigate links with the putative ortholog *NSP2*, analysis of the expression pattern and localisation of AtSCL26 will be carried out. This will determine if the AtSCL26 protein is nuclear localised, following the hypothesis that it acts as a transcription factor, similar to the role that NSP2 plays (Chapter 4). Stable transformation in *A. thaliana* and transient transformation in *Nicotiana tabacum* of GFP-tagged AtSCL26 protein will be used to generate plants that will be analysed using confocal microscopy. This will enable visualisation of where the protein localises within the cell.

1.13.3 Carry out an N-treatment transcriptomic experiment of *atscl26* mutants to investigate possible cell type and root development molecular effects of AtSCL26

Microarray analysis will be used to ask if there is any differential gene expression between *atscl26* mutants and wild-type plants, suggestive of *AtSCL26* controlling the

levels of other genes. An experimental treatment space where nitrogen form and amount is varied will be used to help to ascertain if *AtSCL26* functions vary upon nitrogen level, and thus if there is a N effect. These transcriptome expression profiles will be combined with existing microarray data from sorted epidermal and cortical cell types. The identified differentially expressed genes in *atscl26* mutants will be compared to the Col-0 (wild type) to identify transcriptomic changes based on the presence of *AtSCL26* in N-deplete and N-replete conditions. This will help to determine the molecular mechanisms that *AtSCL26* is involved in. By analysing gene expression variation it will be possible to investigate the function of *AtSCL26* in regulating pathways involved in both root responses to nitrogen in non-legumes, and nodulation in legumes, such as the isoflavonoid/flavonoid biosynthesis pathway.

Chapter 2 Materials and Methods

2.1 Plant growth methods

2.1.1 Plant material

All experiments which used the model organism *Arabidopsis thaliana* used seeds from the Columbia (Col-0) ecotype, unless otherwise stated. This ecotype was also the background for any transgenic lines generated in the lab. Two allelic mutants of the AtSCL26 gene (At4g08250) were used in this project; AtSCL26-1 (SALK_042542) which contains a tDNA insertion 797bps upstream of ATG within the putative promoter region, and AtSCL26-2 (SALK_07660) which contains a tDNA insertion 100bps downstream of the gene within the putative UTR. *Arabidopsis thaliana* seed sterilisation

2.1.2 *Arabidopsis thaliana* growth on agar plates

Seeds were aliquoted into 1.5ml Eppendorf tubes (Eppendorf, Hamburg, Germany) for sterilisation. 750µl 100% ethanol was added to the tube and left for 5 minutes, with regular agitation (inversion of the seeds was avoided where possible so that no seeds were lost into the tube cap). After the 5 minutes had elapsed, the ethanol was removed, and the seeds were then washed again in 750µl of a 10% bleach plus Tween solution (approximately 5µl Tween per 750µl solution). The seeds were agitated as with the ethanol wash. The bleach solution was carefully removed, and the seeds were then washed 4 times with sterile de-ionised water. The seeds were then stored in 200µl of sterile de-ionised water before being sown.

After sterilisation, sterilised seeds were sown onto nutrient-supplemented agar plates. The sterilised seeds were then sown directly onto the plates; where it was necessary to move the seeds between plates during growth, the seeds were sown on

0.7mm strips cut from sterile growth pouches (CYG™ Germination Pouch, West St. Paul, MN, United States).

For experiments where it was necessary to specify the concentration of nitrogen, a growth medium containing 10x basal MS liquid media (M0529 micronutrients only, Sigma-Aldrich) was supplemented with the required concentration of either NH_4NO_3 or KNO_3 (concentrations used in this project were 0.05mM NH_4NO_3, 0.3mM NH_4NO_3, 0.1mM KNO_3, 1mM KNO_3 or 5mM of both NH_4NO_3 and KNO_3), as well as 750mM $MgSO_4$, 625mM K_3PO_4, 30mM sucrose. The media was pH adjusted to 5.7 using KOH and 1% Phytoagar (Duchefa Biochemie, Netherlands) was added prior to autoclaving. Once cooled (~60°C) the media was supplemented with filter-sterilised $CaCl_2$ (1.5M) then poured into 10cm^2 square plates (~50ml per plate). The plates were wrapped in cling film to keep them sterile and stored at 4°C until they were used.

For germination where the N concentration did not have to be varied, 1 x or 0.5 x Murashinge and Skoog (MS) salt and vitamin mix (Sigma-Aldrich, cat. number M5524) and 30mM sucrose was used as the growth medium; 1% Phytoagar was added and the solution was autoclaved before being cooled and poured into plates.

2.2 Nucleic acid techniques

2.2.1 5% Chelex genomic extraction

Leaf tissue (approx. 4mm^2) was collected into a PCR tube. 150µl of a 5% Chelex solution (150µl sterile H_2O with 5% Chelex powder) was then added to each tube and the tissue was homogenised using a yellow pipette tip. The samples were then vortexed for 5 seconds, incubated in a thermocycler at 99°C for 5 minutes and vortexed for 5

seconds again. 100µl of the supernatant was collected and transferred to a fresh tube. The samples were diluted 1/100 and stored at 4°C until use (-20°C for long-term storage).

2.2.2 Edwards genomic DNA extraction

This technique was used as rapid way to obtain genomic DNA from entire seedlings for use in genotyping. The seedling was ground in a microfuge tube (0.5µl) with a sterile 200µl pipette tip for approx. 10-15 seconds. 400µl of Edwards buffer (200mM Tris-HCl pH 7.5, 250mM NaCl, 25mM EDTA pH 8.0, 0.5% SDS) was then added and the samples was ground briefly to clear any tissue from the pestle. The sample was the vortexed for 5 seconds and spun on a benchtop microfuge for 1 minute at full speed. 300µl of supernatant was transferred to a fresh tube and 300µl of isopropanol was added. The solution was left at room temperature for 2 minutes and then spun again at full speed in a microfuge. The supernatant was discarded, and the pellet was allowed to air dry for 10-15 minutes. The pellet was then re-suspended in 25µl TE then 1µl or a 1/20 dilution used as the template for PCR genotyping.

2.2.3 RNA extraction

RNA was extracted using the Monarch® Total RNA Miniprep Kit. 10-day old Seedlings were picked from phytoagar plates and flash frozen in liquid nitrogen (N_2(l)) or roots were removed into a RNase free 2ml Eppendorf and flash frozen; samples were stored at -80°C. For RNA extraction the protocol from the Monarch® Total RNA Miniprep Kit was followed, including the suggested DNase treatment, with no alterations or amendments to an end volume of 30µl. RNA samples intended for use on microarrays were sent for bioanalysis (Aglient 2100 Expert Bioanalyzer,

DE23101786) within the Warwick School of Life Sciences Genomics facility for quality assessment prior to use for microarray work.

2.3 Polymerase Chain reaction (PCR) and gel electrophoresis

2.3.1 PCR using the Gel Red method for genotyping

For each PCR reaction for genotyping a total volume of 20µl (12.9µl H2O, 4µl 5xGelRed enzyme and buffer mix (Biotum, CA, USA), 1µl forward primer, 1µl reverse primer, 0.1µl Taq and 1µl gDNA template) was used from a prepared master-mix. The PCR thermocycler varied depending on the optimal TM of the primers used. tDNA mutant genotyping for the *atscl26-1* and *atscl26-2* lines was carried out using PCR as recommended by The Salk Institute of Genomic Analysis (Alonso et al., 2003). Two parallel reactions were set-up, the first using a left border primer designed against the AtSCL26 gene and a right border primer designed against the AtSCL26 gene to yeild a product in WT and heterozygous lines. The second reaction used the LBb1.3 primer of the tDNA insert (ATTTTGCCGATTTCGGAAC) and the right border primer of the the AtSCL26 gene, to identify a tDNA product (see Table 1).

Table 1: Primers used for mutant genotyping

Genotype	Primer Name	sequence	Tm
	LBb1.3	ATTTTGCCGATTTCGGAAC	51.5
atscl26-1	SALK_042542_LP2	TCTGATCACTCATGGACCTCC	55.8
	SALK_042542_RP2	ATTTGCTGAGCAGACAGAACC	55.5
atscl26-2	SALK_076600_LP1	CAATGCATTCAGCACATCATC	52.6
	SALK_076600_RP1	CGATTCTGAGACGATTTCGAG	53

2.3.2 PCR using the Phusion High Fidelity PCR method for generation of fragments for cloning

For each PCR reaction to amplify products for cloning a total volume of 20µl (12.4µl H_2O, 4µl 5xPhusion HF buffer, 0.4µl 10mM dNTPs, 1µl 20µM forward primer, 1µl 20µM reverse primer, 0.2µl Phusion Taq (Thermofisher) and 1µl gDNA template) was used from a prepared master-mix. The PCR thermocycler varied depending on the optimal TM of the primers used **Table 2**.

Table 2: Primers used in the extraction of genomic amplicons for cloning (A) and primers used for PCR to clone the amplicon into the destination vector (B).

A

Primer name	Primer sequence	Tm (Phusion)	Amplicon size		Gene name and identification
pAtscl26F	CACCGTACAAACCAACCTGTTGGGTT	73.6	987	2439	*Atscl26* (NSP2 homolog) At4g08250
pAtscl26R	GGTCATGCAGGTAAAAATGAAGAAACGG	72.7			
AtSCL26_F	CACCATGAATTATCCTTACGAGGACTTCTTGG	73.6	1452		
AtSCL26_R_STOP	TTACTGATTCGTCTGGCACGAGGC	73.2			
AtSCL26_R_ALANINE	GGCCTGATTCGTCTGGCACGAG	75.4			

B

Primer name	Primer sequence	Tm (Phusion)	Amplicon size	Amplicon in destination vector
patscl26_end_F	AGGACCACAGGTTGTTCGAC	60.01	427	p26 in pBGWFS7
eGFP_beginning_R	gctgaacttgtggccgttta	61.2		
gatscl26_end_F	TACCAACCGTTGTCAAGCAA	60.15	375	p+g26 in pBGWFS7
eGFP_beginning_R	gctgaacttgtggccgttta	61.2		
gatscl26_end_F	TACCAACCGTTGTCAAGCAA	60.15	375	g26a in pK7FWG2
eGFP_beginning_R	gctgaacttgtggccgttta	61.2		
gatscl26_beginning_R	ACTAACCCCATCAGCCACAG	59.99	1055	g26s in pK7WGF2
eGFP_end_F	acgtaaacggccacaagttc	60.04		

2.3.3 Agarose gel electrophoresis for examination of nucleic acid concentration and fragment size

A 1% agarose gel was made by dissolving agarose powder (Sigma-Aldritch, St Louis, MO, USA) in 1X TAE buffer (0.04M Tris acetate, 0.001M EDTA pH8) by autoclaving. 0.0004ug/ml GelRed™ Nucleic Acid Stain (Biotum, CA, USA) was added after cooling. Gels were prepared with a thickness of approximately 10mm in

owl molds (Autogen bioclear, Santa Cruz, CA, USA), and submerged in tanks containing 1xTAE buffer. Samples that were obtained though the GelRed PCR system already contained loading dye and were able to be loaded directly into the wells. Samples which were prepared from the Phusion High Fidelity system were loaded after the addition of 3µl 6x orange loading dye. Gels were run at 100volts at room temperature for approximately 60mins, or until the samples had sufficient separation of the fragments for analysis. 0.5µg of either 1Kb or Log2 ladder (NEB, Beverly, MA, USA) was used as a size and concentration marker (according to manufacturer's guidelines) for DNA or RNA fragments.

2.4 Cell sorting and isolation of specific cell types

Protoplast generation and Fluorescence Activated Cell Sorting. Thee replicates of 9-day-old seedlings were subjected to N treatment, their roots were harvested for protoplast generation, then GFP/YFP cells were isolated on a BD Influx FACS (BD) directly into Qiagen RLT lysis buffer containing 1% (v:v) β-mercaptoethanol which was held at -80°C for RNA extraction (methods according to (Gifford et al., 2008)).

2.5 Microarray hybridisation methods

2.5.1 Epidermis, cortex and pericycle KNO_3-treatment experiment

Data for epidermis and cortex was already available from Lagunas *et al* (In Prep) in this thesis the experiment to generate pericycle data was carried out.

5µg of NuGEN-amplified cDNA from each of the individual cell types was labelled with Cy3 dye for single channel microarray analysis and 4µg of this was hybridized to the array following Nimblegen protocols. Roche-NimbleGen 12x135k

(Roche Applied Science, Upper Bavaria, Germany) NimbleGen microarrays, custom designed for the TAIR10 *Arabidopsis thaliana* genome annotation (Design ID OID37507; see GEO series GSE58046), were used. The arrays were imaged using the MS 200 microarray scanner (480 nm laser) using the autogain feature of the NimbleScan software. Grids were initially automatically aligned and then manually verified. Raw probe (xys) and gene level unnormalized data were obtained using NimbleScan.

2.5.2 Whole root NH_4NO_3- treatment microarray experiment

200 ng of RNA was used for cDNA synthesis and Cy3-labelling using the Low Input Quick Amp Labeling Kit for One-Color Microarray-Based Gene Expression Agilent analysis. 1.65 µg of linearly amplified and labelled cDNA was hybridized for 17 h at 65ºC on 4x44k format 60-mer oligonucleotide probes designed against the *Arabidopsis thaliana* TAIR10 genome annotation (Agilent design ID = 021169). Each array contained a single probe for 44,000 transcripts. Arrays were imaged using an MS200 microarray scanner using only the 480 nm laser using the autogain feature of the NimbleScan software.

2.6 Cloning techniques

Amplicons were created from gDNA using directional cloning and primers designed to create a TAA overhang at the 5' end of the sequence following the pENTR™ Directional TOPO® Cloning Kit (Invitrogen, Waltham, MA, USA) manual (Figure 8). These sequences were ligated into the pENTR/D-TOPO vector and transformed by heat shock into One Shot™ TOP10 Chemically Competent *Escherichia coli* (*E. cole*)

(ThermoFisher Scientific [cat. number c404010], MA, USA) following the protocol provided by the manufacturer. Cells were then spread onto Luria broth agar plates (LBA) containing 25µg/ml kanamycin as a selective agent.

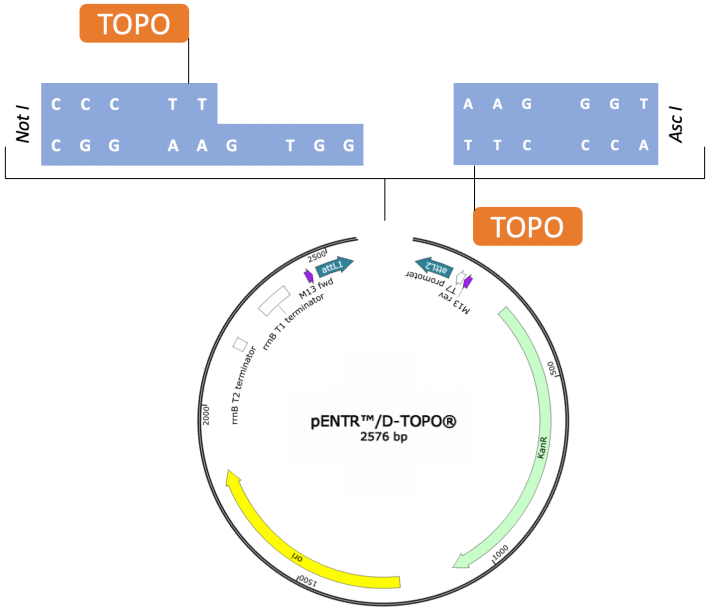

Figure 8: The pENTR/D-TOPO empty vector. At the multiple cloning site there is a 3' antisense overhang needed for successful ligation of the PCR product which contains a 5' CACC sequence at the 5' end of the primer.

Colonies able to grow with antibiotic selection were inoculated into 5ml Luria Broth (LB) (1% tryptone, 0.5% yeast extract, 0.5% NaCl; pH7) containing 25µg/ml kanamycin and incubated at 22°C for 24hrs. After a further 24 hours at 22°C the plasmid DNA was extracted from 3ml of the sample using the QIAprep Spin Miniprep Kit (Qiagen, Germany) following the manufacturer's instructions.

Plasmid DNA was sent for Sanger sequencing (GATC) using the M13 primers provided in the TOPO kit. Sequences were analysed in DNAStar and also in Snapgene. Samples that returned a correct sequence were then selected for transformation into

destination vectors. This was completed using the Gateway Cloning® with Clonase® II (Invitrogen, Waltham, MA, USA) system. The plasmids underwent an LR reaction whereby the amplicon that had been cloned into the pENTR/D-TOPO vector was ligated into a new destination vector which a florescent GFP marker (Figure 9). These vectors were transformed by heat shock into DH5α *E.coli* cells, cultured on LBA or LB then plasmids extracted, and plasmid DNA sequenced as described above.

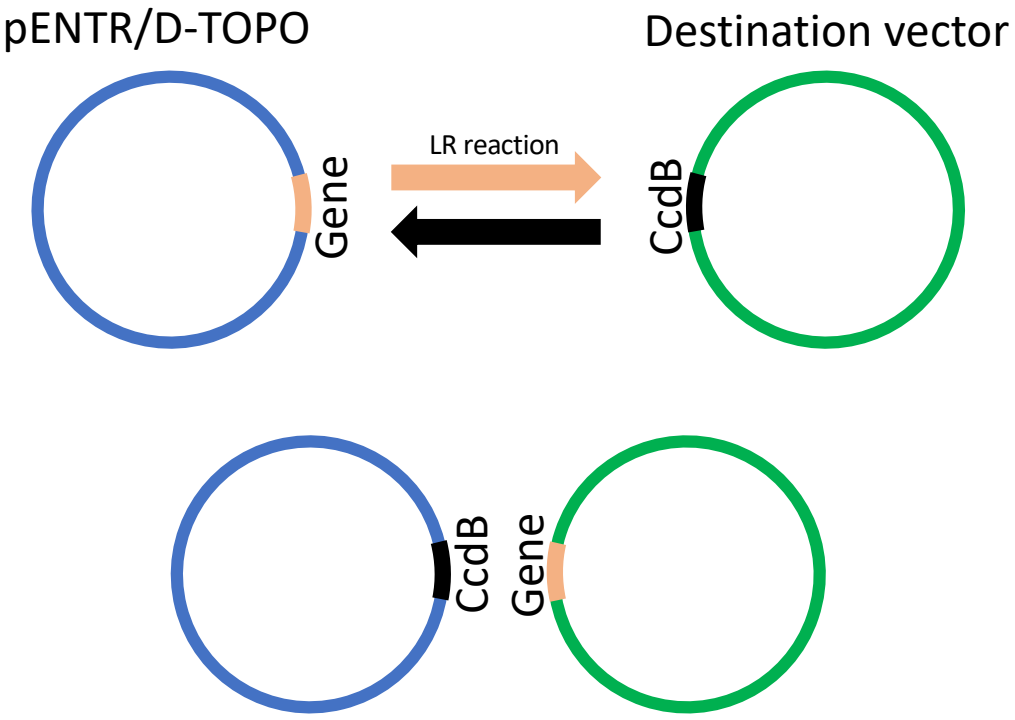

Figure 9: Gateway cloning methodology. The transfer of the gene amplicon (pink) located on the pENTR/D-TOPO vector (blue) with the CcdB gene (black) position on the destination vector (green).

2.7 *Agrobacterium tumefaciens* transformation using electroshock

2µl of destination vector was introduced to a 50µL *A. tumefaciens* aliquot that had been removed from -80°C and allowed to thaw on ice for 2mins. The cells were then gently agitated using a pipette before being transferred to an electroporation cuvette (CellProjects, Geneflow). A micropulser (Heidolph Micropulser™) was loaded with

the cuvette and set to 'Agr' (*A. tumefaciens*) for transformation. Next, 1ml of room temperature LB was added to the cuvette and the total bacterial solution was transferred to a clean labelled Eppendorf. The cells were incubated for 1hour at 28°C on a flatbed shaker (Heidolph Titrmax 1000) at 200rpm then gently pelleted (2mins at 8000rpm) and 850µl of the supernatant was removed. The cells were then resuspended to give a concentrated cell volume and spread onto a LB agar plate with appropriate antibiotics for selection (25µg/mL Kan for constructs in TOPO vector, 50µg/mL Spectomycin with 20µg/mL Gentamycin for constructs in destination vectors). Successful colonies were then inoculated into LB (plus selective antibiotics) for 24hrs at 30°C. Glycerol stocks were prepared using 850µ of 70% glycerol and 150µl inoculated LB.

2.8 Stable transformation of *Arabidopsis thaliana*

2.8.1 Col-0 seeds were sown directly onto soil (approx. 250) to germinate and then transferred to individual pots and left in long day conditions at 22°C until they began to bolt, at which point the main inflorescence bolt was cut using sterile scissors at the base. The plants were kept in 22°C conditions for a further three days at which point they were inoculated with *A. tumefaciens* transformed with destination vectors. The inoculation process involved painting the bacterial solution (overnight culture, spun down and resuspended in infiltration buffer to 10ml) onto every surface of the plant, paying close attention to the underside of the leaves, any flowers, and the wounded bolt.

The seeds were then grown on selective media to assess transformation efficiency. Seedlings were first screened from a plate containing a selective agent (e.g.

50ul/ml Kan), with around 5% transformation efficiency identified. These seedlings were propagated and 100 seeds from each plant were screened again with the same selective agent, then lines which showed a germination rate of 50% were then selected for propagation. Seedlings were selected from lines which showed a 75% transformation rate and replanted in soil for propagation.

2.9 Transient expression in *Nicotiana benthamiana*

Glycerol stocks of transformed *A. tumefaciens* were streaked onto LB plates containing selective antibiotics and left for 48 hours at 28°C. Colonies were picked and inoculated into 10ml selective liquid media and incubated for 24 hours at 28°C 200rpm. Bacterial cells were pelleted (3,000g for 8min) and resuspended in 3ml infiltration buffer (10mM $MgCl_2$, 10mM MES pH5.5). The inoculum concentration was then adjusted to OD_{600} 0.4 in 15ml of infiltration buffer. To infiltrate the leaves, the plants were watered 2 hours prior to infiltration. The inoculum was loaded into a 1mL syringe (no needle), leaves that were selected to be transformed were gently rotated to expose the underside and the syringe was pressed against the abaxial epidermis, pressure was applied by pressing a finger against the nozzle on the other side of the leaf. The infiltrated area is easily identifiable as it goes a darker colour, and a marker pen was used to permanently identify this area.

2.10 Microscopy and phenotyping

2.10.1 Flavonoid staining

A solution of diphenylboric acid-2-amioethyl ester (DPBA) (2.52mg/ml) and 0.01% Triton x-100 was applied to the 12 day old seedlings using a nasal atomiser and left

for 7 minutes before being washed with ddH_2O for a further 7 minutes. The samples were then mounted onto a slide using ddH_2O or first stained with propidium iodide (PI) (500nM) then de-stained and mounted in ddH_2O. DPBA binds to flavonoids and excites when stimulated by the 458nm laser. The emission wave length is specific to the flavonoid, however for the purposes of this investigation, to visualise all fleavenoids stained by DPBA a general GFP filter was used (530/25nm). Visualisation of flavonoids was conducted on the Nikon Omptiphot microscope.

2.11 Phenotyping analysis of root architecture

Plates of seedlings were scanned on a flatbed scanner and analysed using FIJI. PR and LR lengths were measured for each seedling and tabulated in Excel and values for PR length, LR length average, LR number and total LR length were generated. To test for statistical phenotypic differences the data was then analysed using RStudio using a two-tailed t-Test. Boxplots were drawn for root phenotypic data using the ggplot2 function in RStudio.

2.11.1 Confocal microscopy for stable and transient expression analysis

Confocal imaging of transient and stable transformations was completed on the Zeiss LSM 880 or the Zeiss LSM 710 (depending on availability) within the imaging suite at the University of Warwick. Samples were loaded onto the slide with propidium iodide (PI) (500nM) to help identify cell types. The microscopes were set-up to excite at 458 and to detect emission spectra that covered GFP emission wave lengths (530/25 nm).

2.12 Microarray analysis

Image (tiff) files were imported into the Agilent Feature Extraction software for quality control assessment, grid alignment and expression value extraction at the probe and transcript level the RMA algorithm (Tai and Speed, 2012) used to carry out background subtraction, quantile normalization and summarization via median polish, and output $\log_2$ normalized gene expression levels.

For whole root data the Linear Models for Microarray Data (package *limma* in R) was then used to fit linear models to pairs of samples, identifying genes that contrasted the most between the experimental pairs (Ritchie et al., 2015).

For cell type data all genes were put through an ANOVA modeled as follows: $Y = \mu + \alpha_{\text{genotype/cell type}} + \alpha_{\text{nitrogen treatment}} + \alpha_{\text{genotype/celltype* nitrogentreatment}} + \varepsilon$, where Y is the normalized signal of a gene, μ is the global mean and treatment (intercept), the α coefficients correspond to the effects of cell type within each genotype (atscl26-2 and Col-0 epidermal or cortical cells), treatment (nitrogen) and the interaction between cell type/genotype and treatment, and ε represents unexplained variance. Transcripts were termed to be differentially expressed if they showed a Benjamini-Hochberg adjusted P-value ≤ 0.05 in the comparison between treatment and control.

Genes were than analyzed and sorted into lists that were significant based on genotype, cell-type (for KNO_3 cell specific response data) and also for N. For cell type specific data, these lists of cell specific significant responses and the list of significant DEGs due to N were then examined for genes that were present in both to identify overall N-responses.

2.13 Silhouette Plotting and GO term analysis

Genes were clustered using Pearson correlation using the clustergram function in MATLAB and cluster number chosen based on Silhouette plotting, which is an analysis method with generates a series of clusters sizes then analyses the distance between the data points of one cluster to the data points of the neighbouring cluster. A silhouette value is assigned to the cluster number between +1 if the data within the cluster are distinct from the others, and 0, which indicates that there is no distinction between clusters. This technique was used to determine the optimal number of clusters which gave the best overall values in four categories – average silhouette value of worst cluster, average silhouette value of all clusters, median of individual values, and overall average silhouette value of all individual values. After silhouette plotting in Matlab a heatmap was generated for all genes across all clusters using the Matlab clustergram function. The genes in each cluster were then analysed for GO term presence and overrepresentation using http://www.geneontology.org (Chen et al., 2006; Blake et al., 2013; Carbon et al., 2017).

Chapter 3 Phenotypic analysis of *atscl26* mutants and the effects of nitrogen on *atscl26* root development

3.1 Introduction

Investigating orthologous pairs of genes and their functions can help to develop a better idea of how the gene function has evolved in different species, and the extent to which the level of orthology or sequence conservation can be used to predict the extent of similarity of molecular function. The transcription factors *MtNSP2* and *MtNSP1* are two genes that have been previously identified to play a crucial role in Nod factor signalling and the regulation of nodulation in *Medicago truncatula*. These genes are highly conserved between a number of species, including the non-nodulating *Arabidopsis thaliana* (Kaló et al., 2005). Current research (Kaló et al., 2005) suggests that NSP2 acts downstream of both the calcium spiking and calcium-calmodulin dependant protein kinases (CCaMK) activity. It is thought to be involved in signalling for the formation of the infection thread as *nsp2* mutants are unable to form these crucial structures that are required for cortical infection and proper nodule formation.

3.1.1 The links between lateral root development and nodulation

Previous experiments have linked nodulation and lateral root formation together, including through their common regulation by phytohormones (Bensmihen, 2015). These links are important factors that support the theory that lateral root formation was the evolutionary basis of the nodulation pathway. Both of these processes involve cell dedifferentiation, induced or repressed by nutrient availability, and are under the control of phytohormones, as described in Chapter 1.

3.2 Aims and objectives

In order to ask if genes involved in nodulation also had roles in lateral root development a large study in the Gifford lab was carried out. This work used reciprocal best BLAST predictions of orthology to identify transcription factors in *A. thaliana* based on genes that controlled nodulation in *Medicago truncatula*, then asked if these genes had any roles in regulating root development. One gene of note, *AtSCL26*, the putative ortholog of *NSP2*, was found to have a putative nitrogen-related root phenotype (Lagunas et al, 2019 In Prep). The aim of this chapter was to characterise two *atscl26* mutants and thus investigate if *AtSCL26* plays a role in root development in a non legume.

3.3 Results

3.3.1 Investigating the level of orthology between *NSP2* and *AtSCL26*

As previous research suggested that *NSP2* is highly conserved in a number of different plant species, the role of this gene in non-nodulating plants is of great interest as it could provide an insight into the possible specialisation or functional conservation of the gene. *AtSCL26* is a member of the GRAS family, so first, to study AtSCL26 in more detail, the AtSCL26 protein sequence was examined. The decision to investigate the relatedness at the protein, rather than the nucleotide level was made in order to gain achieve a more sensitive comparison that is functionally relevant.

AtSCL26, NSP2 and other NSP2-like protein sequences were obtained using a BLAST (NCBI) search, aligned and then clustered using ClustalOmega. Phylogenetic trees were created using the function available through the ClustalOmega site, using a

neighbour joining method. The comparative distance metrics for each tree were automatically generated.

Analysis of the GRAS family proteins across species reveals clustering of similar protein sequences between in *M. truncatula*, *Oryza sativa*, *Lotus japonicus*, *Glycine Max* and *A. thaliana* (Figure 10), which is consistent with previous reciprocal best BLAST analysis performed to identify potential homologs (Bolle, 2015). It is also in line with research showing that *nsp2* mutants are capable of nodulation when complemented with *NSP2* genes from other plant species (Yokota et al., 2010). *AtSCL26* was found to closely cluster with *M. truncatula* (Figure 10), suggesting that, in line with previous work (Murakami et al., 2007) they are putative orthologs.

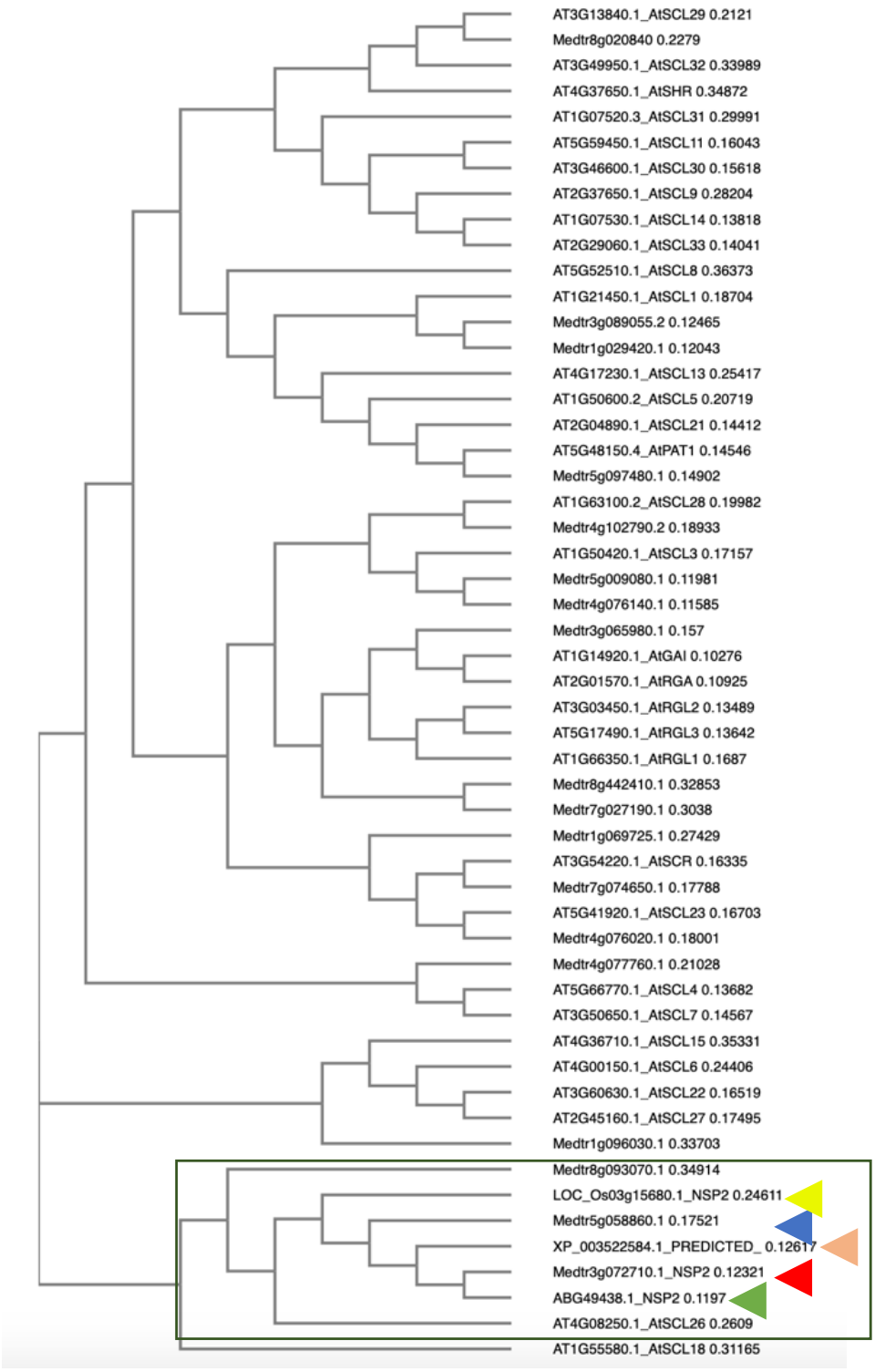

Figure 10: Phylogenetic analysis of GRAS family proteins. AtSCL26 (indicated with red arrow) clusters with MtNSP2 (indicated with a blue arrow), as well as NSP2 sequences from *Oryza sativa* (yellow arrow)), *Lotus japonicus* (green arrow), and *Glycine max* (orange arrow). Number next to each protein name indicates comparative phylogenetic distance.

To examine the specific sequences conserved between AtSCL26 and other NSP proteins from *Medicago truncatula*, *Oryza sativa*, *Glycine max*, and *Lotus japonicus*, the sequences were also aligned using Snapgene®. The alignment, using a 95% similarity threshold, showed that the genes are highly conserved within their functional groups (Figure 11). Within the GRAS gene family, the VHIID motif can be seen, however whilst this motif location is conserved between species, the sequence is only partially conserved. Substitutions have been recorded throughout the sequence, with the P-T-H-D-Q-L residues generally being conserved (Pysh et al., 1999), however AtSCL26 has an asparagine to threonine residue substitution. Conserved regions indicative of GRAS family proteins are evident including the LHR I and II domain. Together with the VHIID motif these sites have been hypothesised as a possible DNA binding site. It is thought that the VHIID motif mediates protein to DNA interactions and the LHR motifs mediating protein-protein interactions (Ellenberger et al., 1992). A nuclear localisation sequence (NLS) within this protein sequence is not evident. A NLS occurs in some but not all GRAS family proteins (Pysh et al., 1999), for example just before the LRI region in SHR (Gallagher and Benfey, 2009). It is possible that a novel NLS in AtSCL26 exists and has not been characterised yet.

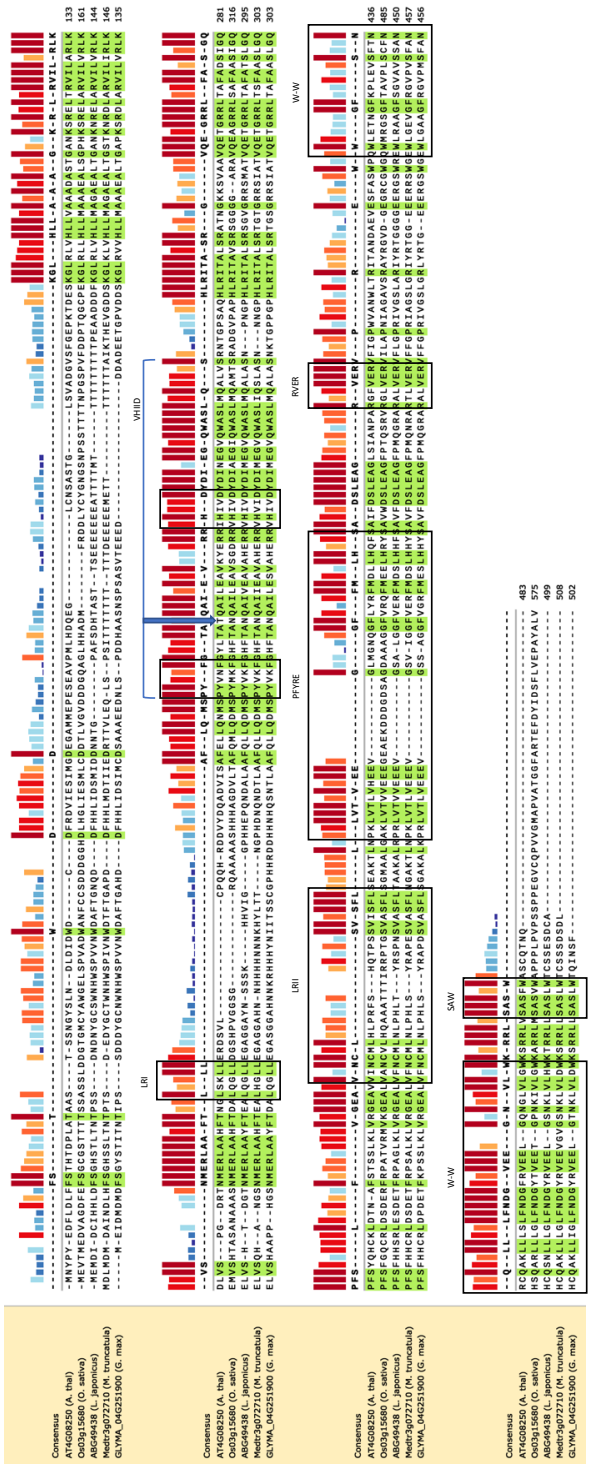

Figure 11: Protein Sequence alignment of AtSCL26/NSP2 sequences from *Medicago truncatula*, *Oryza sativa*, *Glycine max*, *Lotus japonicus* with a 95% similarity threshold show distinct conserved GRAS motifs. The VHIVD domain (blue indicator) shows a partial conservation between the aligned sequences, with conserved histidine (H) and aspartic acid residues (D) residues. The blue arrow indicates a substituted residue on the asparagine residue (N) in AtSCL26, which is otherwise conserved.

To examine the similarity of AtSCL26 with other GRAS proteins in *A. thaliana*, AtSCL26 and the 31 other GRAS protein sequences were obtained from The Arabidopsis Information Resource (TAIR) (The Arabidopsis Information Resource (TAIR), 2018) aligned and then clustered using ClustalOmega (Figure 11). Cluster relationships between SCL family members were in line with previous publications and the subfamilies were identified from (Bolle, 2004) (Figure 12). AtSCL26 does not belong to a sub-family lineage; the protein sequence is distinct from other GRAS family members. The asparagine to threonine residue substitution (Figure 11) could be the potential reason why AtSCL26 is not grouped into any of the sub families.

When the analysis was repeated with a manual change of the threonine residue to an asparagine, the tree structure remains the same, however there is a very slight decrease in the distance metric of the AtSCL26 branch from 0.26090 to 0.25853 for AtSCL26 (red triangle in Figure 10) and a shift from 0.35257 to 0.35200 (red triangle in Figure 12). This substitution therefore does not appear to be the reason for separate branching position of AtSCL26. The lack of a NLS in AtSCL26 could also be the reason why the AtSCL26 clusters apart from other GRAS proteins, but not all GRAS family proteins have an NLS so this is not certain.

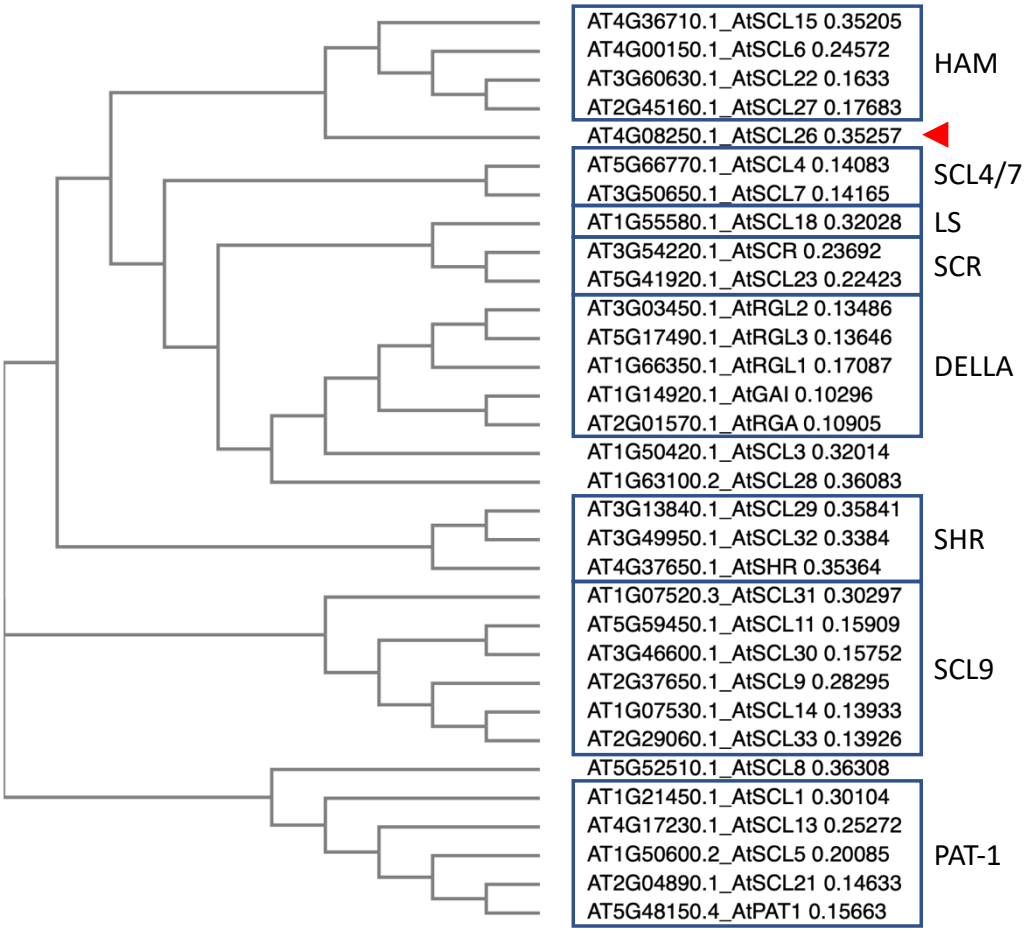

Figure 12: Phylogenetic analysis of known GRAS proteins in Arabidopsis thaliana shows grouping of sequences into the 8 sub-families. Consistent with previous literature, clustering of SCL family member sequences showing grouping of the 32 known GRAS proteins in to their 8 sub families, AtSCL26 (the putative ortholog of MtNSP2 is indicated using a red arrow). As of yet, AT4G08250, AT1G50420, and AT1G63100 are not assigned into a subfamily. Number next to each protein name indicates comparative phylogenetic distance.

3.4 Identification of mutations disrupting *AtSCL26* expression

Two putative mutant alleles of *AtSCL26*, *atscl26-1* (SALK_042542) and *atscl26-2* (SALK_076600) were selected for phenotypic analysis. *atscl26-1* was annotated as containing a T-DNA insertion in the putative promoter region, and *atscl26-2* as containing a T-DNA insertion within the 3'UTR at the end of the gene (Figure 13).

These lines were chosen as seeds were available and there were no other mutant lines which included a tDNA insertion in the coding region of the AtSCL26 gene.

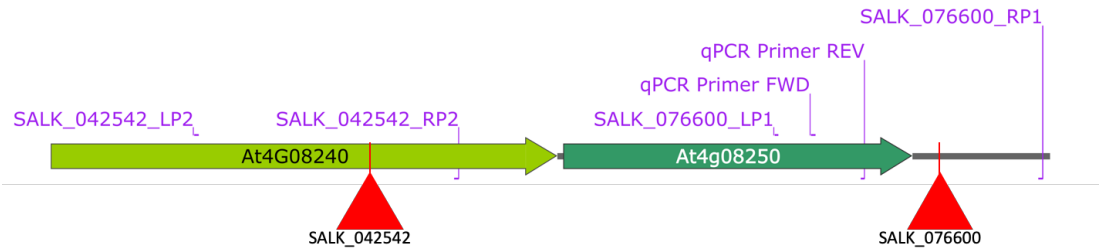

Figure 13: tDNA insertions of the *atscl26-1* mutant (SALK_042542) in the 5' putative promoter region of At4g08250, and the atscl26-2 (SALK_076600) mutant in the 3' UTR of At4g08250. The figure shows the inserted SALK mutation sequences (red), which contain the binding site for the LBb1.3 primer. The SALK_042542 tNDA is within a region of the preceding gene At4g08240, which is annotated as coding region but which also (or alternatively) is the putative promoter region for AtSCL26 (At4g08250). The binding sites of the primers used to genotype the tDNA mutants are included in lilac. The figure also shows the qPCR primer binding sites that were used to confirm that the gene was knocked out.

In order to confirm the effect of the tDNA insertions on the expression of *ATSCL26*, and to test that there is no effect of *atscl26-1* on the closely upstream At4g08240 (Figure 13), qPCR to test the expression of AtSCL26 was carried out (Figure 14) using primers that amplify a region of the 3' coding sequence of the AtSCL26 gene.

AtSCL26 expression levels were tested in roots grown on both deplete (0.1mM) and replete (5mM) levels of KNO_3; previous work had shown that *AtSCL26* is expressed more highly on low levels of nitrogen (Carter, 2013). The *atscl26-2* mutant was found to be a complete knockout, and the *atscl26-1* mutant was found to have very strong loss of expression; both are significantly different to Col-0 based on t-test analysis.

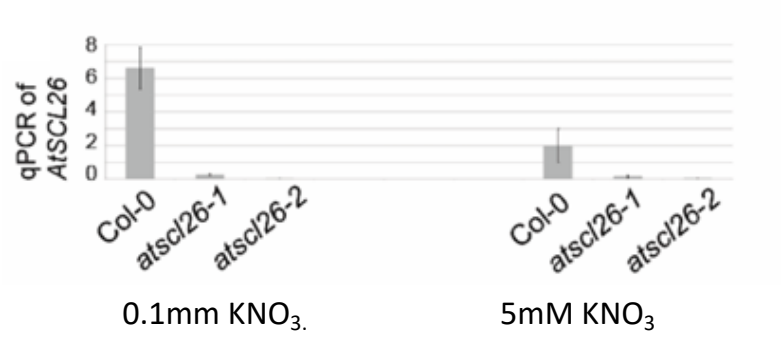

Figure 14: Analysis of *AtSCL26* expression using qPCR in the *atscl26* mutants. Relative expression of *AtSCL26* (using the reference gene At4G14960 - *Tubulin*) is shown in the two *atscl26* mutants and Col-0 wild-type, from roots harvested from seedlings grown on deplete (0.1mM) or replete (5mM) KNO_3. Expression of *AtSCL26* in both mutants is significantly different ($P<0.05$) compared to Col-0 based on t-test analysis.

3.5 *atscl26* seedlings grown on nitrogen deficient growth conditions exhibit an altered root phenotype

3.5.1 Col-0 and *atscl26* seedlings grown on varying KNO_3 levels show different root phenotypes.

In order to determine if *AtSCL26* plays a role in regulating root development, *atscl26* mutants and Col-0 wild-type were grown for 9 days on deplete (0.1mM) and replete (5mM) levels of nitrogen in the form of KNO_3 then seedling root architecture analysed. In total there were 4 biological replicates of 10 seedlings per experimental condition.

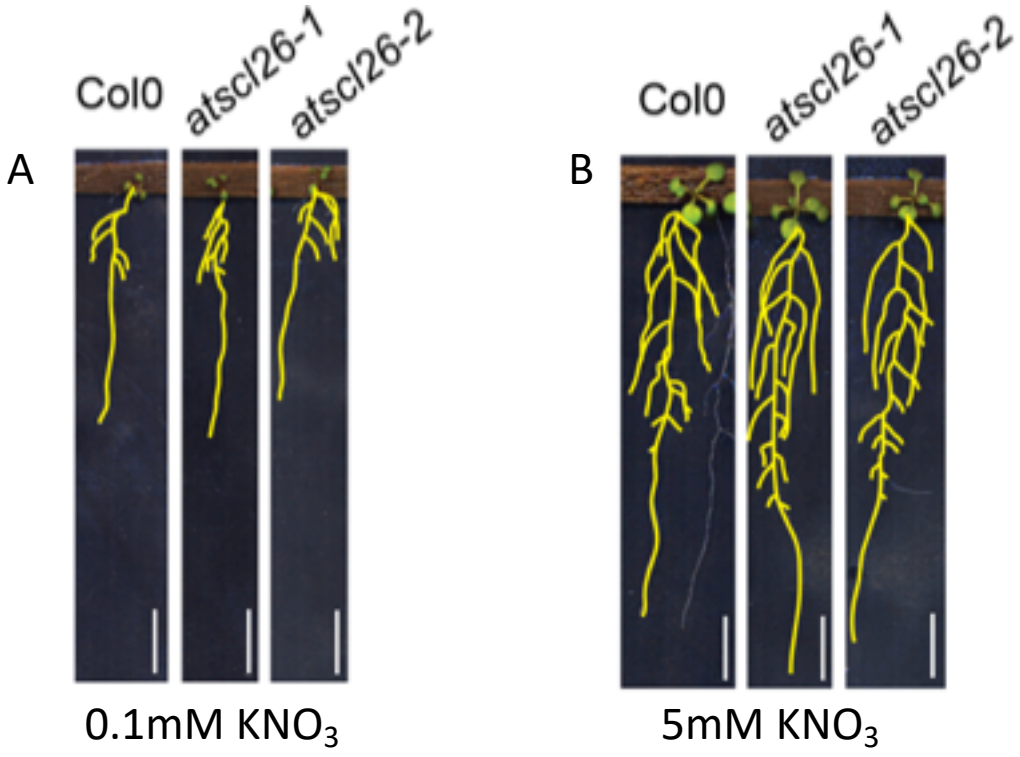

Figure 15: Representative images which show typical growth of Col-0, *atscl26-1* and *atscl26-2* mutants grown for 9 days on deplete (0.1mM) or replete (5mM) KNO_3. Roots have been drawn over with yellow to enable them to be visualised; scale bar = 1 cm.

When grown on replete nitrogen conditions *atscl26-1* and *atscl26-2* mutants both show a significant increase in the overall length of the primary root (PR) (*atscl26-1* having an increase of 0.756cm and *atscl26-2* having an increase of 0.495cm). *atscl26-1* has ~1.8 more LRs and *atscl26-2* has ~1.3 more LRs than Col-0. Total lateral root (LR) length (*atscl26-1* +1.187cm and *atscl26-2* +2.552cm) and LR number are also significantly longer when compared to Col-0 (Figure 15,Table 4); statistical analysis is based on the use of t-testing using the Wilcoxon test statistic.

There are also significant differences in PR length, LR number, and total LR length between *atscl26-2* and *atscl26-1*. *atscl26-1* mutants show a longer PR (the mean is 0.264cm longer), but shorter LR average length and total LR length than *atscl26-2* (mean of 1.365cm shorter). There is a significant increase between Col-0 and *atscl26-*

2 average LR length (increase of 0.103cm in *atscl26-2*), however *atscl26-2* also has a significant increase in growth of 0.101cm when compared to *atscl26-1* (Figure 15, Table 3A).

In deplete N conditions, *atscl26-1* mutants have a significant increase in PR length of 0.56cm, in LR number of 1.4, and in total LR length of 0.545cm (all compared to Col-0). *atscl26-2* mutants also have a significant increase in PR length of 0.651cm, in LR number of 1.5, and in total LR length of 0.615cm compared to Col-0 (Table 3).

Table 3: Root phenotypic analysis of *atscl26* mutants compared to Col-0 wild type. (A) On replete nitrogen both *atscl26* allelic mutants show a significant increase in in PR length, LR number, and total LR length. (B) In the deplete N conditions both *atscl26-1* and *atscl26-2* show a significant increase in total LR length, LR number and PR length. Root measurements were analysed using the Wilcoxon statistical test; n=40.

A

5mM KNO3

Feature Measurement	Genotype		
	Col-0	*atscl26-1*	*atscl26-2*
PR Length (mm)	60.438	67.998	65.361
LR Number	15	17	16
LR length avg. (mm)	6.906	6.932	7.941
Total LR length (mm)	104.435	116.304	129.956
LR density	0.251	0.249	0.251
Feature pval	**Genotype**		
	Col-0 - *atscl26-1*	**Col-0 - *atscl26-2***	***atscl26-1* - *atscl26-2***
PR Length	4.70E-08	5.30E-05	0.011
LR Number	0.0019	0.0099	0.5271
LR length avg.	0.87095	0.00041	0.0003
Total LR length	0.0094	2.50E-05	0.027
LR density	0.5554	0.8318	0.5228

B

0.1mM KNO3

Feature Measurement	Genotype		
	Col-0	*atscl26-1*	*atscl26-2*
PR Length (mm)	21.599	27.204	28.107
LR Number	4	5	5
LR length avg. (mm)	3.482	3.657	3.534
Total LR length (mm)	13.341	18.795	19.493
LR density	0.180	0.196	0.195
Feature pval	**Genotype**		
	Col-0 - *atscl26-1*	**Col-0 - *atscl26-2***	***atscl26-1* - *atscl26-2***
PR Length	2.00E-10	1.30E-11	0.212
LR Number	3.20E-06	3.70E-07	0.5505
LR length avg.	0.95613	0.84104	0.76718
Total LR length	1.40E-05	1.10E-05	0.7655
LR density	2.07E-03	4.41E-03	0.8293

Put together, the phenotypic results from growth on KNO_3 suggest that *AtSCL26* has an inhibitory effect on PR length, LR number, and total LR length. In replete N levels these differences become less dramatic, and the significance between lateral

root average length between *atscl26-1* and Col-0 is lost in replete conditions (Figure 16). Therefore, there is an effect of N level on the function of *AtSCL26*.

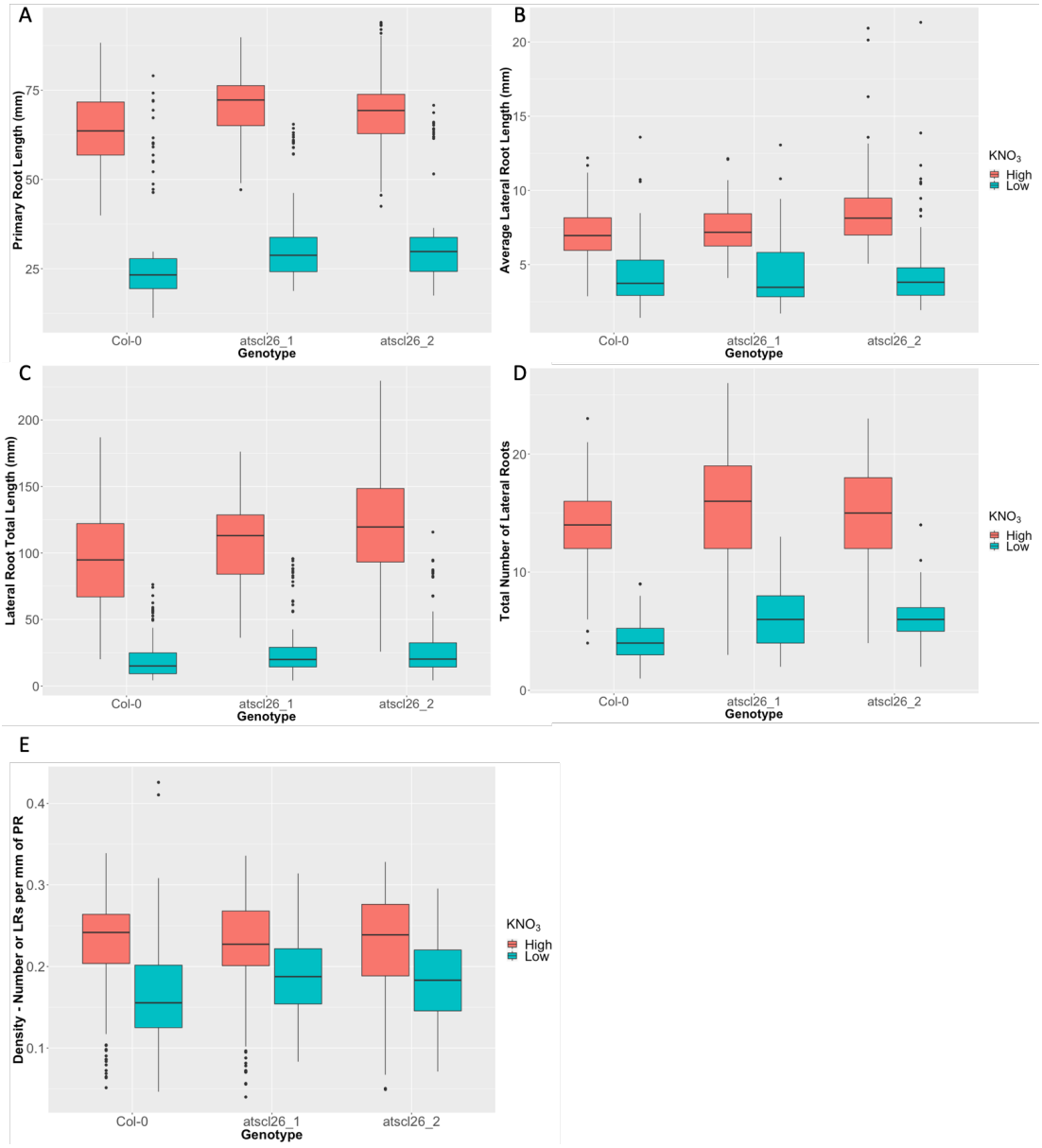

Figure 16: Root phenotype features of seedlings from on deplete and replete KNO_3. The plotted data from Table 3 showing primary root length (A), average lateral root length (B), lateral root total length (C), and total number of lateral roots (D) and lateral root density (E).

3.5.2 *atscl26* mutants grown on deplete and replete NH_4NO_3 conditions show significant root phenotypes

Since nitrogen exists in many forms, and these forms can have different effects on the plant due to regulation of different uptake and utilisation machinery (Shtratnikova et al., 2015), the effect of altering the level of *AtSCL26* expression was also examined when seedlings were grown on varying NH_4NO_3. The two *atscl26* mutants and Col-0 were grown on deplete (0.05mM), sufficient (0.3mM) or replete (5mM) NH_4NO_3 for 9 days and analysed (Figure 17). In total 4 biological replicates of 10 seeds per experimental condition were used.

On deplete NH_4NO_3, in contrast to when grown on deplete KNO_3, the *atscl26-1* mutant had a significant increase in PR length, (+0.398cm) LR number (+0.8), and total LR length (+0.220cm) compared to Col-0. *atscl26-2* was only found to have a statistical increase in PR length (+0.222cm) compared to Col-0, not any significant differences in LR parameters. *atscl26-1* has significantly more LRs (+1.1) as well as an increase in the average LR length (+0.073cm) and the total LR length (+0.333cm) compared to *atcsl26-2* (Table 3A).

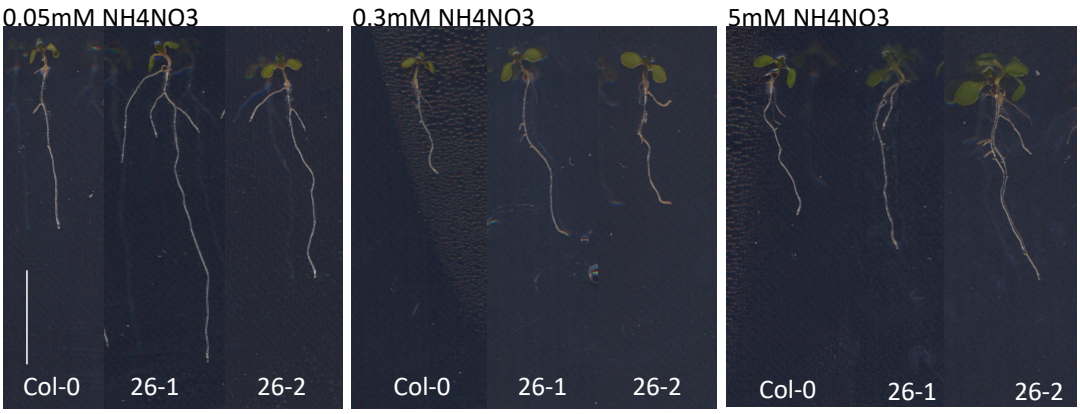

Figure 17: Phenotypic analysis of *atscl26* mutants when grown for 9 days on deplete (0.05mM), sufficient (0.1mM) and replete (5mM) NH_4NO_3 levels. Scale bar = 1cm.

On the 'sufficient' NH_4NO_3 there is a significant increase in total LR length in *atscl26-1* when compared to Col-0 (+0.163cm). Between the two mutants the only significant difference was seen in the number of LRs with *atscl26-2* having +0.5 more LRs than *atscl26-1* (Table 3B).

In replete N conditions *atscl26-1* shows a decrease in LR number (-0.4) when compared to Col-0. There were no other significant differences when comparing Col-0 to either of the mutants, or between the two mutants (Table 4C)

Table 4: Root phenotypic analysis of *atscl26* mutants compared to Col-0 wild type when grown on 0.05mM (A), 0.3mM (B) and 5mM NH_4NO_3 (C).

A

0.05mM NH4NO3

Feature Measurement	Genotype		
	Col-0	*atscl26-1*	*atscl26-2*
PR Length (mm)	10.63836089	14.62260062	12.86396296
LR Number	2.473402758	3.302631579	2.251851852
LR length avg. (mm)	1.860339508	2.1119144	1.381132716
Total LR length (mm)	4.832497537	7.035448916	3.708111111
LR density	0.232498482	0.225858017	0.175051177
Feature pval	**Genotype**		
	Col-0 - *atscl26-1*	Col-0 - *atscl26-2*	*atscl26-1* - *atscl26-2*
PR Length	3.60E-06	5.40E-05	0.84322
LR Number	0.00635	0.90106	0.00516
LR length avg.	1.44E-01	4.20E-01	0.02012
Total LR length	2.13E-03	7.36E-01	0.00642
LR density	9.92E-01	3.01E-02	0.03499

B

0.3mM NH4NO3

Feature Measurement	Genotype		
	Col-0	*atscl26-1*	*atscl26-2*
PR Length (mm)	23.76285788	22.66880921	23.38980994
LR Number	4.366609539	4.338408521	4.799049708
LR length avg. (mm)	2.153749351	2.542350245	2.321827912
Total LR length (mm)	9.270689684	10.71796303	10.89607675
LR density	0.18375776	0.191382286	0.205176943
Feature pval	**Genotype**		
	Col-0 - *atscl26-1*	Col-0 - *atscl26-2*	*atscl26-1* - *atscl26-2*
PR Length	0.15322	0.55565	0.41384
LR Number	0.71814	0.12294	0.0455
LR length avg.	0.02383	0.33762	0.25299
Total LR length	0.10159	0.03476	0.73064
LR density	0.611	0.07395	0.2371

C

5mM NH4NO3

Feature Measurement	Genotype		
	Col-0	*atscl26-1*	*atscl26-2*
PR Length (mm)	20.61227778	19.75259868	20.01418129
LR Number	3.609210526	3.190131579	3.434210526
LR length avg. (mm)	2.145651156	2.599598246	2.578229932
Total LR length (mm)	7.508962719	8.191230263	8.299057018
LR density	5.711021185	6.191781811	5.827884206
Feature pval	**Genotype**		
	Col-0 - *atscl26-1*	Col-0 - *atscl26-2*	*atscl26-1* - *atscl26-2*
PR Length	0.12576	0.25638	0.73142
LR Number	0.03018	0.34381	0.31643
LR length avg.	0.12576	0.25638	0.73142
Total LR length	0.52057	0.52057	0.94418
LR density	0.08402	0.5754	0.353

In combination, the phenotypic results from growth on NH_4NO_3 suggest that AtSCL26 has an inhibitory effect on PR length, LR number, and total LR length in deplete ammonium levels, and that this phenotype is not seen with the increase in ammonia indicating that this could be N-dependant (Figure 18)

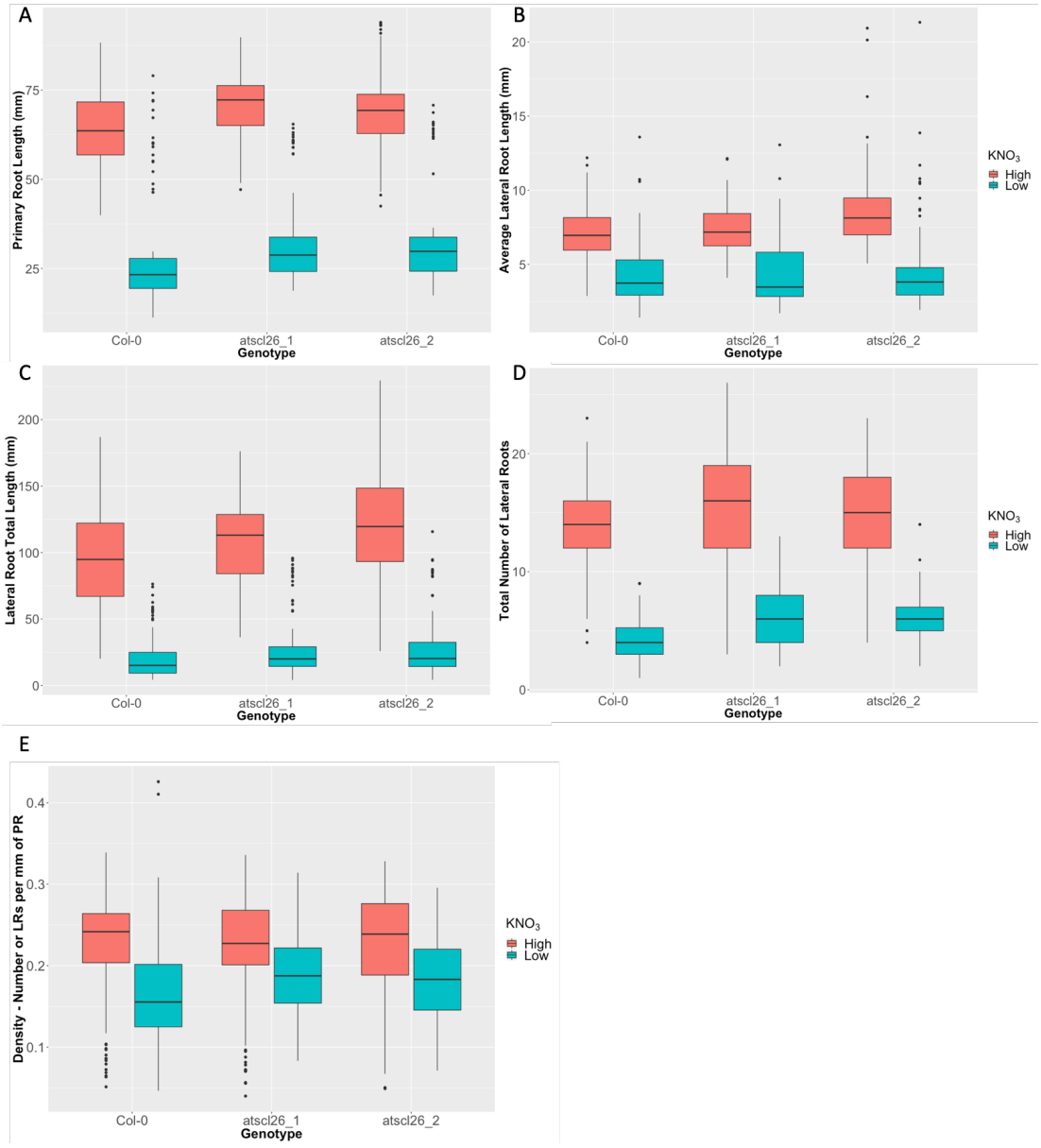

Figure 18: Root phenotype features of seedlings from on deplete, sufficient, and replete NH_4NO_3. The plotted data from Table 4 showing primary root length (A), average lateral root length (B), lateral root total length (C), and total number of lateral roots (D) and lateral root density (E).

3.6 Discussion

Within this chapter the protein sequence of AtSCL26 was analysed and compared to the NSP2 protein sequence as well as other GRAS family proteins. A number of conserved GRAS domains were identified, although a NLS was not found.

AtSCL26 appears to occur in a different phylogenetic tree branch to other GRAS proteins and reasons for this were explored. The asparagine to threonine substitution does not however appear to be the reason for separate branching position of AtSCL26. The difference however could still have a structural or functional consequence. If this were to be investigated further, then it could be of potential interest to use a method such as CRISPR-Cas9 to attempt to edit the seqeunce at this location.

AtSCL26 is N-repressed in whole roots, therefore the effect of N on *atscl26-1/2* root phenotypes was measured. The results of this investigation have shown there is an N-dependent phenotype in KNO_3-supplemented seedlings, and the main finding is that *AtSCL26* acts to repress the growth of the PR and repress LR initiation and also outgrowth. The results also showed that, comparing the two mutants, *atscl26-1* had a longer PR, fewer LRs and a decrease in LR total length when compared to *atscl26-2*.

When seedlings were grown on media supplemented with deplete NH_4NO_3 levels there is a similar phenotype to the deplete KNO_3 supplemented seedlings in that both *atscl26* mutants have an increase in PR length, LR number and total LR length. This shows that *AtSCL26* inhibits the development of PR and LRs in deplete N conditions, no matter the form of N.

When the media contained ‘sufficient’ levels of NH_4NO_3 the only phenotype was an increase in LR length average in *atscl26-1*, whereas on deplete NH_4NO_3 most

measured root parameters were greater in both mutants. There was also a phenotypic difference between the two mutants, as *atscl26-2* had an increase in LR number compared to Col-0 but the *atscl26-1* did not. The only significant difference in replete NH_4NO_3 conditions was an opposite result to growth on replete KNO_3 in that the *atscl26-1* mutant had a decrease in LR number compared to Col-0.

Previous work shows that seedlings grown on ammonia-supplemented plates have reduced PR growth, LR emergence, and LR growth, and that this is due to the absence of nitrate (Shtratnikova et al., 2015). In our experiments all genotypes (including Col-0), when NH_4NO_3- supplemented show a significant difference in phenotype compared to seedlings supplemented with nitrate alone. None of the experiments for this project used ammonia alone as a nitrogen source and so this could be carried out in future work.

The two *atscl26* mutants show some phenotypic differences which is possibly due to the two differing locations of the T-DNA mutation insert sites between *atscl*-1 and atscl26-*2*. There are many instances where allelic mutants can result in different phenotypes (allelic heterogeneity), and this has been attributed to qualitative or quantitative changes in the gene product (Hormozdiari et al., 2017). Our findings show a quantitative mRNA difference between the alleles; future work could examine if any residual AtSCL26 protein is translated and perhaps differs between the two.

In combination, the phenotypic results indicate that *AtSCL26* has both an ammonium-dependant and a nitrate-dependent effect on root development and represses growth of PR and LRs in N-deplete conditions. As ammonium or nitrate levels increase, the repressive effect of *AtSCL26* is reduced and instead LR development is promoted in higher ammonium or nitrate levels. Although there are

both ammonium- and nitrate- dependent effects, the level of *AtSCL26* effect and the precise phenotypes differ. Therefore, it could be possible that *AtSCL26* is involved in regulating pathways unique to ammonium assimilation and distinct from nitrate assimilation, as part of the regulation of root system architecture by N form and level.

Chapter 4 Expression pattern and protein localisation of AtSCL26

4.1 Introduction

It has been hypothesised that the GRAS protein family act as transcription factors, and that the *NSP2* GRAS protein regulates the transcription of genes involved in the nodulation process (Kaló et al., 2005; Hirsch et al., 2009). Transcription factors are important regulatory proteins which can modulate expression of a gene by regulating transcription of that gene into mRNA. This control mechanism is achieved through activity at specific regions of the DNA which act as enhancers, the target binding sites for activator proteins including transcription factors. Transcription factor binding exposes the DNA to transcriptional machinery including RNA polymerase to attach to the promoter region of the DNA and begin transcribing the gene (Figure 19).

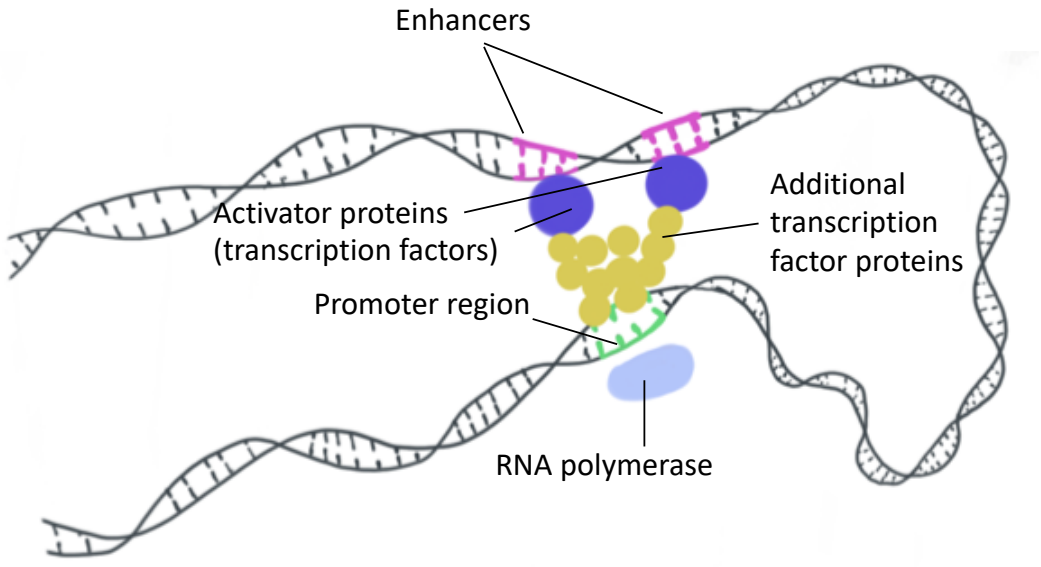

Figure 19: A schematic illustrating the function of transcription factors. Initially, activator proteins (purple) bind to enhancer regions (pink) which cause the DNA to bend towards promoter regions (green). Transcription factors (yellow) complex with the activator protein. This complex enables the DNA polymerase to bind to the promoter region and being transcribing the gene.

4.2 Transcription factor structure

TFs are modular in structure and contain DNA-Binding Domains (DBD), Transactivating Domains (TAD), and in some cases a Signal-Sensing Domain (SSD) (Latchman, 1997). The DBD includes at least one motif which recognises a specific DNA sequence of double or single stranded DNA within a promoter or enhancer region of the gene (as seen in Figure 16). These interactions occur through alpha/beta helices (or disordered regions) with DNA (Pabo and Sauer, 1992). TAD is a scaffold domain which is also known to have activation functions (AFs) and bind to transcription co-regulators (Wärnmark et al., 2003).

4.3 Aims and Objectives

Based on orthology to the *NSP2* gene, it can be hypothesised that *AtSCL26* acts as a transcription factor. To test this hypothesis, the expression pattern of *AtSCL26* was examined and the localisation of the AtSCL26 protein within the cell was tested.

4.4 Generation of GFP-tagged AtSCL26 stable lines for localisation analysis

To investigate the protein localisation and gene expression location of *AtSCL26*, gateway cloning was used to create constructs that would enable generation of GFP-tagged proteins and GFP tagged-promoter marker lines (Table 4).

Table 5: Constructs generated through Gateway cloning for protein localisation and gene expression analysis of *AtSCL26*.

Name	Amplified region	Vector
pAtSCL26:GFP:GUS	promoter	pBGWFS7
pAtSCL26:ATSCL26:GFP:GUS	promoter, gene	pBGWFS7
35s:AtSCL26:GFP	gene (alanine)	pK7FWG2
35s:GFP:AtSCL26	gene	pK7WGF2

Each of the final destination constructs was designed for a particular reason. The constructs that contain the 35S promoter were used for constitutive expression of protein in order to determine localisation. If consistent with the GRAS protein NSP2 localisation AtSCL26 should be nuclear-localised in these lines. To ensure that the eGFP is not interfering with the transcription of the AtSCL26 protein and resulting localisation, the eGFP was fused at both the N-terminus or the C-terminus of the gene sequences. To ensure continuous transcription of the gene and C-terminal eGFP located after the gene sequence, the sequence was mutated using PCR to alter the stop codon into an alanine codon. To visualise gene expression from the native promoter a pAtSCL26:GFP line was also created (Figure 20). Each of the constructs also contains an antibiotic resistance gene which was used as a selective agent during cloning, and in transgenic seedling selection. The constructs which include the native promoter pAtSCL26 confer resistance to Basta. The constructs which include p35S confer resistance to Streptomycin/Spectomycin.

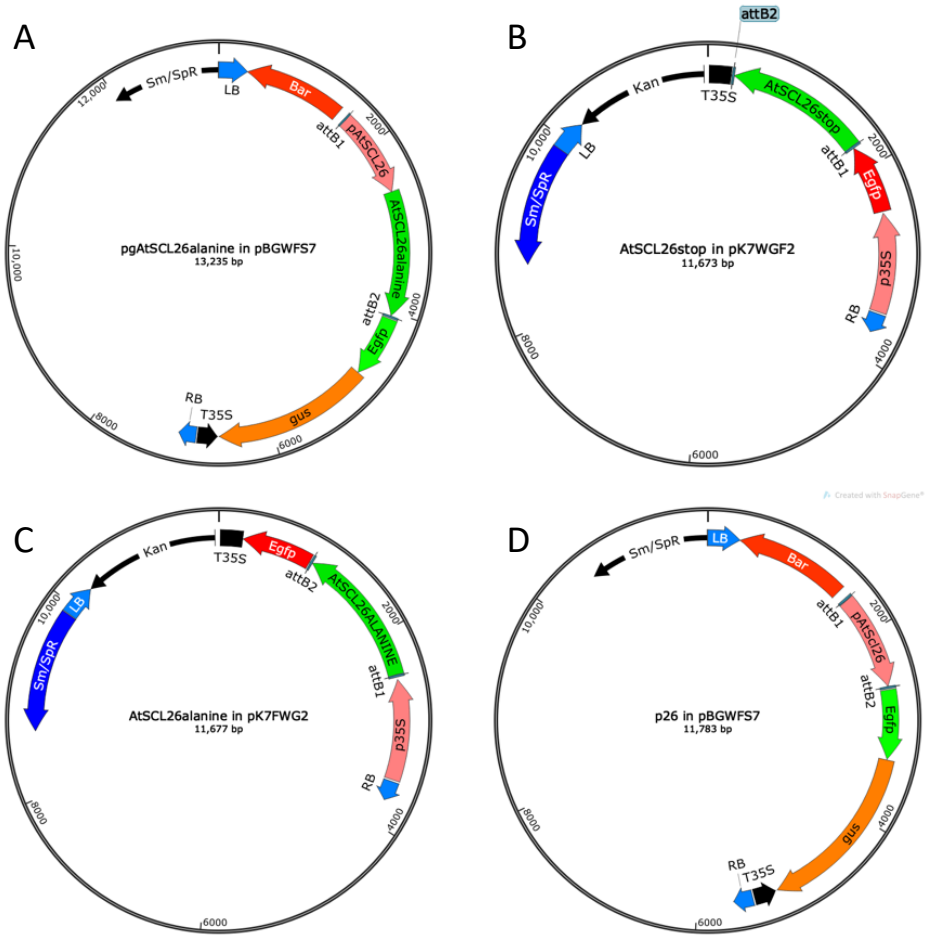

Figure 20: A diagram of each of the four AtSCL26 constructs. A) The native putative p*AtSCL26* sequence followed by the coding sequence of *AtSCL26* was cloned into the pBGWFS7 which includes a Basta resistance resistance marker and eGFP and GUS reporter coding sequences. B) Construct for N-terminal AtSCL26:eGFP expression under the 35S promoter. C) Construct for N-terminal AtSCL26:eGFP/GUS expression under the 35S promoter. D) C Construct for GFP-tagged p*AtSCL26* expression.

4.5 Transient expression of AtSCL26 in *Nicotiana benthamiana* shows putative nuclear localisation for AtSCL26

Localisation of the C-terminally GFP tagged AtSCL26 protein under expression of the 35S promoter and its native stop codon (p35S:GFP:AtSCL26) was investigated using transient expression in 4-6week old *Nicotiana benthamiana* plants. Plant leaves were

infiltrated with *Agrobacterium tumefaciens* carrying the construct then left for 72 hours.

Confocal microscopy of infiltrated leaves revealed a distinct circular GFP expressing pattern within the cells that measured ~5µm in diameter. This size is consistent with the diameter of a *N. benthamiana* plant cell nucleus (Figure 21).

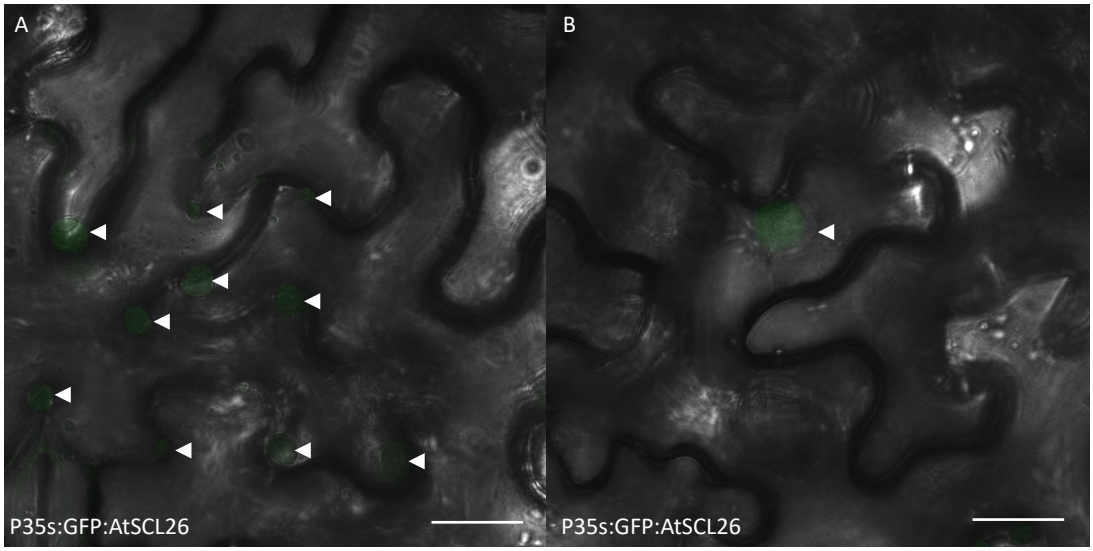

Figure 21: A leaf from 6-week-old *N. benthamiana* plant 3 days after inoculation with *A. tumefaciens* transformed with 35S:GFP:AtSCL26. (A) The white arrows show GFP expression as putative nuclear localisation of AtSCL26; scale bar: 20µm. (B) A second leaf showing GFP expression at a higher magnification; scale bar: 10µm.

Attempts were made to use a nuclear co-stain with DAPI initially tried and then Hoescht tried, however these we unsuccessful. When either DAPI or Hoescht staining was used the GFP expression was not detectable, even when staining was carried out on plant leaf tissue where GFP had previously been strongly detected. The 35S:AtSCL26:GFP N-terminally GFP-tagged AtSCL26 construct was also transiently expressed into *N. benthamiana*. The same circular GFP-expression within cells was detected, similarly indicating nuclear localisation (Figure 22).

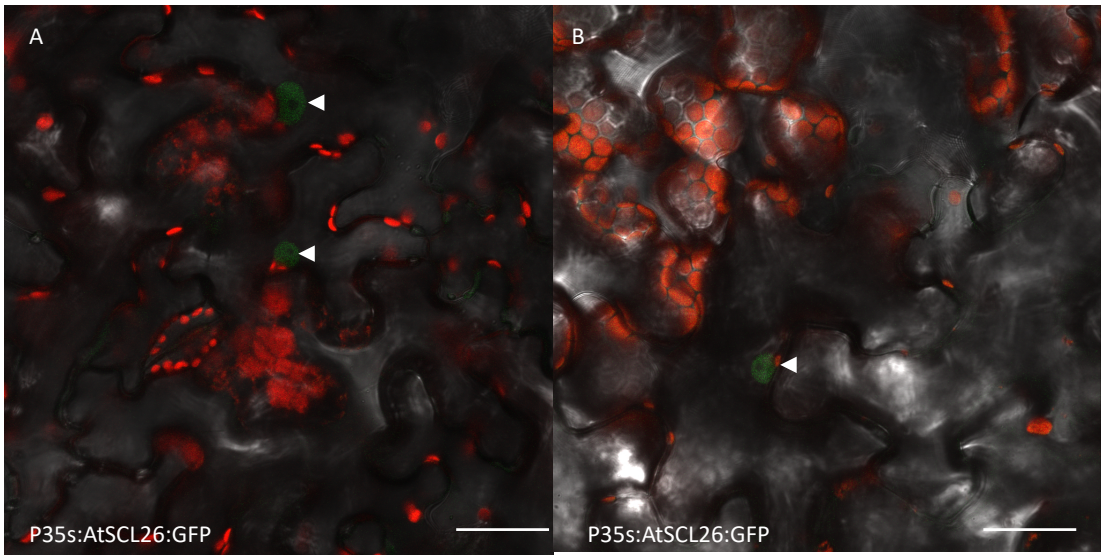

Figure 22: A leaf from 6-week-old *N. benthamiana* plant 3 days after inoculation with *A. tumefaciens* transformed with 35S:AtSCL26:GFP. (A) The white arrows on the show GFP expression and putative localisation in the nucleus; scale bar: 20µm. (B) A second region of cells on the same leaf showing putative nuclear AtSCL26:GFP expression; scale bar: 20µm.

As the only constructs that were transformed so far in this work were the constructs that were driven by the 35S over-expression promotor, it was not possible to ascertain the native localisation of the protein and analysis of cells rather than whole root expression patterns was investigated.

4.6 Stable transformation of *A. thaliana* with AtSCL26 constructs

Stable transformation of the p35S:GFP:AtSCL26 construct into *A. thaliana* (Col-0) plants was carried out using *A. tumefaciens*. Seedlings were inoculated with the bacterial suspension using the painting method as described in Methods. Transformant seeds from these plants were then selected on ½ MS containing 50 µg/mL kanamycin as a selective antibiotic (approx. 1000 seeds per plate). The seeds that successfully germinated were then transferred to 100µg/mL for 4 days and then transferred to soil. The seeds were collected from each of the plants and 100 seeds were sown onto ½ MS

plates with 50µg/mL kanamycin. Germinating seedlings from lines which exhibited 75% germination rates were then selected from propagation. The process was repeated and the lines with 100% germination rate were selected for further propagation and analysis using microscopy. The same limitation exists as with transient expression, in that due to the gene being driven by the 35S promoter, the localisation of this gene under native conditions has not yet been studied.

4.7 AtSCL26 shows nuclear localisation in stably transformed *A. thaliana* plants

Confocal microscopy was used to analyse the localisation pattern of the p35S:GFP:AtSCL26 protein . Similar to the results using transient expression in *N. benthamiana*, putative nuclear localisation was visible (Figure 23).

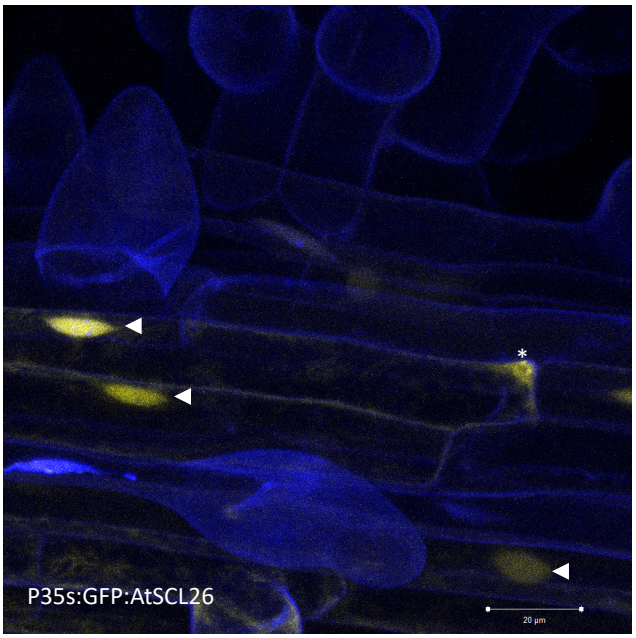

Figure 23: Confocal image of stable p35S:GFP:AtSCL26 line within the primary root of Col-0. Roots were counterstained with PI (false colour blue) The circular GFP-stained structures (false colour yellow) are indicated with white arrows. Asterix indicates an accumulation of GFP expression; scale bar = 20µm.

4.8 Discussion

The results from the experiments in this chapter show a putatively similar nuclear protein localisation pattern between AtSCL26 and NSP2 (Oldroyd, 2003; Kaló et al., 2005). Some staining in the cytoplasm of cells was also seen using confocal microscopy (e.g. see * on Figure 20). It is possible that the cytoplasmic GFP signal that is seen is from disassociated GFP or active diffusion, however this was not confirmed. Plant nuclear pores allow passive diffusion of molecules up to about 60 kDa, however the diffusion of molecules occurs between 50-60kDa is at a reduced rate (Meier, 2007). AtSCL26 has a molecular weight of 53.55 kDa (calculated on http://www.bioinformatics.org), which means that AtSCL26 on its own could passively diffuse across the nuclear membrane into the cytoplasm. However, the addition of eGFP would make AtSCL26:GFP too large to freely pass through the nuclear membrane, thus a NLS would be required. As found in Chapter 3 there is no obvious NLS in the AtSCL26 protein sequence, thus the mechanism enabling putative nuclear-localisation needs to be explored in more detail. For example, a series of point mutation constructs could be designed that modify the region immediately before the LRI domain, where a NLS has been found for SCR (Gallagher and Benfey, 2009).

Although the use of DAPI and Hoescht were attempted as nuclear counterstains for transient expression, experiments using both were initially unsuccessful. Attempts were made to repeat this following the advice of other researchers, including the use of vacuum infiltration, however it was still not possible to visualise either dye using confocal microscopy and also retain the ability to visualise GFP. One hypothesis is that the *N. bethamiana* leaves used could potentially lack the permeability required for the dyes being used, although they have been used successfully by others, so this requires further work.

As mentioned in the results, the limitation of using the 35S promoter is that the native expression pattern of AtSCL26 has not yet been determined. To complement these results there was an intention to use the native promoter of the gene and P35S:GFP:ATSCL26 stable lines have been genotyped, but this work was not completed.

4.9 Future work

Work that was started but not completed was the transformation of the *atscl26-2* mutant line in order to test for molecular complementation and thus confirmation of the *atscl26* phenotype; thus far this has been shown by *atscl26-1/2* mutant trans-allelic non-complementation (Lagunas *et al*. In Prep). The plants of this transformation are currently at the T2 generation. In addition, for expression pattern analysis in stable transformed lines the p*AtSCL26*:GFP:*AtSCL26* line has been transformed into Col-0 and lines are at the T2 generation. Further developing these lines will enable the expression pattern of *AtSCL26* and the localisation of the AtSCL26 protein to be fully examined.

Col-0 has also been successfully transformed with 35S:GFP:AtSCL26 and a stable line has been generated with plants at the T3 generation. Future work in this area will be to take *pAtSCL26*:GFP:GUS and p*AtSCL26*:AtSCL26:GFP:GUS through to the T3 stable line generation. The p*AtSCL26*:GFP lines will enable the gene expression pattern to be assessed and the p*AtSCL26*:AtSCL26:GFP:GUS lines will allow for determination of protein localisation under its own native promoter rather than the non-endogenous 35S promoter. Transgenic lines will be confirmed using genotyping along with confirmation of antibiotic resistance.

Another area which would be of great interest and has been included in future work plans is to test if mutants of *atscl26* and *nsp2* can be cross-species complemented by transforming *atscl26* mutants with the functional *NSP2* gene, and *nsp2* mutants with the functional *AtSCL26* gene. Some progress has been made in this area; *A. tumefaciens* has been transformed with the *pAtSCL26*:AtSCL26:GFP:GUS, 35S:AtSCL26:GFP, and 35S:GFP:AtSCL26 constructs ready for plant transformation. As a complement, 35S:GFP:NSP2 has also been successfully transformed into *A. tumefaciens* ready for *atscl26* plant transformation.

Chapter 5 Molecular phenotyping of AtSCL26

5.1 Introduction

Differentiation of cell types within multicellular organisms enables the partitioning of distinct functions and development of a complex body plan. According to Brady *et al* (2007) the root is comprised of 15 cell types with unique functions and cellular properties (Figure 24). The meristem and quiescent centre are at the tip of each root, with newly dividing cells that arise from the QC in turn elongating then differentiating towards the shoot-end of the root. The root thus represents a developmental gradient of cells with a wide variety of molecular and physiological functions.

In plants, it is well documented that cells have a high degree of plasticity and many cell types are able to dedifferentiate and re-differentiate under particular conditions (Grafi, 2004; Tian et al., 2014). Reactivation of cell division in pericycle cells, enabling lateral root primordia to arise and then develop, as explored in Chapter 1, is a prime example of this feature and underlies the plastic nature of root architecture. Regulation of lateral root development, both numbers and length, is often seen in responses to variation in abiotic or biotic signals that are perceived in outer cell types such as the epidermis and lateral root cap. For formation then emergence and development of a lateral root primordia there must also be coordination of cell division and growth in overlying cells, including the cortex and epidermis (Figure 3).

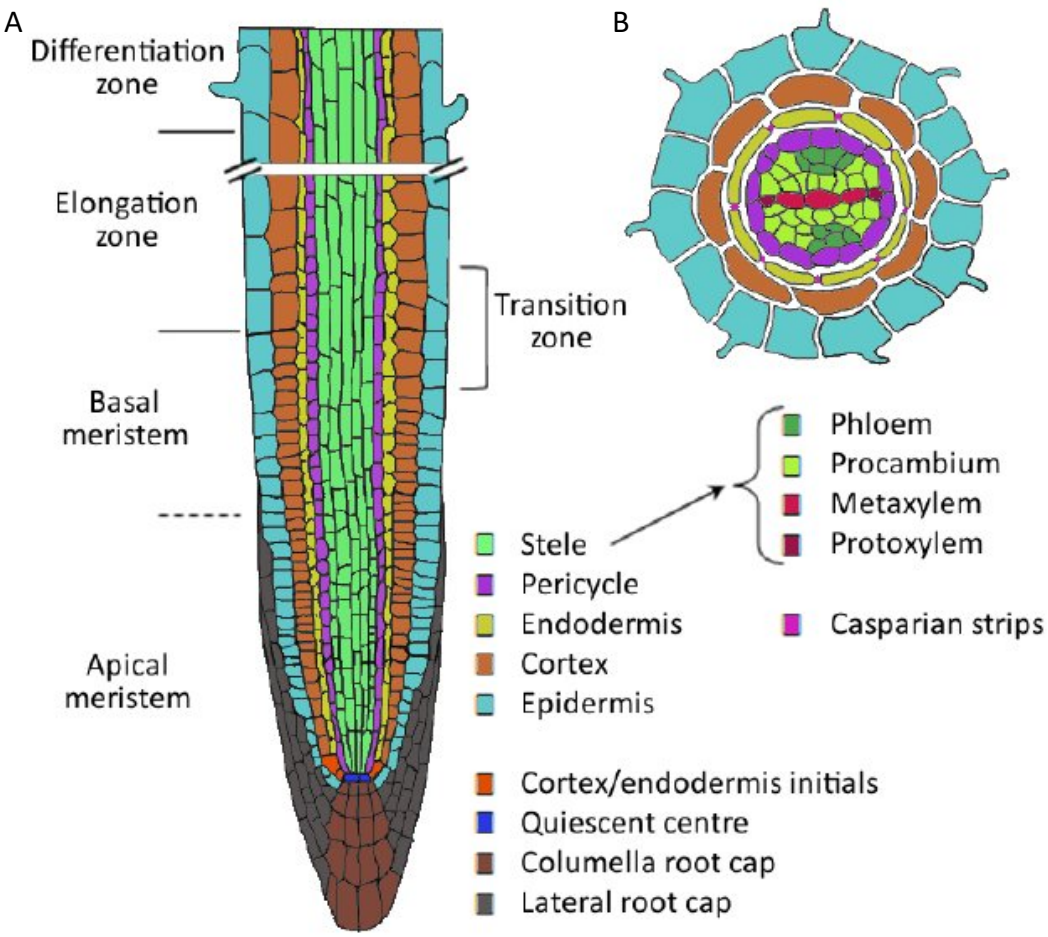

Figure 24: The organisation of root cells in *A. thaliana*. (De Smet et al., 2015). A longitudinal representation of a *A. thaliana* primary root (A) labelled to show the apical meristem, then basal meristem, the elongation zone and the differentiation zone as well as the different cell types. The root has also been sectioned horizontally (cross-section), enabling the concentric patterning of layers of cells to be visible (B).

To analyse the contribution of different cell types during lateral root development it is very informative to be able to separate and then analyse each cell type distinct from each other. Fluorescence Activated Cell Sorting (FACS), as previously mentioned, is a technique that allows for the isolation and separation of fluorescently tagged cells based on their emission wavelength; the fluorescent signal associated with cells can come from the use of dyes or fluorophores expressed in

particular cells or cell types. This invaluable tool provides a rapid and effective way to isolate specific cell types of roots and a number of studies have used FACS to examine the contribution of different cell types during regulation of lateral root development in response to the environment. For example, using a high-resolution time series of nitrogen treatment followed by FACS to isolate cortex and pericycle cells it was found that the coordination of gene expression between cell types and over time is crucial in the regulation of lateral root development in response to an altered nitrogen environment (Walker *et al.*, 2017).

5.2 Aims and objectives

In order to investigate the phenotype of the *atscl26* mutant, a combination of nitrogen treatments and gene expression analysis using microarrays were employed. The first focus was on the whole root level, followed by the use of FACS to examine the contribution of different cell types to the *atscl26* phenotype. The experiments followed the hypothesis that, given the putative role of *ATSCL26* as a transcription factor and its putative role in controlling root nitrogen responses, lack of AtSCL26 (in the *atscl26* mutant) would enable the genes and processes regulated by AtSCL26 to be revealed. As described in the introduction, the AtSCL26 homolog NSP2 dimerises with NSP1. AtSCL29 appears be the homolog of NSP1. If AtSCL26 interacts with AtSCL29 in Arabidopsis it could be that there is regulation between these genes at the mRNA level. Therefore analysis of microarray data is highly relevant to start to ask if there is any relationship between the AtSCL26 and AtSCL29 genes.

5.3 Microarray analysis of RNA extracted from whole root samples of *atscl26* and wild-type *A. thaliana* seedlings grown on NH_4NO_3

In order to investigate gene expression variation in the *atscl26-1* and *atscl26-2* mutants and the influence of the level of nitrogen, seedlings were grown for 9 days on 0.3mM or 5mM NH_4NO_3 then RNA extracted from roots. The mRNA expression levels were analysed using the Agilent One Colour Microarray system (see Methods). After the expression levels of each of the genes was normalised using LIMMA, implemented in RStudio, the data was analysed to identify genes with significant variance (Pvalue <0.01) in their expression values depending on the treatment level (nitrogen-treated or not) or genotype (*atscl26-2* or Col-0 wild-type) a 2-way ANOVA was run in MATLAB. Thus, the generated data was analysed to determine a transcriptomic profile of each of the conditions to enable evaluation of the *AtSCL26*-effect and the nitrogen**ATSCL26* (nitrogen by genotype interaction) effect on the transcriptome.

Using qPCR analysis it had been found that nitrogen repressed the expression of *AtSCL26* (Figure 14). Here, using microarrays, the expression of *AtSCL26* in Col-0 between deplete and replete samples was not found to be significantly different (Figure 25). Microarray analysis is less sensitive than qPCR, which could account for the difference, particularly if variation in expression level is at the cell type level.

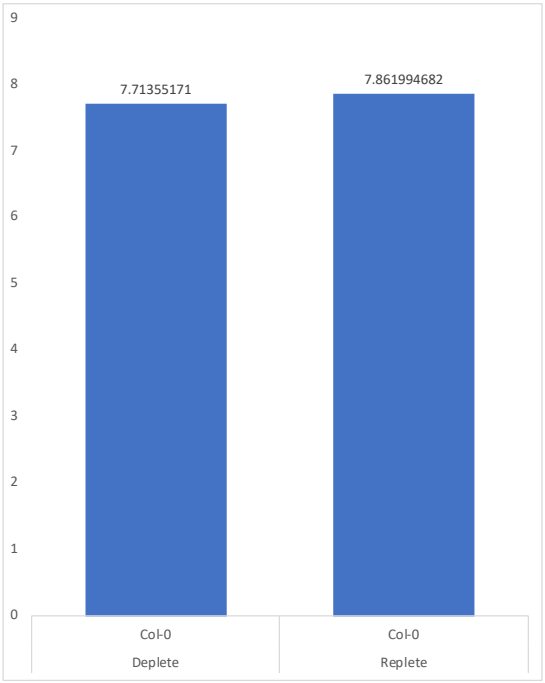

Figure 25: The effects of N on AtSCL26 whole root data. There is no significant difference in AtSCL26 expression between deplete and replete N conditions (pVal=0.44 calculated using a two tailed t-test assuming heteroscedasticity) when looking at the whole root data (SE deplete = 0.543, SE replete = 0.85).

The whole root gene expression data was initially filtered to only include values of genes that were significantly differentially expressed when analysing the genotype effect. There were 226 genes mis-regulated in both the *atscl26-1* and the *atscl26-2* mutant compared to Col-0 and thus are putatively under *ATSCL26* control. 7565 genes were found to vary upon nitrogen influx (nitrogen effect responsive genes). There were 893 genes that had a nitrogen*genotype effect, which were genes which were significantly differentially expressed due to the lack of *AtSCL26* under the influence of nitrogen.

The expression of *AtSCL26* and *AtSCL29* was found not to change across the experiments. *AtSCL26* has been found to be induced by KNO_3 (Lagunas *et al*. In Prep) but does not seem to be induced by NH_4NO_3. Expression of *AtSCL26* is still seen in *atscl26-1* and *atscl26-2* on the microarray, despite being loss of expression mutants

validated using qPCR. This could be because the microarray probes for *AtSCL26* are not specific (perhaps hybridising to *AtSCL29*), or because they detect non full-length sequence, upstream of the qPCR primers. A BLAST search was used and it was found that the probes are specific to *AtSCL26* and they are spread across the full transcript (Figure 26). Expression of *AtSCL26* and presence of AtSCL26 protein should be tested further in the *atscl26* lines.

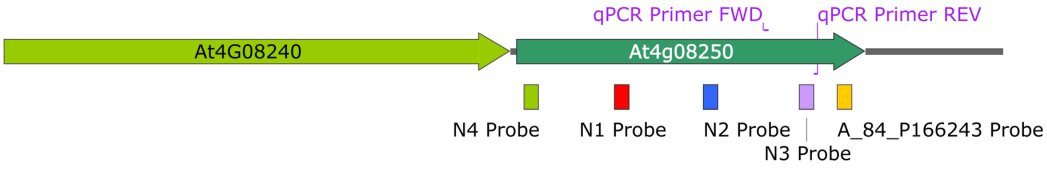

Figure 26: A map schematic showing the locations of the probes used in microarray analysis. Probes that were used to measure expression ofAtSCL26 during the microarray were all firmly within the transcript. The N1 (red), N2(blue), N3 (purple) and N4 (green) are the probes used for the Nimblegen system. A_84_P166243 (yellow) is the probe used by the Aligent system.

A number of nitrogen-responsive genes were analysed to confirm the effects of nitrogen influx including nitrate and ammonium transporters, N-assimilation enzymes and N-metabolism components (Figure 27). A list of these genes was assembled from a search in VirtualPlant and many of these genes are known to be N-responsive in roots from previous studies ((Gifford et al., 2013; Walker et al., 2017). Supporting the N-treatment here, *NRT2.1* and *AtAMT1.1* were found to be N-repressed and *NRT1.1*, *AtAMT1.2* and *AtAMT2.1* were found to be N-induced. N-regulation of these genes occurred similarly in Col-0 and both *atscl26* mutants, suggesting that they do not have global N-uptake phenotypes. However, the N-regulation of expression of *NRT1.1* and *AtAMT2.1* was reduced in *atscl26*, because the level of expression in N-deplete conditions was greater.

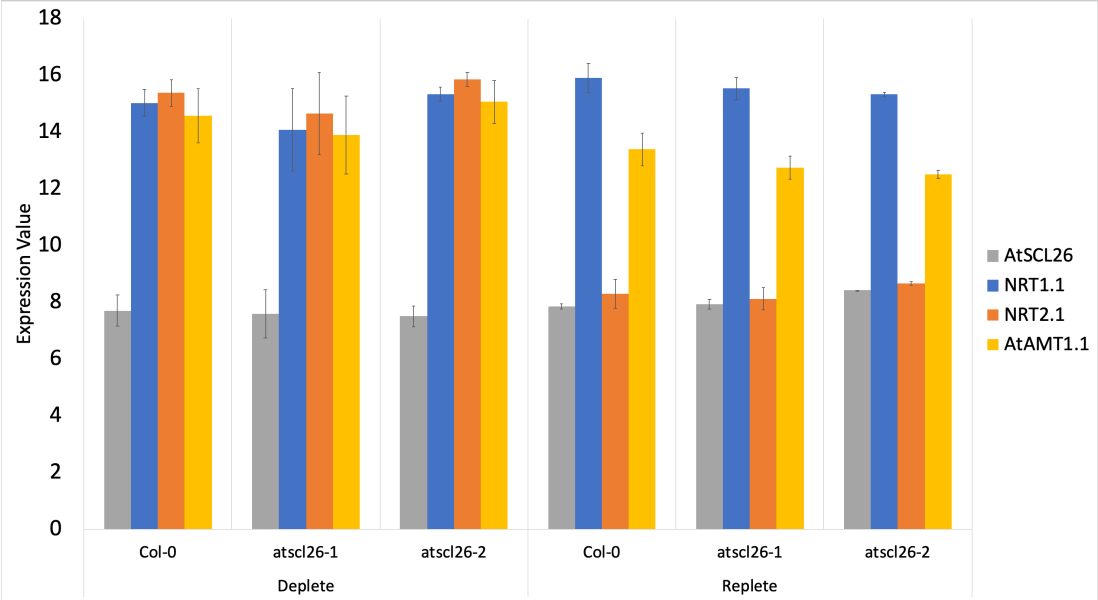

Figure 27: The average expression of a selection of key N-responsive genes as well as GRAS family transcription factor *AtSCL26*. *NRT2.1* and *AtAMt1.1* were found to be N-repressed in the presence of nitrogen in all genotypes, consistent with the known N-responses of these genes. *NRT1.1*. These results are in-line with published literature (Gifford et al., 2008; Walker et al., 2017)

In order to examine the expression patterns of genes with significant expression variance, gene expression values for the 893 genes were clustered in MATLAB and silhouette plotting used to determine how many clusters would separate genes optimally (see Methods). 11 clusters was chosen since this number performed well across all cluster statistics but also enabled major trends in the data to be distinguished (Figure 28).

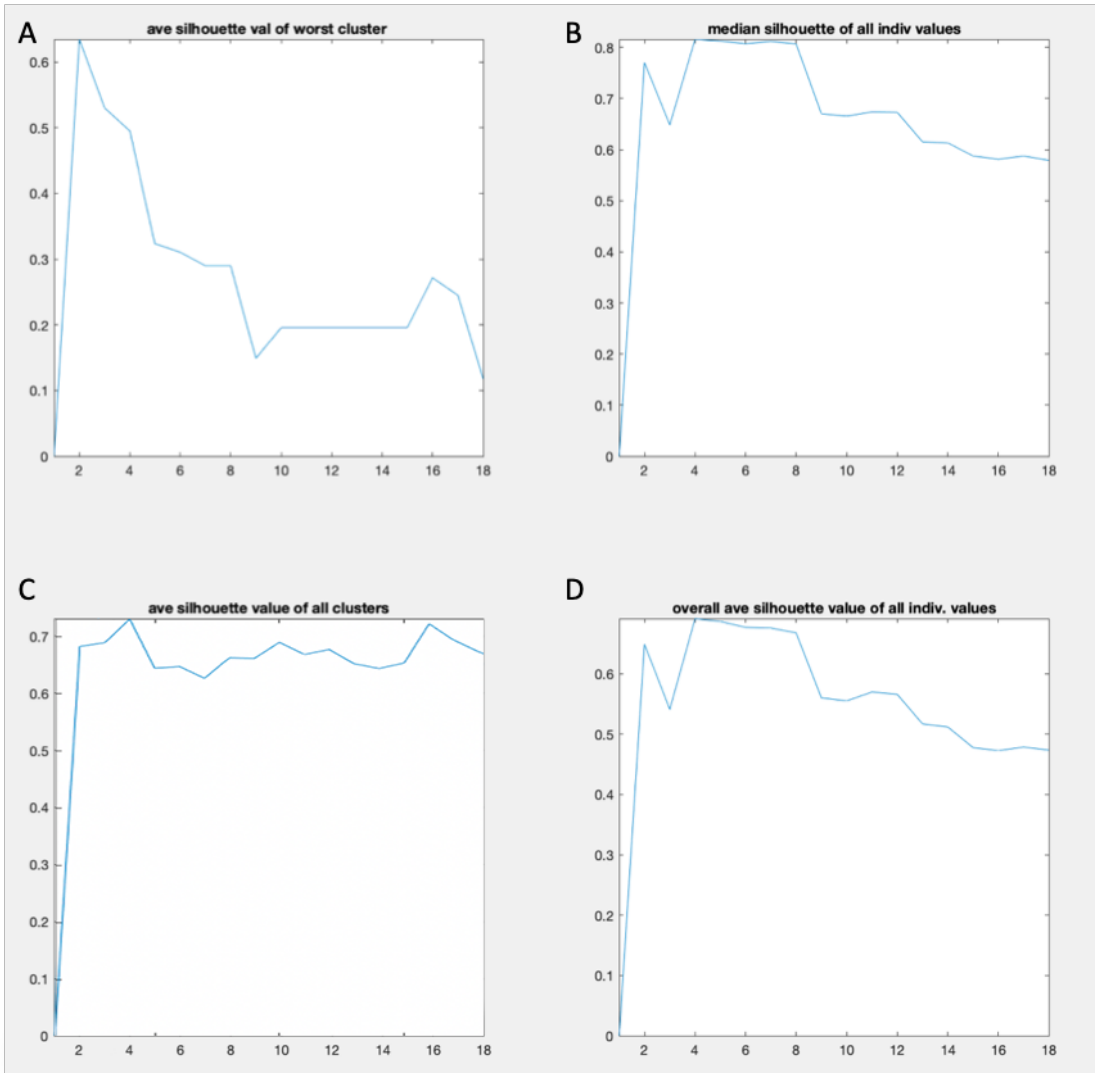

Figure 28: Silhouette plots for the data generated from the microarray data from whole roots grown on NH_4NO_3. A-D show measures of cluster evaluation; 11 clusters were chosen based on this number having high values across all four cluster evaluation statistics.

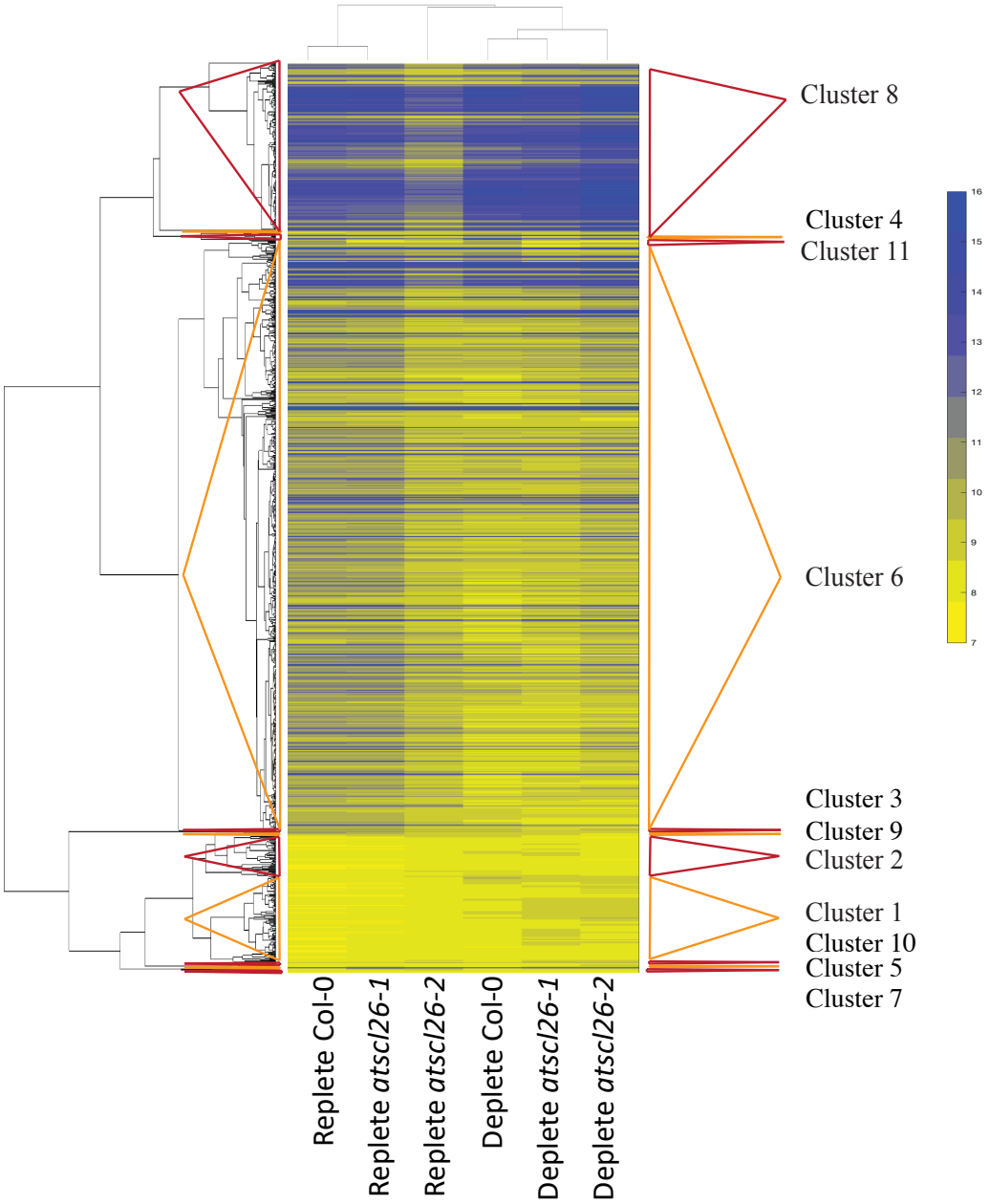

Figure 29: Heatmap showing the expression values for the 11 clusters of genes that are differentially expressed in the NH_4NO_3 whole root experiment. Colour bar shows the log2 expression level of genes within the heatmap.

The dendrogram showing relatedness between the transcriptome data samples shows a closer clustering between the replete Col-0 and replete *atscl26-1* samples. The N-replete *atscl26-2* sample has a distinct transcriptome profile from other datasets with greater differences between this sample and the others. The N-deplete transcriptome

data sets cluster together, with Col-0 and *atscl26-1* being the most similar to each other.

Across all data the major patterns are cluster 6 and cluster 8, which are the two largest clusters (table 6) and also the only clusters which had over represented GO terms.

Table 6: The number of clusters generated from analysis of the microarray data obtained using seedlings grown on NH_4NO_3

Cluster Number	Number of genes
1	108
2	54
3	2
4	2
5	1
6	736
7	1
8	208
9	14
10	6
11	2

In cluster 8 there are a large number of genes that are downregulated in N-replete conditions in *atscl26-2,* compared to the other transcriptome profiles in replete conditions, and also upregulation in *atscl26-2* N-deplete conditions compared to Col-0 and *atscl26-1* N-deplete conditions. Cluster 6 contains genes that show overall higher levels of expression in Col-0 and *atscl26-1* in N-replete conditions compared to in *atscl26-2* N-replete conditions, in which levels are more similar to genotypes in N-deplete conditions. Genes in the next largest cluster, cluster 1, have reduced expression in all N-replete transcriptome conditions compared to N-deplete conditions.

5.4 Genes in cluster 6 are induced in the presence of nitrogen and are involved in cell differentiation and auxin polar transport

Genes in cluster 6 (Figure 30) are N-induced in Col-0. A similar response is seen in *atscl26-1*, however not in *atscl26-2*, suggesting that the N-induction of these genes is dependent a functional copy of *AtSCL26* that is absent in *atscl26-2*. In addition, there is an overall increase in the expression of cluster 6 genes in the *atscl26-2* mutant in N-deplete conditions, indicating that *AtSCL26* could also have a repressive effect in the absence of nitrogen. In the replete conditions, the opposite effect is seen, in that *atscl26*-2 mutants have a reduction in expression of cluster 6 genes, indicating that there is an overall inductive effect of *AtSCL26* on these genes in nitrogen replete conditions.

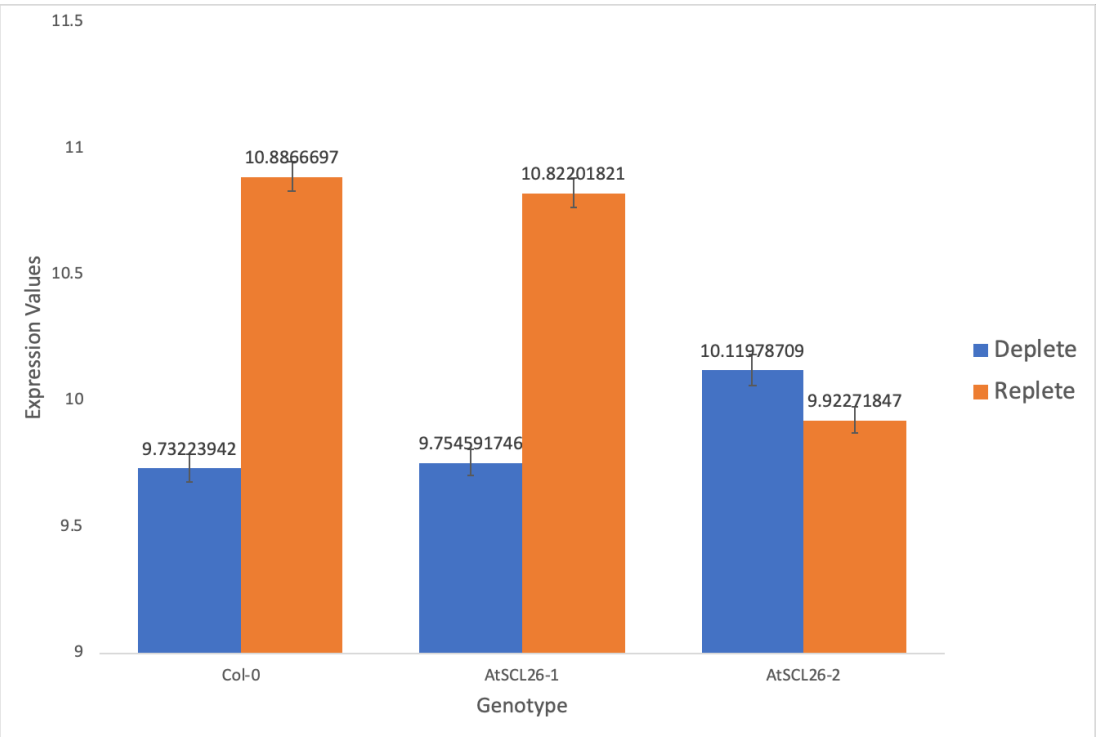

Figure 30: Average expression value of genes in cluster 6. In roots of seedlings grown on deplete (blue) NH_4NO_3 conditions there is no difference in expression levels between *atscl26-1* and Col-0, however the *atscl26-2* mutant shows increased expression of these genes. In replete conditions (orange) expression in *atscl26-1* and Col-0 are again similar, both higher than expression in *atscl26-2*.

In order to ask if the cluster represents a groups of genes involved in the same function or process a GO term overrepresentation analysis was carried out in VirtualPlant using Biomaps (Katari et al., 2010). In cluster 6 there is an overrepresentation of genes involved in a range of molecular functions (GO term classification), including "transmembrane receptor protein tyrosine kinase signalling pathway (pval=2.3 E-11), "xylem and phloem pattern formation" (pval=0.02) including the genes TORNADO 1 (TRN1), "auxin polar transport" (pval=0.02), and "cell differentiation" (pval=0.03) including the gene *BETA AMYLASE 1* (*BAM1*). GO biological processes overrepresented in this cluster include: "ATP binding" (pval=7.33E-6), "adenyl ribonucleotide binding" (pval=7.66E-6) and "microtubule motor activity" (pval=4.28E-4). Based on the Munich Information Centre for Protein Sequences (MIPS) classification there are very similar functions overrepresented, including "plant cell differentiation" (pval=6.6 E-4), and "ribosome biogenesis" (pval=1.87E-07).

In summary, in the presence of nitrogen in the form of NH_4NO_3, *AtSCL26* appears to regulate the N-induction of genes involved in cell differentiation, auxin polar transport, which are known to be important processes in lateral root formation (de Smet, 2012).

5.5 Genes in cluster 8 are repressed by *AtSCL26* in deplete nitrogen conditions and induced by *AtSCL26* in nitrogen replete conditions.

The main pattern in cluster 8 (Figure 31) is that there is a higher level of gene expression in the *atscl26-2* mutant, indicating that in low nitrogen conditions *AtSCL26* could play a repressive effect on the expression of these genes. In N-replete conditions, the expression of cluster 8 genes in the *atscl26-2* mutant are reduced, which suggests that in the presence of nitrogen, *AtSCL26* has an overall inductive effect on cluster 8 genes. Similarly, to the case in cluster 6, the expression levels in Col-0 and *atscl26-1* were similar.

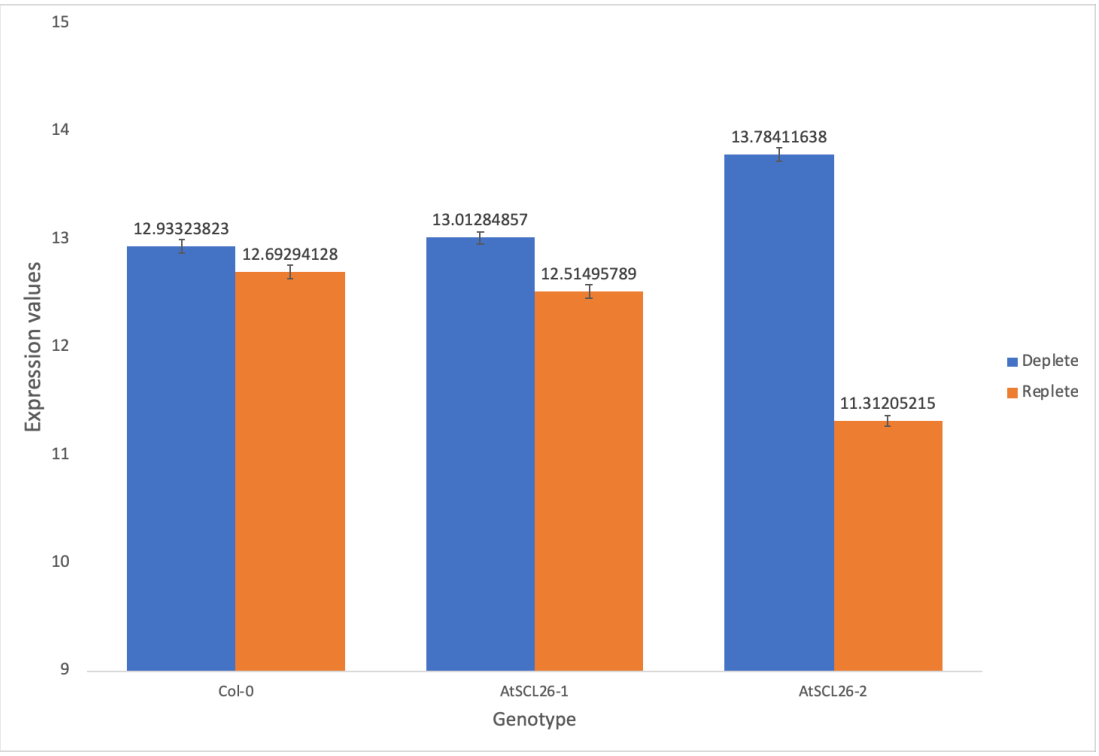

Figure 31: Average expression values of genes in cluster 8. In roots of seedlings grown on deplete (0.3mM) NH_4NO_3 (blue) genes in *atscl26-2* are more highly expressed than in Col-0 wild-type or *atscl26-1*. In N-replete conditions (orange) the genes have reduced expression in each genotype.

Molecular processes overrepresented in this cluster included functions in "ribosome biogenesis" (pval=1.73E-22), the gene *TRANSMEMBRANE AMINO ACID TRANSPORTER* FAMILY PROTEIN (AT2G41190) which functions in "translation" (pval=1.73E-54) and genes involved in "cellular biosynthetic processes" (pval=1.97E-24). Biological functions overrepresented in this cluster included "ribosome structure" (pval=1.52E-66) and analysis of MIPS terms suggested that the proteins were involved in "protein synthesis" (pval=5.5972-41) and "translation" (pval=3.83E-37). Genes that were clustered together here were

In summary, based on the genes in cluster 8, *AtSCL26* has a repressive effect on genes involved in ribosome biogenesis, transport, translation and protein synthesis when nitrogen is limiting, and an overall inductive effect on these genes when nitrogen is replete.

5.6 Microarray analysis of RNA extracted from specific cell types of *atscl26-2* and wild-type *A. thaliana* seedlings treated with KNO_3

Whilst data from whole roots is informative for understanding gene expression changes that are occurring on a systemic level within the root, investigating individual cell types enables key changes in gene expression that feed into changes in root development to be located. For analysis of the *atscl26* mutant, the *atscl26-2* mutant was crossed with pericycle, cortex, and epidermis lines containing a GFP tag (Gifford et al., 2008). Only *atscl26-2* was used, since it was the allele with the strongest loss of expression and also strongest phenotype (as presented in earlier chapters). The aim of this experiment was to assess transcriptomic differences occurring in key locations involved in responses to changing N levels in the environment (epidermis) and locations involved in lateral root emergence (cortex and pericycle).

GFP cell type-specific promoter-tagged *atscl26-2* and Col-0 seedlings were grown on deplete (0.1mM) KNO_3-containing agar plates for 9-days and then exposed to a two-hour treatment of either deplete (no change) or replete (5mM) KNO_3. The roots of the seedlings were then harvested, and protoplasts generated for isolation of individual cell types using FACS. RNA was then extracted, and microarrays hybridised as for whole root expression analysis. Microarray data was normalised, and a 2-way ANOVA used to determine genes that were significantly differentially expressed according to genotype and/or nitrogen treatment within each cell type.

5.7 The effect of nitrogen on the expression of *AtSCL26*

By analysing the Col-0 microarray data from isolated cell types it is possible to determine the effects that nitrogen has on the expression of *ATSCL26* on a cellular level (Figure 32). In cortex cells *ATSCL26* was found to be N-induced and in pericycle and epidermal cells *ATSCL26*was found to be N-repressed.

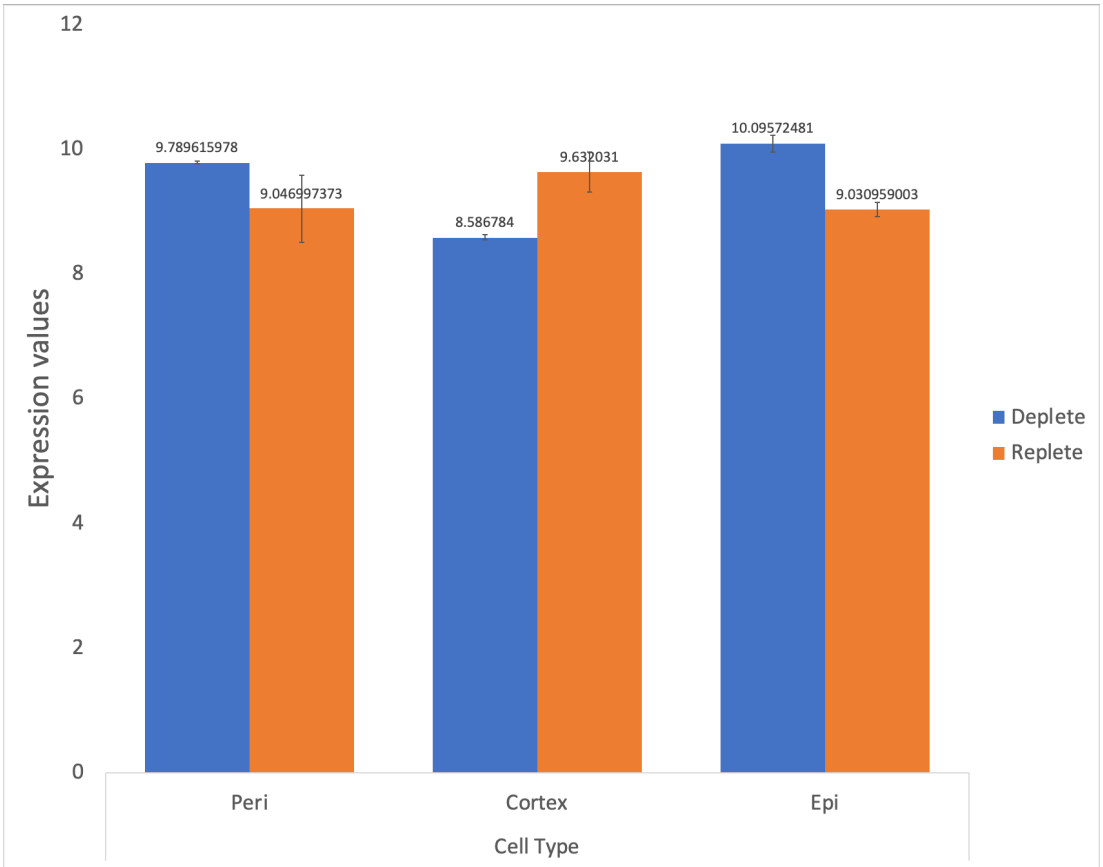

Figure 32: Expression levels of *AtSCL26* across three root cell types treated with replete nitrogen or grown on deplete nitrogen. In peri (pericycle) and epidermal (epi) cells there is reduced *AtSCL26* expression in N-replete conditions, whereas there is an increase of *AtSCL26* expression in the cortex when roots are KNO_3-treated.

The use of cell type analysis was very important for examining the N-regulation of *AtSCL26*. Despite N-regulation of *AtSCL26* being obvious in individual cell types, when *AtSCL26* expression is examined in whole roots, the N-regulation is not discernible (Figure 25) at least using microarrays; when using qPCR it was possible to detect overall N-repression of *AtSCL26* (Figure 14).

In order to examine the expression patterns of genes with significant expression variance in cell types according to nitrogen, expression values for all 2259 genes with a genotype*nitrogen effect were analysed. This enabled us to focus specifically on genes whose N-regulation in specific cell types was controlled by *AtSCL26*. Expression of these genes were clustered in MATLAB and silhouette plotting used to

form an optimal number (12) of clusters (Figure 33). then plot a dendrogram and heat map of expression values (Figure 34), as carried out previously.

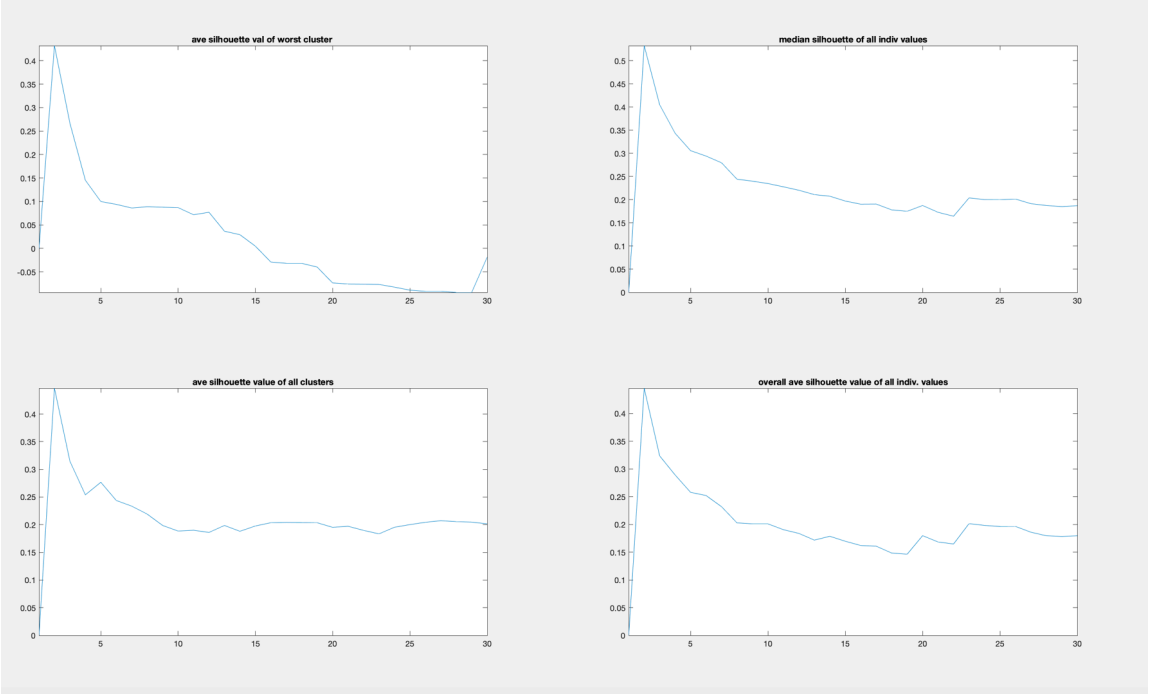

Figure 33: Silhouette plots for the data generated from the microarray data using whole roots grown on KNO_3. A-D show measures of cluster evaluation; 12 clusters were chosen based on this number having high values across all four cluster evaluation statistics.

Cell types from N-deplete or N-replete levels tend to cluster together (Figure 34). The pericycle samples are the most tightly clustered cell type; cortex and epidermis samples cluster in a mixed fashion, with N-deplete and N-replete samples closer to each other than samples of the same cell type. Cluster 6 was the largest cluster generated (see Figure 34) from this analysis, and the only cluster to have over represented GO terms. Cluster 6 genes have reduced expression in the epidermis and cortex. In the pericycle some of the genes in cluster 6 have higher expression in Col-0 than *atscl26-2* in N-replete conditions. Conversely, the second largest cluster (cluster 11) includes genes that have higher expression in the cortex and epidermis compared to the pericycle.

Table 7: The number of clusters generated from analysis of the microarray data obtained using seedlings grown on KNO_3

Cluster Number	Number of genes
1	11
2	40
3	19
4	55
5	39
6	918
7	60
8	121
9	89
10	27
11	868
12	12

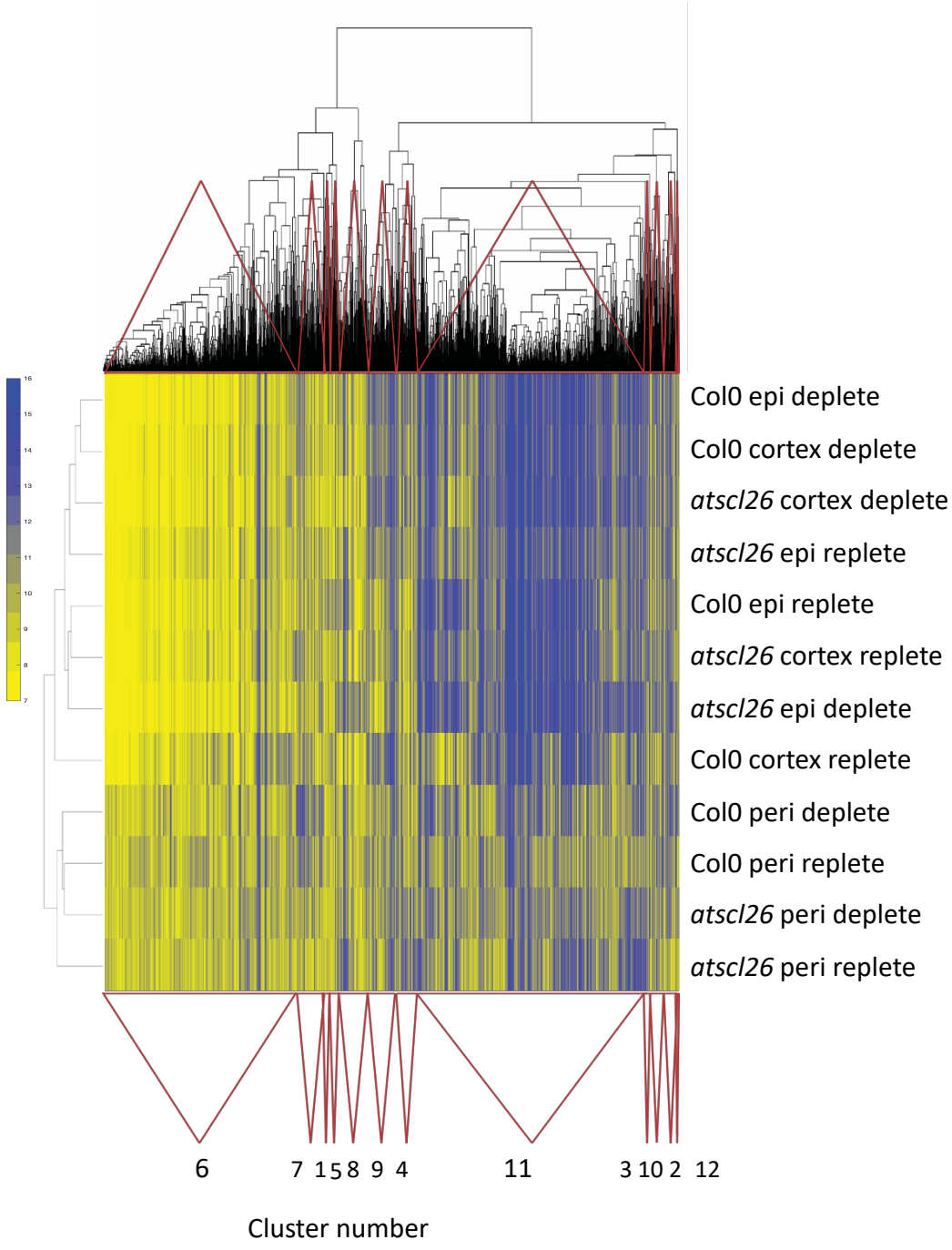

Figure 34: Heatmap showing the expression values for the 12 clusters of genes that are differentially expressed in the KNO_3 cell type experiment. Colour bar shows the log2 expression level of genes within the heatmap; deplete=KNO_3-deplete conditions; Replete = KNO_3-replete conditions.

5.8 Analysis of cluster 6 genes show that *AtSCL26* has a nitrogen dependent repressive effect in pericycle and cortex in replete conditions, and a repressive effect in epidermal cells in deplete conditions.

One of the largest clusters, cluster 6 (886 genes), contained genes overrepresented in molecular mechanisms including "response to steroid hormone stimulus" (*GRF8, GRF6, AFT1*) (pval=4.E-2) and "intracellular transport" (*ATGOS11, TIM13, ATRAB2A*) (pval=4.E-2). In the pericycle in Col-0 cluster 6 genes are N-repressed, however the expression of these genes does not vary in the *atscl26-2* mutant, suggesting that these genes are N-repressed by *AtSCL26*. In N-deplete conditions there is only a slight decrease in the level of expression for the genes in this cluster when comparing Col-0 to *atscl26*-2, however in replete conditions, these genes are more highly expressed in the *atscl26-2* mutant, indicating that *AtSCL26* has a repressive effect on the expression on the genes in this cluster in the presence of nitrogen. Similar to in pericycle cells, cluster 6 is N-repressed in Col-0 cortex cells but not in *atscl26-2*, again suggesting that *AtSCL26* represses expression of these genes. In the epidermis, in contrast, cluster 6 genes are N-induced in Col-0 but this N-induction is almost absent in *atscl26-2*. Cluster 6 is however expressed more highly in *atscl26-2* compared to Col-0, suggesting that *AtSCL26* represses the expression of these genes when N is limiting.

To summarise these results, genes that are involved in intracellular transport and in regulating responses to steroid hormone stimuli when subjected to deplete nitrogen conditions appear to be repressed by *AtSCL26* in the pericycle and cortex when N is replete and repressed by *AtSCL26* in the epidermis when N is deplete.

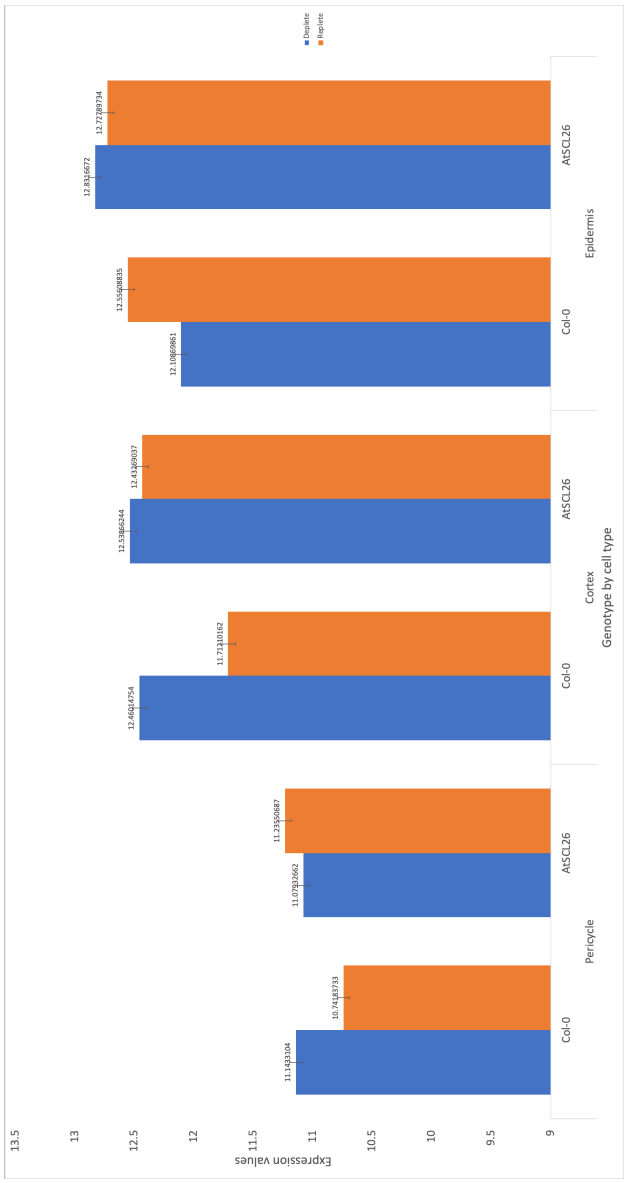

Figure 35: Expression of genes in cluster 6 in specific cell types from seedlings grown on deplete and replete KNO. In depleted N, genes in cluster 6 appear to be repressed by AtSCL26 in the pericycle and cortex when N is replete and repressed by AtSCL26 in the epidermis when N is deplete.

5.9 Genes involved in flavonoid biosynthesis have altered expression levels in *atscl26* mutants and between cell types

A number of genes that are involved in the synthesis of flavonoids in *A. thaliana* were identified across gene expression clusters in the experiments detailed

above. Thus, the expression of all genes annotated to be involved in the flavonoid biosynthesis pathway were analysed; the 17 genes were identified via NCBI. The expression values obtained through analysis of the microarray data was then plotted for these 17 genes on a heatmap to visualise the up- or down- regulation of the genes from the experiments involving KNO_3 treatment then isolation of different cell types (Figure 36), and the experiment involving NH_4NO_3 treatment of whole roots (Figure 37).

Almost all of the genes exhibit some degree of variation, however small. When looking at deplete conditions there are 11 genes which show genotype effect on expression and only 7 where the effect looks to be induced by N, with 4 of common genes common to both. Genotype N-dependant effects in replete conditions appear to identify 12 genes which have either an up – or – down regulation to their expression; *F3H* and *CHS* are amongst those genes and are directly involved in the flavonoid biosynthesis pathway.

The difference in expression does not seem to be nitrogen dependant for all genes. For example, in the epidermis there were some genes whose expression level was N-regulated but in other cell types there was no N-effect. *F3H* codes for FLAVONE 3-HYDROXLASE (Figure 6), an enzyme that regulates the synthesis of flavonoids by hydroxylation of naringenin into dihydrokaempferol. *F3H* is also co-ordinately expressed with CHS and CHI, which are important enzymes in chalcone synthesis (Nabavi et al., 2018). In epidermal cells, *F3H* has reduced expression in the *atscl26-2* when compared to Col-0 in N-deplete conditions, yet in N-replete conditions *F3H* has increased expression in *atscl26-2* compared to Col-0. In contrast, in *atscl26* (compared to Col-0), *F3H* has reduced expression in cortex but slightly increased

expression in *atscl26* pericycle in both N-replete and N-deplete conditions. The documented relationship between expression of *F3H* and the co-ordinately expressed *AtCHS* (Nabavi, *et al*, 2018) is similarly seen in the data here. *AtCHS* has reduced expression in N-deplete conditions in the *atscl26* mutant epidermis, and increased expression in N-replete *atscl26* mutant epidermis, as seen for *F3H*. It also has reduced expression in *atscl26* cortex cells at both N levels and but slightly increased expression in *atscl26* pericycle in both N-replete and N-deplete conditions.

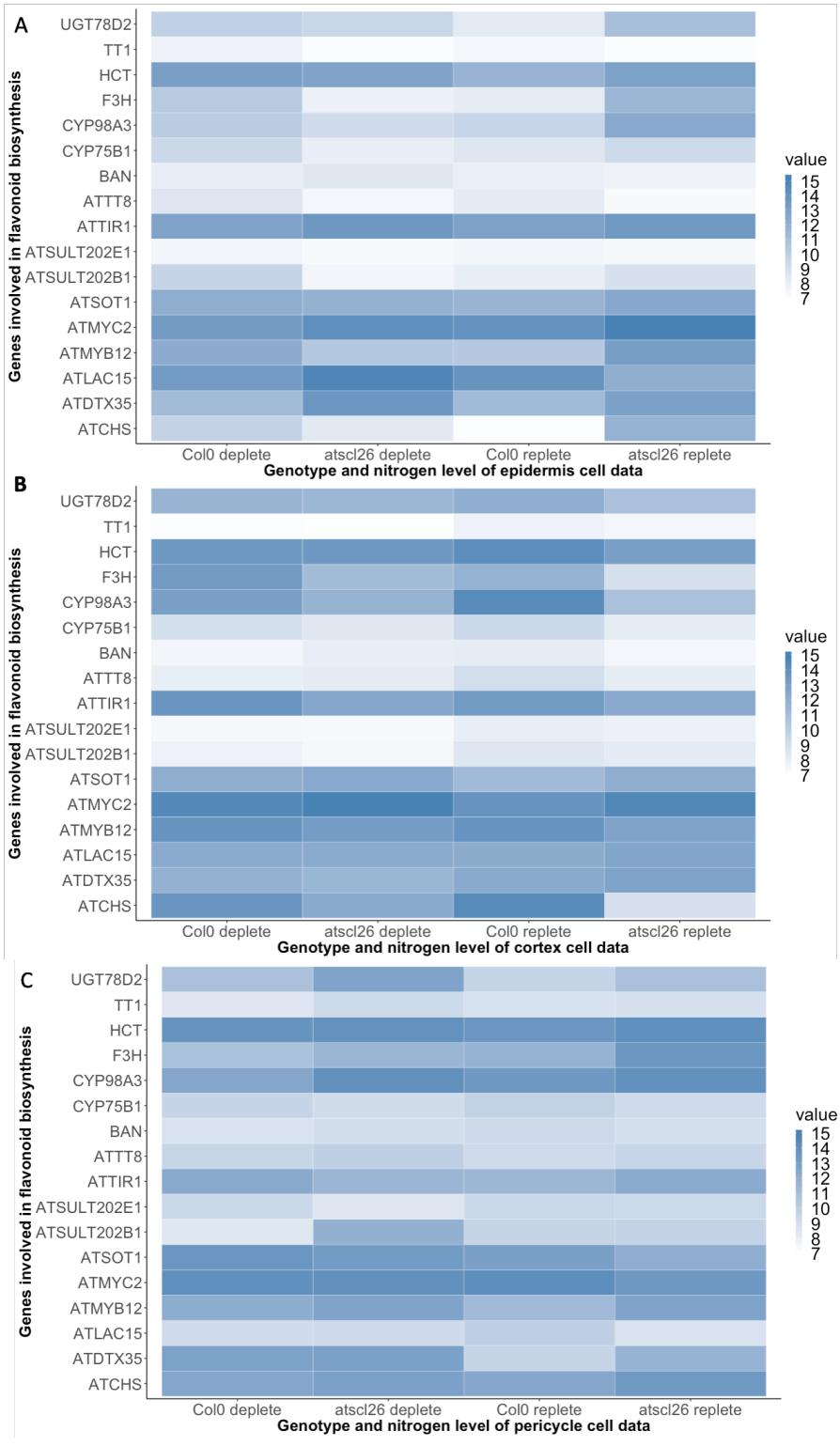

Figure 36: Expression levels of flavonoid biosynthesis genes in Col-0 and *atscl26-2* cell-type specific data of *A. thaliana* grown in replete and deplete NH_4NO_3 conditions. Cell type specific data generated through microarray analysis of gene expression of isolated epidermal cells (A), cortex cells (B) and pericycle cells (C).

The cell type specific heat map reveals the cell type detail of expression levels when comparing the wild type Col-0 to *atscl26-2*, which can help to elucidate the potential regulatory function of the *AtSCL26* gene on flavonoid biosynthesis. When gene expression is analysed on a whole root level, the complexities of the gene expression shifts are lost and the data gives a misleading impression that there is little to no variation between *atscl26* and Col-0 (Figure 36).

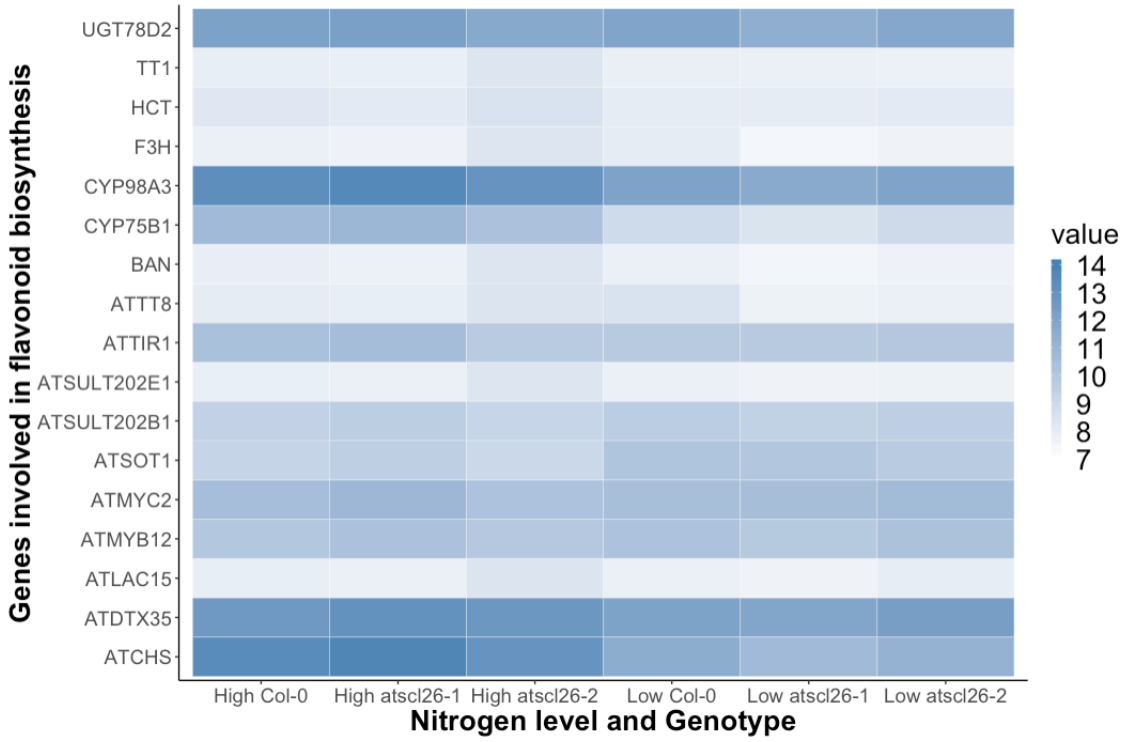

Figure 37: The expression values of genes involves in flavonoid biosynthesis in *A. thaliana* in whole roots treated with KNO_3. The heatmap shows that there is a slight increase in expression for some of the genes in *atscl26-2* when compared to Col-0 when grown on replete-N (high), with there being a difference change for *atscl26-2* than when comparing Col-0 and *atscl26-1*. On N-deplete (low) levels, there is only a slightly reduced expression of genes in the two *atscl26* mutants compared to Col-0.

5.10 *AtSCL26* is involved in flavonoid biosynthesis

To ask if the altered levels of flavonoid biosynthesis genes translated into altered levels of flavonoids in the roots, *atscl26-2* mutants were grown for 12-days on deplete or replete KNO_3 then total flavonoid abundance visualised by staining roots with DPBA.

DPBA binds to flavonoids and emits wavelengths between 520nm and 550nm when excited with the 488nm laser.

In roots of *atscl26-2* mutants grown on 0.1mM KNO_3 there is a large flavonoid abundance that is absent in Col-0, particularly in lateral root primordia (Figure 37). On N-replete (5mM KNO_3) levels, both *atscl26-2* and Col-0 have abundant flavonoid content, except for the root tip of Col-0 where flavonoid expression was reduced (Figure 38); analysis of more roots would enable this difference to be more fully explored. Overall, the flavonoid staining data suggests that *AtSCL26* acts to repress flavonoid formation in roots in N-deplete conditions.

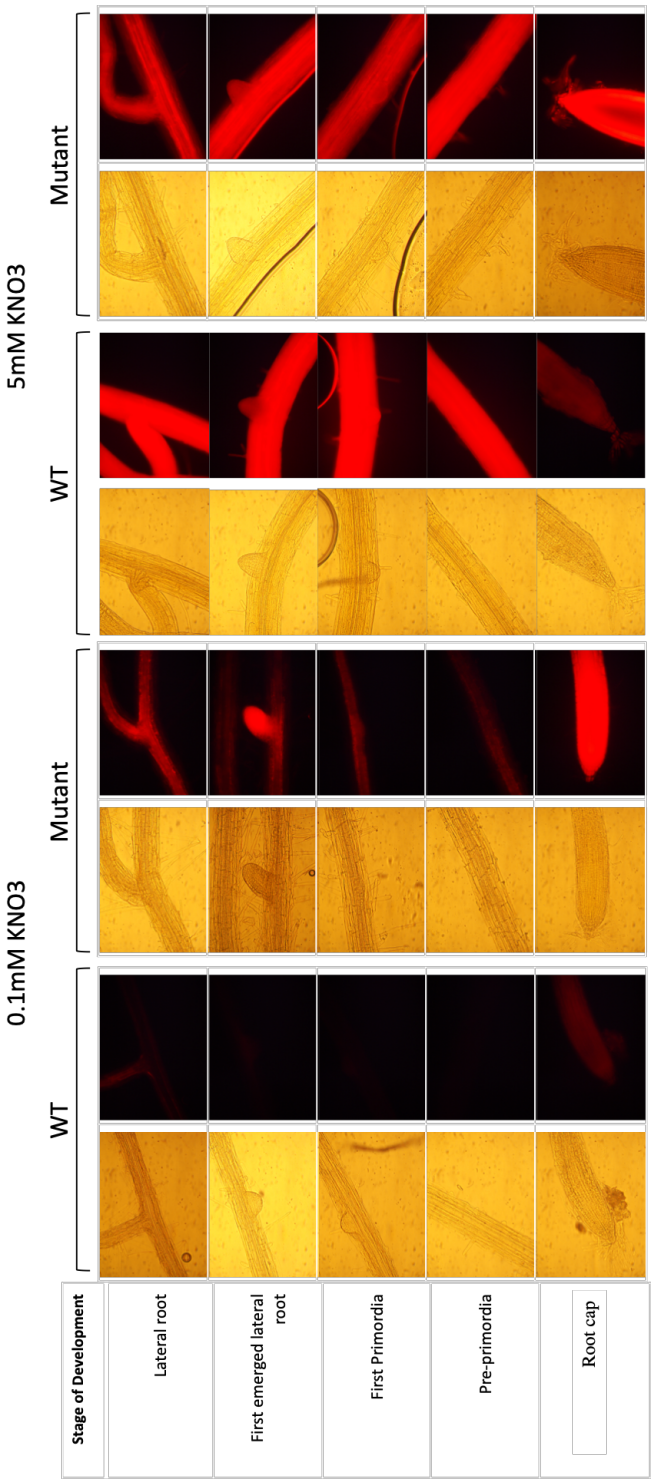

Figure 38: Flavonoid localisation levels in wild type (Col-0 WT) and mutant (*atscl26-2*) seedling roots. In roots of *atscl26-2* mutants grown on 0.1mM KNO_3 there is a large flavonoid abundance, that is absent in Col-0. On N-replete (5mM KNO_3) levels, both *atscl26-2* and Col-0 have abundant flavonoid content. Scale bar = 1cm.

5.11 Discussion

Combining the findings from expression analysis of the *atscl26* mutant with phenotypic analysis we are able to gain a better understanding of how *AtSCL26* affects gene expression in response to N. In deplete conditions there is a lower level of *AtSCL26* in the cortex, however in higher N conditions there is the reverse with a higher level of expression in the cortex and lower levels in the epidermis and pericycle cells. Accordingly, the *AtSCL26* effect and the influence of N on this effect varies by cell type. Analysis of individual cell types in *atscl26-2* showed that intracellular transport and responses to steroid hormone stimuli were repressed by *AtSCL26* in deplete N conditions in the cortex and pericycle and repressed by *AtSCL26* in replete conditions in the epidermis.

Flavonoid staining suggests that *AtSCL26* acts to repress flavonoid localisation in roots in N-deplete conditions. Flavonoids are important secondary metabolites which serve as versatile enzymes within the plant. In the leaves their accumulation gives protection against UV damage. Flavonoid abundance appears to be reduced by *AtSCL26* in low N conditions but there is no difference between *atscl26* and Col-0 in higher N levels. Therefore, we can postulate that the flavonoid expression N-upregulation does not require *AtSCL26*. *AtSCL26* instead seems to only limit flavonoid levels when N is deplete.

Cell type variation in flavonoid expression was not obvious. However, the presence of greater flavonoid levels particularly in *atscl26* lateral roots could potentially be down to the increased expression of *F3H* and *CHS* in pericycle, from which lateral roots originate. It would be interesting to investigate this in more detail. Alternatively, it could be that be the total level of DPBA staining was saturated in order to visualise these differences, or that that greater level of magnification was

required to visualise the differences. Alternatively, since there are a wide range of flavonoids it is possible that that more detailed analysis of different flavonoid forms could reveal cell type differences linked to the gene expression cell type differences.

As mentioned previously, it is postulated that the nodulation pathway co-opted the 'genetic blueprint' for lateral root growth (Bensmihen, 2015). Successful nodulation relies heavily on the timed expression of flavonoids as part of signalling a compatible plant root-rhizobia interaction and thus the link between *AtSCL26*, flavonoid expression and N is very interesting. It has been found that flavonoids can act in a similar way to synthetic auxin inhibitors, since the phenotype of flavonoid mutants was found to be similar to plants which had increased levels of auxin transport (Brown, 2001).

Based on the gene expression data presented in this chapter it can be hypothesised the regulation of flavonoid biosynthesis could be linked to the repression of genes involved in the polar transport of auxin across the cell membranes that was found in N-deplete conditions. This could be tested by analysing auxin levels in the *atscl26* mutants and by analysing flavonoid and *AtSCL26* levels in auxin transport mutants.

Chapter 6 Discussion and overall conclusion

In order to characterise the function of *AtSCL26* the aims of the project were to characterise the mutant phenotype of *atscl26* and to ascertain if this was N-dependant, to determine the cellular localisation of AtSCL26, based on the hypothesis that it is nuclear localised as NSP2, and to profile the molecular phenotype of *atscl26* in response to N using transcriptomic analysis. This work advances what we know of the relationship between NSP2 and AtSCL26 from previous studies that focussed on a comparison at the sequence level (Kaló *et al*, 2005).

In Chapter 3 it was shown that there is a strong root system architecture phenotype of *atscl26* mutants compared to Col-0 wild-type with overall an increase in lateral root numbers, lateral root length and primary root length. The phenotype was stronger in the *atscl26-2* mutant compared to the *atscl26-1* mutant, which seemed to be related to the more complete loss of *AtSCL26* expression in *atscl26-2*. There were also differences in the phenotypic effect between seedlings grown on replete and deplete N conditions, indicating that there is an N-dependant root phenotype and thus that *AtSCL26* has N-dependent effects on roots.

Interestingly the work also showed that the root phenotype was dependent on the source of N. In both seedlings grown on KNO_3 and NH_4NO_3 in deplete N levels *AtSCL26* inhibits the growth of PR, LR number, and LR outgrowth. However, when N levels increase and *AtSCL26* expression is reduced, the repressive effects of *AtSCL26* are thus reduced. In higher KNO_3 levels the root phenotype is less dramatic. In sufficient levels of NH_4NO_3, there is a stronger reduction of the repressive effects of *AtSCL26* and *atscl26-2* seedlings have a wild-type RSA with the only statistically significant difference being an increase in length in *atscl26-1*mutants (with the role of

AtSCL26 thus being to repress LR average length). On replete NH_4NO_3, the opposite effect is seen, in that *AtSCL26* activity still seems to control RSA, since there is an increase in the number of LRs in *atscl26* mutants. This adds another molecular player in the regulation of lateral root development according to nitrogen, to extend what we know about how nitrogen controls system architecture (Krouk et al., 2011).

When studying flavonoid abundance in roots a strong increase in flavonoid expression was seen in *atscl26-2* specifically in N-deplete conditions. This suggested that *AtSCL26* could be involved in regulating pathways that inhibit the flavonoid production in roots in N-deplete conditions. This adds additional information to help explain what was already known about the importance of flavonoid biosynthesis in nitrogen starvation responses during root development (Peng et al., 2008). Due to flavonoids being key communicators during the nodulation process in legumes, this was also an interesting discovery in the non-nodulating *A. thaliana*.

This project was able to draw putative conclusions as to the relatedness of the GRAS family member *AtSCL26* in *A. thaliana* and the GRAS transcription factor *NSP2* in *M. truncatula* by comparing analysis of protein localisation in the cell. An important similarity is that *AtSCL26* appears to have nuclear localisation similar to *NSP2* (Oldroyd, 2003; Kaló et al., 2005), indicating that it localises to a region where it could act as a regulator of gene expression. When aligned with other GRAS proteins, *AtSCL26* does not belong to any of the families that have been previously identified by Bolle *et al* (2016) (Figure 10). After investigating the sequence of the *AtSCL26* protein sequence, there is one key amino acid substitution, however this was not found to be responsible for the separate branch position compared to other *A. thaliana* GRAS proteins. According to Kaló *et al* (2005) across the GRAS family there is a conservation of residues within the VHIID motif and this includes NSP2. However, in

AtSCL26 this conservation is reduced and there is an asparagine to threonine residue substitution (this work and (Pysh et al., 1999)). The substitution could be important for function and is worthy of further investigation.

The use of transcriptomic profiling of *atscl26* mutants has enabled the hypothesis to be made that in deplete N conditions *AtSCL26* acts to repress genes involved in polar transport of auxin, as well as repress genes that are involved in regulation in response to steroid hormone detection, cell elongation, as well as intracellular transport of proteins.

Using the transcriptome data generated from this (pericycle and whole roots) and previous (epidermis and cortex) microarray experiments this project has also been able to draw conclusions on the effects of N on *AtSCL26* in individual cell types and in whole roots. As mentioned in Chapter 5, in replete KNO_3 there is a higher level of *AtSCL26* expression in cortical cells, however in deplete KNO_3 conditions, roots have higher levels of *AtSCL26* in the pericycle and epidermis. This work added has enabled finer detail to be gained about the role of *AtSCL26* in roots, since if there are opposite N-effects on gene expression in different cell types, as has been found here, the complexity is not possible to identify when all cell types are combined and analysed together (whole root sampling).

6.1 Possible links between *AtSCL26*, auxin, and GA

Another important hormone in signalling relating to plant growth is gibberellin (GA). One of the functions of this hormone is to degrade GAI and RGA, two DELLA growth repressor proteins (Gupta and Chakrabarty, 2013; Fonouni-Farde et al., 2016). GA signalled degradation was found to be responsible not only for cell elongation,

supporting previous research (Hirsch and Oldroyd, 2009), but also for cell proliferation. It has previously been shown that auxins upregulate GA biosynthesis genes (GA 3-oxidase and GA 20-oxidase) and down-regulate the genes that lead to GA catabolism (GA 2-oxidases), which in turn increases the levels of bioactive auxin (Reid et al., 2011). Therefore, if auxin is upregulated, leading to more GA which degrades growth inhibiting DELLA proteins, this would lead to more cell elongation and proliferation. However, it has been shown that in deplete N levels, *AtSCL26* inhibits the polar transport of auxin which would lead to a reduction in cell elongation and cell proliferation, as there would be a decrease in the level of GA. In deplete N conditions we found that *AtSCL26* had increased expression in the pericycle (the location of LR initiation) where it appeared to inhibit expression of genes involved in auxin transport, as well as cellular differentiation. Thus *AtSCL26* appears to inhibit important processes in LR initiation and cellular priming or the xylem pole pericycle cells for division.

6.2 Future work and suggested areas of investigation

To further investigate the developmental root phenotypes that differed based on the source of N used, it would be interesting to run a large-scale experiment looking at the effects of combinations of variable amounts of KNO_3, NH_4NO_3, and NH_4 as N sources for *A. thaliana* and also for the legume *M. truncatula*. The use of cell type specific RNAseq on epidermis, cortex, endodermis, and pericycle cells can enable localised effects related to regulation by N source to be characterised. Carrying this out for the *atscl26-2* mutant, treated with NH_4NO_3 in future work to would help to determine to what extent *AtSCL26* in involved in an ammonium-specific assimilation regulatory pathway.

A number of genes were found to have altered levels of expression or N-regulation in the *atscl26* mutants using transcriptomic analysis. There are presumably under *AtSCL26* control, thus the promoters of the putatively regulated genes should be examined to search for GRAS-binding sites, and investigated to elaborate understanding of the *atscl26* phenotype and the *AtSCL26*-controlled network.

Future work on this project should also include completing the complementation of *atscl26* mutants with *AtSCL26* and also testing trans-complementation of the *nsp2* mutant with *AtSCL26*. The trans-complementation of *atscl26* mutants with *NSP2* would provide a complementary investigation to ask to what extent the functions of these putative orthologs can be substituted. The experiment would ask to what extent the lateral root development and nodulation phenotypes in each case can be complemented and wild-type development restored.

An important piece of future work would be to create a profile of the hormones and flavonoids involved in LR growth in both *M. truncatula* and also in *A.thaliana* (as well as the trans-complemented mutants). This would involve comparing the abundance of flavonoids in response to *NSP2*/*AtSCL26* activity, following the hypothesis that flavonoids are less abundant in *nsp2* mutants.

Investigating links between GA, auxin and *AtSCL26* will also form the basis of future work since it would offer the chance to locate *AtSCL26* within the wider regulatory framework of lateral root development and more comprehensively assess links underlying possible co-option of the control of nodulation and lateral root development.

6.3 Conclusion

Overall this thesis has shown that *AtSCL26* has a repressive effect on root development in nitrogen-deplete conditions, and this is also nitrogen source dependant. This investigation suggests that, like *NSP2*, *AtSCL26* could be a nitrogen-regulated transcription factor that coordinates root development according to environmental cues. Investigating this putative ortholog pair enables us to gain insight into the potential shared pathways underpinning two key root architecture programmes – nodulation and lateral root development.

Chapter 7 References

Alonso, J. M., Stepanova, A. N., Leisse, T. J., Kim, C. J., Chen, H., Shinn, P., Stevenson, D. K., Zimmerman, J., Barajas, P., Cheuk, R., Gadrinab, C., Heller, C., Jeske, A., Koesema, E., Meyers, C. C., Parker, H., Prednis, L., Ansari, Y., Choy, N., Deen, H., Geralt, M., Hazari, N., Hom, E., Karnes, M., Mulholland, C., Ndubaku, R., Schmidt, I., Guzman, P., Aguilar-Henonin, L., Schmid, M., Weigel, D., Carter, D. E., Marchand, T., Risseeuw, E., Brogden, D., Zeko, A., Crosby, W. L., Berry, C. C. and Ecker, J. R. (2003) Genome-wide insertional mutagenesis of *Arabidopsis thaliana*. *Science*, 301(5633) pp. 653–657.

Alvarez, J. M., Riveras, E., Vidal, E. A., Gras, D. E., Contreras-López, O., Tamayo, K. P., Aceituno, F., Gómez, I., Ruffel, S., Lejay, L., Jordana, X. and Gutiérrez, R. A. (2014) Systems approach identifies TGA1 and TGA4 transcription factors as important regulatory components of the nitrate response of *Arabidopsis thaliana* roots. *Plant Journal*, 80(1) pp. 1–13.

Araya, T., Miyamoto, M., Wibowo, J., Suzuki, A., Kojima, S., Tsuchiya, Y. N., Sawa, S., Fukuda, H., von Wirén, N. and Takahashi, H. (2014) CLE-CLAVATA1 peptide-receptor signaling module regulates the expansion of plant root systems in a nitrogen-dependent manner. *Proceedings of the National Academy of Sciences*, 111(5) pp. 2029–2034.

Bensmihen, S. (2015) Hormonal control of lateral root and nodule development in legumes. *Plants*, 4(3) pp. 523–547.

Birnbaum, K., Jung, J. W., Wang, J. Y., Lambert, G. M., Hirst, J. A., Galbraith, D. W. and Benfey, P. N. (2005) Cell type-specific expression profiling in plants via cell sorting of protoplasts from fluorescent reporter lines. *Nature Methods*, 2(8) pp.

615–619.

Blake, J. A., Dolan, M., Drabkin, H., Hill, D. P., Ni, L., Sitnikov, D., Bridges, S., Burgess, S., Buza, T., McCarthy, F., Peddinti, D., Pillai, L., Carbon, S., Dietze, H., Ireland, A., Lewis, S. E., Mungall, C. J., Gaudet, P., Chisholm, R. L., Fey, P., Kibbe, W. A., Basu, S., Siegele, D. A., McIntosh, B. K., Renfro, D. P., Zweifel, A. E., Hu, J. C., Brown, N. H., Tweedie, S., Alam-Faruque, Y., Apweiler, R., Auchinchloss, A., Axelsen, K., Bely, B., Blatter, M. C., Bonilla, C., Bougueleret, L., Boutet, E., Breuza, L., Bridge, A., Chan, W. M., Chavali, G., Coudert, E., Dimmer, E., Estreicher, A., Famiglietti, L., Feuermann, M., Gos, A., Gruaz-Gumowski, N., Hieta, R., Hinz, U., Hulo, C., Huntley, R., James, J., Jungo, F., Keller, G., Laiho, K., Legge, D., Lemercier, P., Lieberherr, D., Magrane, M., Martin, M. J., Masson, P., Mutowo-Muellenet, P., ODonovan, C., Pedruzzi, I., Pichler, K., Poggioli, D., Porras Millan, P., Poux, S., Rivoire, C., Roechert, B., Sawford, T., Schneider, M., Stutz, A., Sundaram, S., Tognolli, M., Xenarios, I., Foulger, R., Lomax, J., Roncaglia, P., Khodiyar, V. K., Lovering, R. C., Talmud, P. J., Chibucos, M., Gwinn Giglio, M., Chang, H. Y., Hunter, S., McAnulla, C., Mitchell, A., Sangrador, A., Stephan, R., Harris, M. A., Oliver, S. G., Rutherford, K., Wood, V., Bahler, J., Lock, A., Kersey, P. J., McDowall, M. D., Staines, D. M., Dwinell, M., Shimoyama, M., Lauledерkind, S., Hayman, T., Wang, S. J., Petri, V., Lowry, T., DEustachio, P., Matthews, L., Balakrishnan, R., Binkley, G., Cherry, J. M., Costanzo, M. C., Dwight, S. S., Engel, S. R., Fisk, D. G., Hitz, B. C., Hong, E. L., Karra, K., Miyasato, S. R., Nash, R. S., Park, J., Skrzypek, M. S., Weng, S., Wong, E. D., Berardini, T. Z., Li, D., Huala, E., Mi, H., Thomas, P. D., Chan, J., Kishore, R., Sternberg, P., Van Auken, K., Howe, D. and Westerfield, M. (2013) Gene ontology annotations and resources. *Nucleic Acids Research*, 41(D1).

Bolle, C. (2004) The role of GRAS proteins in plant signal transduction and development. *Planta*, 8(5) pp. 683–692.

Bolle, C. (2015) Structure and Evolution of Plant GRAS Family Proteins. *Plant transcription factors: evolutionary, structural and functional aspects*. Elsevier Inc. pp. 153–161.

Bouguyon, E., Brun, F., Meynard, D., Kubeš, M., Pervent, M., Leran, S., Lacombe, B., Krouk, G., Guiderdoni, E., Zazímalová, E., Hoyerová, K., Nacry, P. and Gojon, A. (2015) Multiple mechanisms of nitrate sensing by Arabidopsis nitrate transceptor NRT1.1. *Nature Plants*, 1(15015).

Brady, S. M., Orlando, D. A., Lee, J. Y., Wang, J. Y., Koch, J., Dinneny, J. R., Mace, D., Ohler, U. and Benfey, P. N. (2007) A high-resolution root spatiotemporal map reveals dominant expression patterns. *Science*, 318(5851) pp. 801–806.

Bren dAmour, C., Reitsma, F., Baiocchi, G., Barthel, S., Güneralp, B., Erb, K.-H., Haberl, H., Creutzig, F. and Seto, K. C. (2016) Future urban land expansion and implications for global croplands. *Proceedings of the National Academy of Sciences*, 114(34) p. 201606036.

Brown, D. E. (2001) Flavonoids act as negative regulators of auxin transport *in vivo* in Arabidopsis. *Plant Physiology*, 126(2) pp. 524–535.

Carbon, S., Dietze, H., Lewis, S. E., Mungall, C. J., Munoz-Torres, M. C., Basu, S., Chisholm, R. L., Dodson, R. J., Fey, P., Thomas, P. D., Mi, H., Muruganujan, A., Huang, X., Poudel, S., Hu, J. C., Aleksander, S. A., McIntosh, B. K., Renfro, D. P., Siegele, D. A., Antonazzo, G., Attrill, H., Brown, N. H., Marygold, S. J., Mc-Quilton, P., Ponting, L., Millburn, G. H., Rey, A. J., Stefancsik, R., Tweedie, S., Falls, K., Schroeder, A. J., Courtot, M., Osumi-Sutherland, D., Parkinson, H.,

Roncaglia, P., Lovering, R. C., Foulger, R. E., Huntley, R. P., Denny, P., Campbell, N. H., Kramarz, B., Patel, S., Buxton, J. L., Umrao, Z., Deng, A. T., Alrohaif, H., Mitchell, K., Ratnaraj, F., Omer, W., Rodríguez-López, M., C. Chibucos, M., Giglio, M., Nadendla, S., Duesbury, M. J., Koch, M., Meldal, B. H. M., Melidoni, A., Porras, P., Orchard, S., Shrivastava, A., Chang, H. Y., Finn, R. D., Fraser, M., Mitchell, A. L., Nuka, G., Potter, S., Rawlings, N. D., Richardson, L., Sangrador-Vegas, A., Young, S. Y., Blake, J. A., Christie, K. R., Dolan, M. E., Drabkin, H. J., Hill, D. P., Ni, L., Sitnikov, D., Harris, M. A., Hayles, J., Oliver, S. G., Rutherford, K., Wood, V., Bahler, J., Lock, A., De Pons, J., Dwinell, M., Shimoyama, M., Laulederkind, S., Hayman, G. T., Tutaj, M., Wang, S. J., DEustachio, P., Matthews, L., Balhoff, J. P., Balakrishnan, R., Binkley, G., Cherry, J. M., Costanzo, M. C., Engel, S. R., Miyasato, S. R., Nash, R. S., Simison, M., Skrzypek, M. S., Weng, S., Wong, E. D., Feuermann, M., Gaudet, P., Berardini, T. Z., Li, D., Muller, B., Reiser, L., Huala, E., Argasinska, J., Arighi, C., Auchincloss, A., Axelsen, K., Argoud-Puy, G., Bateman, A., Bely, B., Blatter, M. C., Bonilla, C., Bougueleret, L., Boutet, E., Breuza, L., Bridge, A., Britto, R., Hye- A-Bye, H., Casals, C., Cibrian-Uhalte, E., Coudert, E., Cusin, I., Duek-Roggli, P., Estreicher, A., Famiglietti, L., Gane, P., Garmiri, P., Georghiou, G., Gos, A., Gruaz-Gumowski, N., Hatton-Ellis, E., Hinz, U., Holmes, A., Hulo, C., Jungo, F., Keller, G., Laiho, K., Lemercier, P., Lieberherr, D., Mac- Dougall, A., Magrane, M., Martin, M. J., Masson, P., Natale, D. A., ODonovan, C., Pedruzzi, I., Pichler, K., Poggioli, D., Poux, S., Rivoire, C., Roechert, B., Sawford, T., Schneider, M., Speretta, E., Shypitsyna, A., Stutz, A., Sundaram, S., Tognolli, M., Wu, C., Xenarios, I., Yeh, L. S., Chan, J., Gao, S., Howe, K., Kishore, R., Lee, R., Li, Y., Lomax, J., Muller, H. M., Raciti, D., Van Auken, K., Berriman, M., Stein,

Paul Kersey, L., W. Sternberg, P., Howe, D. and Westerfield, M. (2017) Expansion of the gene ontology knowledgebase and resources: The gene ontology consortium. *Nucleic Acids Research*, 45(D1) pp. 331–338.

Carter, A. (2013) *Cell-type specific comparative analysis of lateral root and nodule development at phenotypic and genomic levels*. University of Warwick PhD Thesis.

Carter, A. D., Bonyadi, R. and Gifford, M. L. (2013) The use of fluorescence-activated cell sorting in studying plant development and environmental responses. *International Journal of Developmental Biology*, 57(6–8) pp. 545–552.

Casimiro, I., Marchant, A., Bhalerao, R. P., Beeckman, T., Dhooge, S., Swarup, R., Graham, N., Inze, D., Sandberg, G., Casero, P. J. and Bennett, M. (2001) Auxin transport promotes arabidopsis lateral root initiation. *The Plant Cell*, 13(4) p. 843.

Chen, J., Zhang, D., Shen, B., Zhang, X., Xu, B. and Xu, X. (2006) Enantioseparation of D,L-α-amine acid on crown ester chiral stationary phases. *Fenxi Huaxue/Chinese Journal of Analytical Chemistry*, 34(11) pp. 1535–1540.

Devaiah, B. N., Karthikeyan, A. S. and Raghothama, K. G. (2007) WRKY75 transcription factor is a modulator of phosphate acquisition and root development in Arabidopsis. *Plant Physiology*, 143(4) pp. 1789–1801.

Downie, J. A. (2014) Legume nodulation. *Current Biology*. Elsevier, 24(5) pp. 184–190.

Eckardt, N. A. (2009) Nodulation signaling in legumes depends on an NSP1-NSP2 complex. *Plant Cell*, 21(2) pp. 367–367.

Ellenberger, T. E., Brandl, C. J., Struhl, K. and Harrison, S. C. (1992) The GCN4

basic region leucine zipper binds DNA as a dimer of uninterrupted α Helices: Crystal structure of the protein-DNA complex. *Cell*, 71(7) pp. 1223–1237.

FAO (2015) Current world fertilizer trends and outlook to 2018. *Food and Agriculture Organization of the United Nations* p. 66.

Fenn, M. E., Baron, J. S., Allen, E. B., Rueth, H. M., Nydick, K. R., Geiser, L., Bowman, W. D., Sickman, J. O., Meixner, T., Johnson, D. W. and Neitlich, P. (2003) Ecological effects of nitrogen deposition in the western United States. *BioScience*, 53(4) pp. 404–420.

Fonouni-Farde, C., Tan, S., Baudin, M., Brault, M., Wen, J., Mysore, K. S., Niebel, A., Frugier, F. and Diet, A. (2016) DELLA-mediated gibberellin signalling regulates Nod factor signalling and rhizobial infection. *Nature Communications*, 7, article number 12636.

Fossum, J.-P. (2014) Calculation of carbon footprint of fertilizer production, *Yara HESQ* 1, (3) pp. 4–9.

Gallagher, K. L. and Benfey, P. N. (2009) Both the conserved GRAS domain and nuclear localization are required for SHORT-ROOT movement. *Plant Journal*, 57(5) pp.785-97

Gibson, K. E., Kobayashi, H. and Walker, G. C. (2008) Molecular determinants of a symbiotic chronic infection. *Annual Review of Genetics*, 42(1) pp. 413–441.

Gifford, M. L., Banta, J. A., Katari, M. S., Hulsmans, J., Chen, L., Ristova, D., Tranchina, D., Purugganan, M. D., Coruzzi, G. M. and Birnbaum, K. D. (2013) Plasticity regulators modulate specific root traits in discrete nitrogen environments. *PLoS Genetics*, 9(9).

Gifford, M. L., Dean, A., Gutierrez, R. A., Coruzzi, G. M. and Birnbaum, K. D. (2008) Cell-specific nitrogen responses mediate developmental plasticity. *Proceedings of the National Academy of Sciences*, 105(2) pp. 803–808.

Gojon, A., Krouk, G., Perrine-Walker, F. and Laugier, E. (2011) Nitrate transceptor(s) in plants. *Journal of Experimental Botany*, 62(7) pp. 2299–2308.

Gonzalez-Rizzo, S., Crespi, M. and Frugier, F. (2006) The *Medicago truncatula* CRE1 cytokinin receptor regulates lateral root development and early symbiotic interaction with *Sinorhizobium meliloti*; *The Plant Cell*, 18(10) p. 2680 LP-2693.

Grafi, G. (2004) How cells dedifferentiate: A lesson from plants. *Developmental Biology*, 268(1) pp. 1–6.

Gruber, B. D., Giehl, R. F. H., Friedel, S. and von Wiren, N. (2013) Plasticity of the Arabidopsis root system under nutrient deficiencies. *Plant Physiology*, 163(1) pp. 161–179.

Gupta, R. and Chakrabarty, S. K. (2013) Gibberellic acid in plant: Still a mystery unresolved. *Plant Signaling and Behavior*, 8(9) pp. 1–5.

Heckmann, A. B., Lombardo, F., Miwa, H., Perry, J. A., Bunnewell, S., Parniske, M., Wang, T. L. and Downie, J. A. (2006) *Lotus japonicus* nodulation requires two GRAS domain regulators, one of which is functionally conserved in a non-legume. *Plant Physiology*, 142(4) pp. 1739–1750.

Heo, J.-O., Chang, K. S., Kim, I. A., Lee, M.-H., Lee, S. A., Song, S.-K., Lee, M. M. and Lim, J. (2011) Funneling of gibberellin signaling by the GRAS transcription regulator SCARECROW-LIKE 3 in the *Arabidopsis* root. *Proceedings of the National Academy of Sciences*. National Academy of Sciences, 108(5) pp. 2166–2171.

Hirsch, S., Kim, J., Munoz, A., Heckmann, A. B., Downie, J. A. and Oldroyd, G. E. D. (2009) GRAS proteins form a dna binding complex to induce gene expression during nodulation signaling in *Medicago truncatula*. *Plant Cell*, 21(2) pp. 545–557.

Hirsch, S. and Oldroyd, G. E. D. (2009) GRAS-domain transcription factors that regulate plant development. *Plant Signaling and Behavior*. Landes Bioscience, 4(8) pp. 698–700.

Hoffman, B. M., Lukoyanov, D., Dean, D. R. and Seefeldt, L. C. (2013) Nitrogenase: A draft mechanism. *Accounts of Chemical Research*, 46(2) pp. 587–595.

Hormozdiari, F., Zhu, A., Kichaev, G., Ju, C. J. T., Segrè, A. V., Joo, J. W. J., Won, H., Sankararaman, S., Pasaniuc, B., Shifman, S. and Eskin, E. (2017) Widespread allelic heterogeneity in complex traits. *American Journal of Human Genetics*, 100(5) pp. 789–802.

Journet, E.-P., El-Gachtouli, N., Vernoud, V., de Billy, F., Pichon, M., Dedieu, A., Arnould, C., Morandi, D., Barker, D. G. and Gianinazzi-Pearson, V. (2001) *Medicago truncatula ENOD11* : A novel RPRP-encoding early nodulin gene expressed during mycorrhization in arbuscule-containing cells. *Molecular Plant-Microbe Interactions*, 14(6) pp. 737–748.

Kaló, P., Gleason, C., Edwards, A., Marsh, J., Mitra, R. M., Hirsch, S., Jakab, J., Sims, S., Long, S. R., Rogers, J., Kiss, G. B., Downie, J. A. and Oldroyd, G. E. D. (2005) Nodulation signaling in legumes requires NSP2, a member of the GRAS family of transcriptional regulators. *Science*, 308(5729) pp. 1786–1789.

Karlowski, W. M. and Hirsch, A. M. (2003) The over-expression of an alfalfa RING-H2 gene induces pleiotropic effects on plant growth and development. *Plant Molecular Biology*, 52(1) pp. 121–133.

Kassaw, T., Nowak, S., Schnabel, E. and Frugoli, J. A. (2017) ROOT DETERMINED NODULATION1 is required for M. truncatula CLE12, but not CLE13 peptide signaling through the SUNN receptor kinase. *Plant Physiology*, 174(4).

Katari, M. S., Nowicki, S. D., Aceituno, F. F., Nero, D., Kelfer, J., Thompson, L. P., Cabello, J. M., Davidson, R. S., Goldberg, A. P., Shasha, D. E., Coruzzi, G. M. and Gutierrez, R. A. (2010) VirtualPlant: A Software Platform to Support Systems Biology Research. *Plant Physiology*, 152(2) pp. 500–515.

Kiba, T. and Krapp, A. (2016) Plant nitrogen acquisition under low availability: Regulation of uptake and root architecture. *Plant and Cell Physiology*, 57(4) pp. 707–714.

Kim, J. and Rees, D. C. (1994) Nitrogenase and biological nitrogen fixation. *Biochemistry*, 33(2) pp. 389–397.

Krapp, A., Berthome, R., Orsel, M., Mercey-Boutet, S., Yu, A., Castaings, L., Elftieh, S., Major, H., Renou, J.-P. and Daniel-Vedele, F. (2011) Arabidopsis roots and shoots show distinct temporal adaptation patterns toward nitrogen starvation. *Plant Physiology*, 157(3) pp. 1255–1282.

Krouk, G., Ruffel, S., Gutiérrez, R. A., Gojon, A., Crawford, N. M., Coruzzi, G. M. and Lacombe, B. (2011) A framework integrating plant growth with hormones and nutrients. *Trends in Plant Science*, 16(4) pp. 178–182.

Lagunas, B., Schäfer, P. and Gifford, M. L. (2015) Housing helpful invaders: The evolutionary and molecular architecture underlying plant root-mutualist microbe interactions. *Journal of Experimental Botany*, 66(8) pp. 2177–2186.

Latchman, D. S. (1997) Transcription factors: An overview. *International Journal of*

Biochemistry and Cell Biology pp. 1305–1312.

Lin, S.-H., Kuo, H.-F., Canivenc, G., Lin, C.-S., Lepetit, M., Hsu, P.-K., Tillard, P., Lin, H.-L., Wang, Y.-Y., Tsai, C.-B., Gojon, A. and Tsay, Y.-F. (2008) Mutation of the Arabidopsis NRT1.5 nitrate transporter causes defective root-to-shoot nitrate transport. *The Plant Cell*, 20(9) p. 2514 LP-2528.

Liu, C.-W. and Murray, J. (2016) The role of flavonoids in nodulation host-range specificity: An update. *Plants*, 5(3) p. 33.

Ma, W., Li, J., Qu, B., He, X., Zhao, X., Li, B., Fu, X. and Tong, Y. (2014) Auxin biosynthetic gene TAR2 is involved in low nitrogen-mediated reprogramming of root architecture in Arabidopsis. *Plant Journal*, 78(1) pp. 70–79.

Malamy, J. E. and Benfey, P. N. (1997) Organization and cell differentiation in lateral roots of *Arabidopsis thaliana*. *Development*, 124(1) p. 33-44.

Masson-Boivin, C. and Sachs, J. L. (2018) Symbiotic nitrogen fixation by rhizobia — the roots of a success story. *Current Opinion in Plant Biology*. Elsevier Ltd, 44 pp. 7–15.

Medici, A., Marshall-Colon, A., Ronzier, E., Szponarski, W., Wang, R., Gojon, A., Crawford, N. M., Ruffel, S., Coruzzi, G. M. and Krouk, G. (2015) AtNIGT1/HRS1 integrates nitrate and phosphate signals at the Arabidopsis root tip. *Nature Communications*, p. 6274.

Meier, I. (2007) Composition of the plant nuclear envelope: Theme and variations. *Journal of Experimental Botany*, 58(1) pp. 27–34.

Mok, D. W. S. and Mok, M. C. (2001) Cytokinin metabolism and action. *Annual Review of Plant Physiology nad Plant Molecular Biology*, 52 pp. 89–118.

Moshelion, M. and Altman, A. (2015) Current challenges and future perspectives of plant and agricultural biotechnology. *Trends in Biotechnology*, 33(6) pp. 337–342.

Murakami, Y., Miwa, H., Imaizumi-Anraku, H., Kouchi, H., Downie, J. A., Kawaguchi, M. and Kawasaki, S. (2007) Positional cloning identifies *Lotus japonicus* NSP2, a putative transcription factor of the GRAS family, required for NIN and ENOD40 gene expression in nodule initiation. *DNA Research*, 13(6) pp. 255–265.

Nabavi, S. M., Šamec, D., Tomczyk, M., Milella, L., Russo, D., Habtemariam, S., Suntar, I., Rastrelli, L., Daglia, M., Xiao, J., Giampieri, F., Battino, M., Sobarzo-Sanchez, E., Nabavi, S. F., Yousefi, B., Jeandet, P., Xu, S. and Shirooie, S. (2018) Flavonoid biosynthetic pathways in plants: Versatile targets for metabolic engineering. *Biotechnology Advances*, (November).

Nacry, P., Bouguyon, E. and Gojon, A. (2013) Nitrogen acquisition by roots: Physiological and developmental mechanisms ensuring plant adaptation to a fluctuating resource. *Plant and Soil* pp. 1–29.

Van Norman, J. M., Xuan, W., Beeckman, T. and Benfey, P. N. (2013) To branch or not to branch: the role of pre-patterning in lateral root formation. *Development*, 140(21) pp. 4301–4310.

Oldroyd, G. E. D. (2003) Identification and characterization of nodulation-signaling pathway 2, a gene of *Medicago truncatula* involved in nod factor signaling. *Plant Physiology*, 131(3) pp. 1027–1032.

Overvoorde, P., Fukaki, H. and Beeckman, T. (2010) Auxin control of root development. *Cold Spring Harbor perspectives in biology*, 2(6) p. 16.

Pabo, C. O. and Sauer, R. T. (1992) Transcription factors: Structural families and principles of DNA recognition. *Annual Review of Biochemistry*, 61(1) pp. 1053–1095.

Peng, M., Hudson, D., Schofield, A., Tsao, R., Yang, R., Gu, H., Bi, Y.-M. and Rothstein, S. J. (2008) Adaptation of Arabidopsis to nitrogen limitation involves induction of anthocyanin synthesis which is controlled by the NLA gene. *Journal of experimental botany*. 2008/06/13, Oxford University Press, 59(11) pp. 2933–2944.

Péret, B., De Rybel, B., Casimiro, I., Benková, E., Swarup, R., Laplaze, L., Beeckman, T. and Bennett, M. J. (2009) Arabidopsis lateral root development: an emerging story. *Trends in Plant Science*, 14(7) pp. 399–408.

Population, W. and History, G. (2008) *World Population Growth History*. Growth (Lakeland). [Online] [Accessed on 1st September 2018] https://ourworldindata.org/world-population-growth.

Pysh, L. D., Wysocka-Diller, J. W., Camilleri, C., Bouchez, D. and Benfey, P. N. (1999) The GRAS gene family in Arabidopsis: Sequence characterization and basic expression analysis of the SCARECROW-LIKE genes. *Plant Journal*. Blackwell Science Ltd, 18(1) pp. 111–119.

Rabalais, N., Turner, R. and Scavia, D. (2002) Beyond science into policy: Gulf of Mexico hypoxia. *Bioscience*, 52(2) p. 129.

Rees, D. C. and Howard, J. B. (2000) Nitrogenase: Standing at the crossroads. *Current Opinion in Chemical Biology*, 4(5) pp. 559–566.

Reid, J. B., Davidson, S. E. and Ross, J. J. (2011) Auxin acts independently of DELLA proteins in regulating gibberellin levels. *Plant Signaling and Behavior*, 6(3) pp. 406–408.

Ritchie, M. E., Phipson, B., Wu, D., Hu, Y., Law, C. W., Shi, W. and Smyth, G. K. (2015) Limma powers differential expression analyses for RNA-sequencing and microarray studies. *Nucleic Acids Research*, 43(7) p. e47.

Salonen, M., Urho, L. and Engström-Öst, J. (2009) Effects of turbidity and zooplankton availability on the condition and prey selection of pike larvae. *Boreal Environment Research*, 14(6) pp. 981–989.

Shtratnikova, V. Y., Kudryakova, N. V., Kudoyarova, G. R., Korobova, A. V., Akhiyarova, G. R., Danilova, M. N., Kusnetsov, V. V. and Kulaeva, O. N. (2015) Effects of nitrate and ammonium on growth of *Arabidopsis thaliana* plants transformed with the *ARR5::GUS* construct and a role for cytokinins in suppression of disturbances induced by the presence of ammonium. *Russian journal of plant physiology* 62(6) pp. 792–803.

Simonson, R. E. (1956) Variations on the theme mental health in nursing. *Public health reports*, 71(7) pp. 700–704.

de Smet, I. (2012) Lateral root initiation: One step at a time. *New Phytologist* pp. 867–873.

De Smet, S., Cuypers, A., Vangronsveld, J. and Remans, T. (2015) Gene networks involved in hormonal control of root development in *Arabidopsis thaliana*: A framework for studying its disturbance by metal Stress. *International Journal of Molecular Sciences*, 16(8) pp. 19195–19224.

Smit, P., Raedts, J., Portyanko, V., Debellé, F., Gough, C., Bisseling, T. and Geurts, R. (2005) NSP1 of the GRAS protein family is essential for rhizobial nod factor-induced transcription. *Science*, 308(5729) pp. 1789–1791.

Stougaard, J. (2000) Regulators and regulation of legume root nodule development. *Plant Physiology*, 124(2) p. 531-540.

Suzaki, T., Yoro, E. and Kawaguchi, M. (2015) Leguminous plants: Inventors of root nodules to accommodate symbiotic bacteria. *International Review of Cell and*

Molecular Biology, 316 pp. 111–158.

Tai, Y. C. and Speed, T. P. (2012) A multivariate empirical Bayes statistic for replicated microarray time course data. *In Selected Works of Terry Speed*, pp. 617–642.

The Arabidopsis Information Resource (TAIR) (2018) Arabidopsis GRAS gene family.. [Online] [Accessed on 15th September 2018] https://www.arabidopsis.org/browse/genefamily/gras_genefamily.jsp.

Tian, H., Jia, Y., Niu, T., Yu, Q. and Ding, Z. (2014) The key players of the primary root growth and development also function in lateral roots in Arabidopsis. *Plant Cell Reports*, 33(5) pp. 745–753.

Tian, X. and Doerner, P. (2013) Root resource foraging: does it matter? *Frontiers in Plant Science*, 4 pp. 2–5.

Tischner, R. (2000) Nitrate uptake and reduction in plants. *Plant, Cell and Environment*, 23(2) pp. 1005–1024.

Turner, A. M. and Chislock, M. F. (2010) Blinded by the stink: Nutrient enrichment impairs the perception of predation risk by freshwater snails. *Ecological Applications*, 20(8) pp. 2089–2095.

United Nations News Service (2013) World population projected to reach 9.6 billion by 2050 – UN report. *United Nations News Service*. [Online] [Accessed on 1st October 2016] http://www.un.org/apps/news/story.asp?NewsID=45165#.VEe-qVfZq5c.

Walker, L., Boddington, C., Jenkins, D., Wang, Y., Grønlund, J. T., Hulsmans, J., Kumar, S., Patel, D., Moore, J. D., Carter, A., Samavedam, S., Bomono, G., Hersh, D. S., Coruzzi, G. M., Burroughs, N. J. and Gifford, M. L. (2017) Root

architecture shaping by the environment is orchestrated by dynamic gene expression in space and time. *The Plant Cell*, 29 pp. 2393–2412.

Wärnmark, A., Treuter, E., Wright, A. P. H. and Gustafsson, J.-Å. (2003) Activation functions 1 and 2 of nuclear receptors: Molecular strategies for transcriptional activation. *Molecular Endocrinology*, 17(10) pp. 1901–1909.

Worrell, E., Bernstein, L., Roy, J., Price, L. and Harnisch, J. (2009) Industrial energy efficiency and climate change mitigation. *Energy Efficiency*, 2(2) pp. 109–123.

Xia, X., Ma, C., Dong, S., Xu, Y. and Gong, Z. (2017) Effects of nitrogen concentrations on nodulation and nitrogenase activity in dual root systems of soybean plants. *Soil Science and Plant Nutrition*, 63(5) pp. 470–482.

Yokota, K., Soyano, T., Kouchi, H. and Hayashi, M. (2010) Function of GRAS proteins in root nodule symbiosis is retained in homologs of a non-legume, rice. *Plant and Cell Physiology*, 51(9) pp. 1436–1442.

Yu, L. H., Miao, Z. Q., Qi, G. F., Wu, J., Cai, X. T., Mao, J. L. and Xiang, C. Bin (2014) MADS-Box transcription factor AGL21 regulates lateral root development and responds to multiple external and physiological signals. *Molecular Plant*, 7(11) pp. 1653–1669.

Yuan, L., Loque, D., Kojima, S., Rauch, S., Ishiyama, K., Inoue, E., Takahashi, H. and von Wiren, N. (2007) The organization of high-affinity ammonium uptake in Arabidopsis Roots depends on the spatial arrangement and biochemical properties of AMT1-type transporters. *Plant Cell*, 19(8) pp. 2636–2652.